university of groningen

faculty of science and engineering

Determining Gauge Field Induced Primordial Non-Gaussianity by Calculation of the Bispectrum employing Green's Functions

Author:
Giacomo BELLERI
(S4759141)

Supervisor:
Dr. E. DIMASTROGIOVANNI
Second examiner :
Prof. Dr. A. MAZUMDAR

Bachelor's Thesis
To fulfill the requirements for the degree of
Bachelor of Science in Physics
at the University of Groningen

July 9, 2024

Contents

Abstract

Cosmological late-time observables are characterized by small deviations from homogeneity and isotropy. These originate in quantum fluctuations produced during inflation, a period of rapid expansion during the earliest moments of the universe. The nature of this process depends on its field content. More than one field may have been present and their interactions often result in sourced quantum fluctuations. These generally introduce non-Gaussian features in the distribution of the anisotropies. Therefore, non-Gaussianity is often used as a probe of inflation. This paper analyzes the effects and evolution of sourced quantum fluctuations originating from interactions of the inflaton with Gauge fields. After a discussion of the mechanism involved, the power spectrum and bispectrum related to these interactions are computed using Green's functions. For most configurations of parameters, the bispectrum exhibits an equilateral shape with large non-Gaussianities. The application of PLANCK constraints ($-73 \leq f_{\mathrm{NL}}^{\mathrm{equil}} \leq 21$) imposes $\xi \leq 2.5$ and $H(\alpha/f) \leq 1.44 \cdot 10^{-3}$. These correspond to configurations in which Gauge interaction effects are small. In fact, for these values, the primordial amplitude deviates from its inflaton-only counterpart by a maximum of 1.98%. In addition, a comparison with the self-interaction bispectrum ($f_{\mathrm{NL}} \ll 1$) suggests that self-interactions are minor corrections to the larger contribution produced by interactions with Gauge fields.

Acknowledgments

First of all, I would like to thank Dr. E. Dimastrogiovanni for their excellent guidance, invaluable feedback, and for the opportunity to study this interesting new topic. I would also like to thank Amelie Rudek for being the best study companion throughout the past few months. She was there for all my mental breakdowns and rants and I will always thank her for letting me annoy her with useless study breaks. My thanks go to Marike Schneider for being my best friend and the best lab partner I could ask for. The same can be said for Sidney Schwarz but he is best remembered for his cake(s). An important mention goes to Diana Ionescu, Balázs Kovács, Tim Van Der Meer, Douglas Kant, and the rest of *Community*.

I would also like to thank my parents Alessandro and Francesca, my brother Vittorio, and my grandparents Franco, Donatella, Anna, and Bruno for always supporting me (financially and emotionally). Lastly, I would like to thank my pets (of which you can find pictures below) for always bringing me joy.

(a) *Lilu*

(b) *Molly*

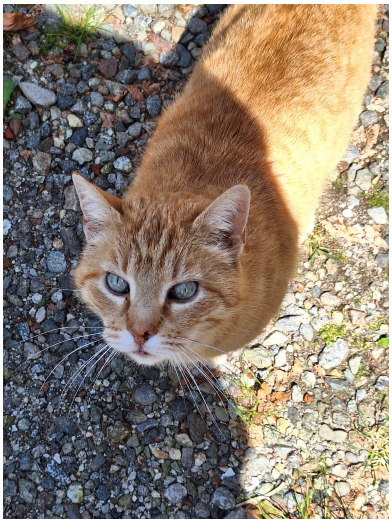

(c) *Garfield*

1 Introduction

First introduced in 1981 by A.H. Guth [1] and preceded by the works of Starobinsky [2], the inflation paradigm is now accepted by most cosmologists as a valid addition to the standard cosmic evolution (Fig.1) and is currently one of the most stimulating aspects of both theoretical and observational cosmology.

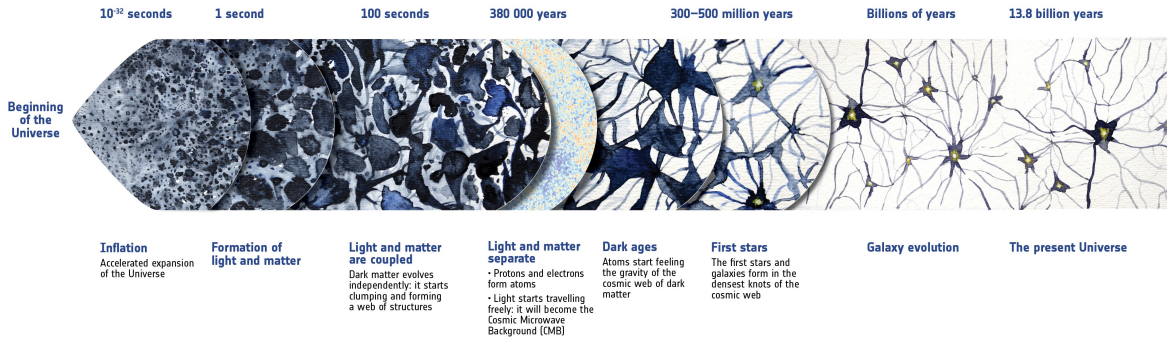

Figure 1: *Diagrammatic representation of the cosmic history, including the inflationary phase, according to current data. The Big Bang is taken as the origin of time. The numbers presented approximately indicate the starting moment of each evolutionary phase. Source: [3].*

Cosmic inflation refers to a brief (timescale of 1×10^{-33} s [4]) period of accelerated, rapid, and almost exponential expansion of the universe that took place shortly after the Big Bang. Due to these characteristics, inflation can explain the approximate flatness of the universe, its complete thermal equilibrium, and its lack of magnetic monopoles [5–7]. In standard cosmology (Sec. 2.2), these cosmological features lack a justification and are thus referred to as ”Flatness”, ”Horizon”, and ”Monopole” problems.

The length and energy scale of the inflationary period vary with different models. However, all models of inflation are described by the dynamics of one or multiple fields known as inflatons [6–9]. These fields may vary in nature but all govern the universe's evolution due to their non-negligible contributions to its energy density and pressure. There often are additional fields with small contributions to the energy density but relevant effects on inflatons or observables. For example, Gauge fields [10] might have been present. The field content and the corresponding dynamics actively shape the observables that can now be measured.

Of particular observational importance are the *Cosmic Microwave Background* (CMB) and the *Large Scale Structure* (LSS) distribution (Fig.2). The latter refers to the spatial distribution of matter on cosmological scales, which are much larger than the size of any galaxy or galaxy cluster. On the other hand, the CMB is the ensemble of primordial photons that have been streaming freely since their last scattering shortly after recombination [6, 8, 11]. Recombination refers to the moment free protons and electrons combined to form the first hydrogen atoms, which led to a considerable decrease in the free electron's number density. Consequentially, the scattering probability of photons reduced considerably and the universe transitioned from being photon-opaque to its current photon-transparent state. As such, both the CMB and the LSS distribution constitute valuable observables for cosmologists as they provide information on primordial conditions and their gravitational evolution.

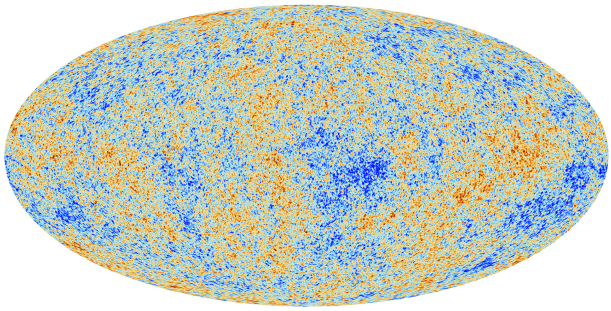

(a) *Full-sky map of the Cosmic Microwave Background. Orange and blue spots correspond to positive and negative fluctuations with respect to the mean temperature. The fluctuations are in the order of* 1×10^{-5} K. *Source: [12].*

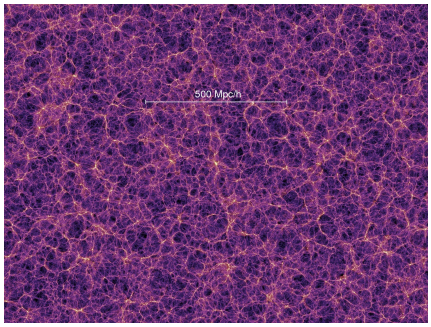

(b) *Simulated partial sky map of the Large Scale Structure distribution on the scale of* 500 Mpc/h *in the present. Brighter and darker portions correspond to positive and negative density fluctuations. Source: [13].*

Figure 2: *Sky maps of CMB and LSS distribution.*

On cosmological scales, the CMB appears to be homogeneous and isotropic. However, precise measurements of the CMB from COBE[14], WMAP[15], and PLANCK[16], evidenced the presence of small anisotropies. A similar analysis applies to the LSS distribution. The reasons for these deviations can be found in inflation. During inflation, the quantum fluctuations of the fields involved grow to super-horizon scales and evolve according to gravitational non-linear dynamics [9]. However, due to the stronger coupling of gravity to matter than to radiation, the initial quantum fluctuation conditions have a smaller effect on the LSS distribution than on the CMB, as the gravitational evolution quickly masks them [17]. Therefore, the CMB anisotropies are the ideal probe of primordial cosmology [17, 18].

Consequently, statistical analyses of the CMB have the potential to unveil specific characteristics of inflation and provide new information on its field content and related dynamics. To extract this information, *n-point correlation functions*, and their Fourier transforms are often computed [9, 17, 18]. The 2-point correlation function and the corresponding *power-spectrum* are particularly significant. However, measurements of these statistics do not provide a complete picture of the statistical distribution of primordial anisotropies. To determine whether quantum fluctuations are entirely Gaussian or if they present small deviations from Gaussianity, one has to compute the *3-point correlation function* and its *bispectrum* [9, 17, 18]. These statistics are related to the *non-linearity parameter* f_{NL}, a measure of the strength of the *Primordial non-Gaussianity*. The latest constraints on this parameter allow f_{NL} to be non-zero and do not exclude values up to order 10^1.

Research Scope and Outline

The amount of primordial non-Gaussianity allows cosmologists to discern between different inflationary models. However, for such a task to be efficient, cosmologists have to predict the primordial deviations from Gaussianity produced by each model.

In this paper, the deviations from Gaussian distributions are analyzed for two different models. In the first model, quantum fluctuations produced by the inflaton self-interactions and the related non-Gaussianity are considered. The second model extends the first by introducing Gauge fields. Given the scope of the research, the justification and history of this addition are not treated but its phenomenology is. Consequentially, the latter's ability to source inflaton's quantum fluctuations is studied.
A comparison between the two models is performed through an analysis of the bispectra. This allows for the following research questions to be answered:

Q1. *What is the effect of Gauge-field induced interactions on primordial non-Gaussianity?*

Q2. *How do Gauge field interactions affect the shape of the bispectrum?*

Q3. *How does the f_{NL} parameter compare to the PLANCK measurements?*

Sec.2 establishes the necessary theoretical background for an accurate analysis of primordial non-Gaussianity arising from inflaton interactions. Sec.3, discussed the evolution of quantum fluctuations and the effects of sourced quantum fluctuations on field statistics. The latter are then discussed in the context of Gauge field interactions in Sec. 4.

2 Theoretical Background

This section briefly outlines relevant concepts of General Relativity (GR) and Quantum Field Theory (QFT). The reader is also introduced to Friedmann-Lemaître-Robertson-Walker (FLRW) cosmology and inflation.

2.1 Notation Conventions

In the following sections, several notation conventions are used. In particular, Einstein's summation convention is assumed whenever an index is repeated. Greek indices range from 0 to 3 i.e. $\mu, \ldots = 0, \ldots, 3$ while Latin indices range from one to three i.e. $i, \ldots = 1, 2, 3$. Partial derivatives with respect to any variable k are represented with the shorthand notation ∂_k while over-dots and primes indicate full derivatives with respect to proper time τ and cosmic time t respectively. In addition, natural units ($\hbar = c = 1$) are used.

2.2 General Relativity and FLRW Cosmology

The universe is neutral and several orders of magnitude larger than a nucleus or an atom. As such, gravity is the relevant interaction (Tab.1) for cosmological evolution [5]. When distances and energy contents are comparable to the ones of our solar system, the latter is theoretically described by the familiar Newtonian formalism. However, Einstein's General Relativity is the appropriate framework for analyzing high-energy systems like the universe.

Interaction	Range (m)	Associated Boson
Weak	10^{-18}	W, Z
Strong	10^{-15}	Gluon
Electromagnetic	∞	Photon
Gravity	∞	Graviton

Table 1: *Properties of the four fundamental interactions. For each interaction, the range and strength relative to gravity are presented together with the associated boson(s). The only boson that has not yet been experimentally observed is the Graviton. Source: [19]*

2.2.1 Einstein's Equations

General relativity extends special relativity to accelerated reference frames. This is summarised in the two following principles [6]:

The Equivalence Principle:
The laws of physics in a freely falling reference frame take the same form as the ones in an inertial reference frame.

Curved Path of a Moving Object:
Objects move through spacetime following geodesics, the shortest possible trajectories on curved spacetime manifolds.

The equivalence principle finds its roots in the idea that a freely falling observer is unable to determine whether they are freely falling or are immobile. A familiar example is a person in a closed and opaque elevator moving with constant acceleration. Said person is unable to determine whether they

are moving or not. The second principle can be understood by considering a light beam propagating with a freely falling observer. According to the latter, the light will propagate in a straight line. On the other hand, for a different observer light will appear to have a curved trajectory as the light source moves with respect to the observer.

The two principles suggest a relation between gravity, curved spacetime, and energy. The latter is one of the main differences from Newtonian gravity as even massless particles can follow curved trajectories. Indeed, General Relativity establishes a relationship between the curvature of spacetime, its local energy content, and the related gravity in the form of *Einstein's Equations* [6, 8]:

$$\underbrace{G_{\alpha\beta} + g_{\alpha\beta}\Lambda}_{\text{Curvature}} = \kappa \overbrace{T_{\alpha\beta}}^{\text{Energy}} \tag{1}$$

For the sake of brevity and simplicity, an intuitive description of these equations is favored over the often challenging mathematical description. On the left-hand side of Eq.1, the *Einstein tensor* $G_{\alpha\beta}$ depends on the *spacetime metric* $g_{\alpha\beta}$, a quantity that encodes the curvature of spacetime and relates them to the spacetime interval $ds^2 = g_{\alpha\beta}dx^{\alpha}dx^{\beta}$. The quantity Λ is the *cosmological constant* generally associated with dark energy. On the right-hand side, the *energy-momentum tensor* $T_{\alpha\beta}$ encodes the local energy content and is scaled by the constant κ.

Einstein's Equations (Eq.1) suggest a bilateral relation between spacetime's curvature and its energy content. That is, the energy generates spacetime's curvature which in turn affects the motion of its energy content. The resulting changes in the energy distribution lead to further changes in the metric/curvature and this process repeats. Therefore, gravity is the manifestation of the spacetime's curvature's effect on the local energy density. However, modeling gravity is not an easy task. As the Einstein, metric, and energy tensors are symmetric, Einstein's Equations (Eq.1) are ten coupled non-linear equations that are often difficult to solve.

2.2.2 The Cosmological Principle and the FLRW Metric

Solving Einstein's equations is a task that is greatly simplified by the *Cosmological Principle* [5] which states that the universe is *maximally symmetric*, and thus homogenous and isotropic, on cosmological scales. This principle is deeply rooted in observation. The CMB, LSS distribution, and many other observables present negligible discrepancies from homogeneity and isotropy on scales much larger than the ones of the largest galaxy clusters.

Each manifold has a curvature K. Out of all the possible curved spacetime manifolds, only three are consistent with the cosmological principle: uniformly positively curved, negatively curved, and not curved. These correspond to the spherical, hyperbolic saddle, and flat (Minkowski) manifolds respectively (Fig.3). These constraints simplify the metric tensor to the following *FLRW metric* [6, 8] in spherical coordinates:

$$g_{\alpha\beta} = \begin{bmatrix} -1 & 0 \\ 0 & a^2(t)\gamma_{ij} \end{bmatrix} \qquad \gamma_{ij}dx^i dx^j = \frac{dr^2}{1-Kr^2} + r^2\left(d\theta^2 + sin^2(\theta)d\varphi^2\right) \tag{2}$$

Eq.2 is expressed in terms of time t and the *comoving coordinates* (r, θ, ϕ). These coordinates do not stretch and change as the universe expands over time. Evidence for this expansion was found by E.

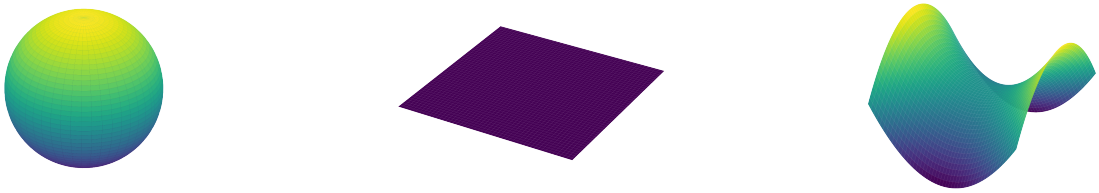

(a) *Spherical manifold with curvature $K > 0$.*

(b) *Euclidean manifold with curvature $K = 0$.*

(c) *Hyperbolic (Saddle) manifold with curvature $K < 0$.*

Figure 3: *Three-dimensional representation of the spacetime manifolds consistent with the cosmological principle. It includes spherical/positively curved (3a), flat (3b), and saddle/negatively curved (3c) manifolds.*

Hubble in 1929 [20]. His research forced many cosmologists to move away from a static universe model in favor of the current dynamic universe. This led to the introduction of the *scale factor* $a(t)$ which quantifies the expansion of cosmological distances. This allows for the definition of the *proper time* $d\tau = dt/a(t)$. The rate of expansion is related to the *Hubble parameter* H or to its proper time equivalent $\mathcal{H}$:

$$H = \frac{a'}{a} \qquad\qquad \mathcal{H} = \frac{\dot{a}}{a} \tag{3}$$

2.2.3 The Friedmann Equations and Cosmological Evolution

In a universe with FLRW metric, the energy-momentum tensor simplifies to the tensor of a perfect fluid $T^{\mu}{}_{\nu} = \mathrm{diag}\,(-\rho,\, P,\, P,\, P)$ where ρ and P are the energy density and pressure associated with the universe's energy content. The metric and the associated energy-momentum tensor reduce Einstein's Equations (Eq.1) to two coupled equations for the scale factor $a(t)$ and its rate of change $a'(t)$. These equations, known as *Friedmann Equations*, are reported below together with the continuity equation.

$$1^{st}\ \textit{Friedmann Equation:} \qquad H^2 = \left(a'/a\right)^2 = \rho(3M_p^2)^{-1} - Ka^{-2} \tag{4}$$

$$2^{nd}\ \textit{Friedmann Equation:} \qquad H' + H^2 = \left(a''/a\right) = -(\rho + 3P)(6M_p^2)^{-1} \tag{5}$$

$$\textit{Continuity Equation:} \qquad \dot{\rho} + 3H(\rho + P) = 0 \tag{6}$$

In the case of a flat, single-component universe, the equations above reduce to:

$$H = \frac{a'}{a} = a^{-\frac{3}{2}(1+w)} H_0 \qquad\qquad w = \frac{P}{\rho} \tag{7}$$

The equation above is of fundamental importance for discussions of the inflationary phase (Sec.2.4).

2.3 Quantum Field Theory and Field Dynamics

Most of modern physics is built on (relativistic) fields and their dynamics. Like the familiar electric and magnetic fields, fields describe a quantity's value and its changes at every point in spacetime. Classically, this ensures that the physical system and the related equations satisfy *locality* [21] and thus ensure agreement with special relativity.

These concepts can be expanded to quantum physics. Planck and Einstein suggested that electric and magnetic fields can be described entirely by *photons*, the particle *quanta* of said fields [22]. Indeed, once fields are quantized, fundamental particles naturally manifest as their quanta.

Therefore, Quantum Field Theory provides a framework for the analysis of particles and their interactions, which will be introduced after a discussion of field dynamics. For detailed discussions on these topics, the reader is referred to [21, 22], the resources on which the following sections are based on.

2.3.1 Scalar and Gauge Field Dynamics

Relativistic field dynamics are analyzed through the Lagrangian formalism. In this formalism, the Lagrangian $L = E_k - V$ is defined as the difference between the field's kinetic energy E_k and its potential energy V. It is often useful to deal with the Lagrangian density $\mathcal{L}$ i.e. Lagrangian per unit volume. The field's equations of motion can be found by minimizing the *action* S (Eq.8) using the *Euler-Lagrange* equations. These are reported below for a scalar field $\phi(t,\vec{x})$ but can easily be extended to vector and tensor fields.

$$S = \int dx^4 \sqrt{-g}\mathcal{L} \qquad\qquad \partial_\mu \left(\frac{\partial \mathcal{L}}{\partial(\partial_\mu \phi)} \right) - \frac{\partial \mathcal{L}}{\partial \phi} = 0 \tag{8}$$

The factor $\sqrt{-g} = \sqrt{-\det(g)}$ in Eq.8 arises as a result of the change from the locally flat system of coordinates to the generalized (curved) system. It constitutes a generalization of the action to curved spacetime manifolds.

Using Eq.8 it is now possible to analyze the dynamics of a general case. For the sake of clarity, details of these derivations are reported in Sec.A.1 A possible Lagrangian density for the scalar field $\phi(t,\vec{x})$ is given in Eq.9 [8]. The minimization of the action leads to the following equations of motion [8]:

$$\mathcal{L}_\phi = -\frac{1}{2} g^{\alpha\beta} \partial_\alpha \phi \partial_\beta \phi - V(\phi) \tag{9}$$

$$\frac{1}{\sqrt{-g}} \partial_\alpha \left(\sqrt{-g} g^{\alpha\beta} \partial_\beta \phi \right) + \partial_\phi V(\phi) = 0 \tag{10}$$

As explained in Sec.A.1, Eq.10 can be simplified by using the FLRW metric As explained in Sec.A.1. In conformal time the equation reads:

$$\ddot{\phi} + 2\mathcal{H}\dot{\phi} - \nabla^2 \phi + a^2 \partial_\phi V(\phi) = 0 \tag{11}$$

The same procedure can be applied to the Gauge field[1] $A^\mu(t,\vec{x})$. The Lagrangian density and the equations of motion associated with this particular field are given below:

$$\mathcal{L}_{A^\mu} = -\frac{1}{4}F^{\alpha\beta}F_{\alpha\beta} \qquad F_{\alpha\beta} = \partial_\alpha A_\beta - \partial_\beta A_\alpha \tag{12}$$

$$-\sqrt{-g}\,g_{\mu\beta}\partial_\alpha F^{\alpha\beta} = 0 \tag{13}$$

The detailed derivation of the equations of motion can be found in Sec.A.1.2, together with the details of its simplification when the FLRW metric and Coulomb gauge are used in Eq.13. The Coulomb gauge sets $A^0 = \vec{\nabla}\cdot\vec{A} = 0$ such that the equations of motion reduce to:

$$\partial_\tau^2\vec{A} - \nabla^2\vec{A} = 0 \tag{14}$$

2.3.2 Quantization and Creation/Annihilation Operators

So far, fields have been treated purely classically. To introduce quantum effects, the fields need to be promoted to operator-valued functions, a task that can be performed by analyzing the fields' behavior in momentum space. When spacetime is flat, this can be done by considering the fields' Fourier transform, as can be seen below for the scalar and gauge fields:

$$\phi(t,\vec{x}) = \int \frac{d^3\mathrm{k}}{(2\pi)^{3/2}}\phi_{\vec{\mathrm{k}}}(t)e^{i\vec{\mathrm{k}}\cdot\vec{x}} \qquad \vec{A}(t,\vec{x}) = \int \frac{d^3\mathrm{k}}{(2\pi)^{3/2}}\vec{A}_{\vec{\mathrm{k}}}(t)e^{i\vec{\mathrm{k}}\cdot\vec{x}} \tag{15}$$

In the limit of a flat, non-expanding universe the equations of motion of the free scalar and gauge fields simplify to the equations of motion of harmonic oscillators in momentum space:

$$\left(\partial_t^2 - \nabla^2\right)\phi(t,\vec{x}) = \left(\partial_t^2 + k^2\right)\phi_{\vec{\mathrm{k}}}(t) = 0 \qquad \left(\partial_t^2 - \nabla^2\right)\vec{A}(t,\vec{x}) = \left(\partial_t^2 + k^2\right)\vec{A}_{\vec{\mathrm{k}}}(t) = 0 \tag{16}$$

Following Eq.15-16, fields can be interpreted as an infinite collection of harmonic oscillators in momentum space. Therefore, similarly to the quantum harmonic oscillator, the Fourier modes can be quantized by introducing creation and annihilation operators which excite (create) and de-excite (annihilate) specific modes (particles). This quantization can be extended to an expanding flat space. Therefore, the scalar field is given by [6, 23]:

$$\phi(\tau,\vec{x}) = \int \frac{d^3\mathrm{k}}{(2\pi)^{3/2}}\left[b_{\vec{\mathrm{k}}}v_{\vec{\mathrm{k}}}(\tau) + b^\dagger_{-\vec{\mathrm{k}}}v^*_{-\vec{\mathrm{k}}}(\tau)\right]e^{i\vec{\mathrm{k}}\cdot\vec{x}} \tag{17}$$

$$\left[b_{\vec{\mathrm{k}}},\, b_{\vec{q}}\right] = \left[b^\dagger_{\vec{\mathrm{k}}},\, b^\dagger_{\vec{q}}\right] = 0 \qquad \left[b_{\vec{\mathrm{k}}},\, b^\dagger_{\vec{q}}\right] = \delta(\vec{\mathrm{k}} - \vec{q}) \tag{18}$$

where $v_{\vec{\mathrm{k}}}(\tau)$, $b_{\vec{\mathrm{k}}}$ and $b^\dagger_{\vec{\mathrm{k}}}$ are the amplitude of the mode, the annihilation operator, and the creation operator respectively. Similarly, the Gauge field can be promoted to an operator using the following expression [10, 24]:

$$\vec{A}(\tau,\vec{x}) = \sum_{\lambda=\pm}\int \frac{d^3\mathrm{k}}{(2\pi)^{3/2}}\left[\vec{\varepsilon}_\lambda(\vec{\mathrm{k}})a_\lambda(\vec{\mathrm{k}})A_\lambda(\tau,\vec{\mathrm{k}}) + \vec{\varepsilon}^*_\lambda(-\vec{\mathrm{k}})a^\dagger_\lambda(-\vec{\mathrm{k}})A^*_\lambda(\tau,-\vec{\mathrm{k}})\right]e^{i\vec{\mathrm{k}}\cdot\vec{x}} \tag{19}$$

$$\left[a_{\lambda_1}(\vec{\mathrm{k}}),\, a_{\lambda_2}(\vec{q})\right] = \left[a^\dagger_{\lambda_1}(\vec{\mathrm{k}}),\, a^\dagger_{\lambda_2}(\vec{q})\right] = 0 \qquad \left[a_{\lambda_1}(\vec{\mathrm{k}}),\, a^\dagger_{\lambda_2}(\vec{q})\right] = \delta_{\lambda_1\lambda_2}\delta(\vec{\mathrm{k}} - \vec{q}) \tag{20}$$

[1] While the Gauge field $A^\mu(t,\vec{x})$ is virtually equivalent to the photon field of Quantum Electrodynamics, in this research the Gauge Field is not required to have standard model features and as such it will be considered as a general field.

where $A_\lambda(\tau,\vec{k})$, $a_\lambda(\vec{k})$, and $a^\dagger_\lambda(\vec{k})$ are the amplitude of the mode, the annihilation operator, and the creation operator respectively. The field's polarisation is determined by $\vec{\varepsilon}_\lambda(\vec{k})$, which takes on multiple values depending on the wavevector ($\vec{k}$) and the direction of polarisation (λ). These vectors have the following characteristics [24]:

$$\vec{k}\cdot\vec{\varepsilon}_\lambda(\vec{k})=0 \quad \vec{k}\times\vec{\varepsilon}_\lambda(\vec{k})=-ik\lambda\vec{\varepsilon}_\lambda(\vec{k}) \quad \vec{\varepsilon}_\lambda(\vec{k})=\vec{\varepsilon}^*_\lambda(-\vec{k}) \quad \vec{\varepsilon}^*_{\lambda_1}(\vec{k})\cdot\vec{\varepsilon}_{\lambda_2}(\vec{k})=\delta_{\lambda_1\lambda_2} \tag{21}$$

2.4 Scalar Field Inflation

2.4.1 Inflation and Its Importance

While not a part of standard cosmology, inflation has quickly become accepted as a fundamental part of the universe's evolution. This is due to its ability to solve issues that plague FLRW cosmology, including the "horizon problem" [6].

The "horizon problem" corresponds to the apparent thermal equilibrium of regions of the sky that would have never been causally connected in the standard cosmological evolution. For example, CMB photons produced at diametrically opposite positions are in thermal equilibrium even though they were not in causal contact at the time of last scattering (Fig.4a). Causal connection is determined by the "particle horizon" χ, defined as the maximum distance traveled by a signal produced at time t_i. Given this definition, and noting that $c=1$, the horizon distance can be expressed as shown below [25]:

$$\chi=\int_{t_i}^{t}\frac{dt}{a(t)}=\int_{\ln a_i}^{\ln a}(aH)^{-1}\equiv\tau-\tau_i \tag{22}$$

where $R_H=(aH)^{-1}$ is the comoving Hubble radius. By substitution of Eq.7, the particle horizon can be expressed in the following way [25]:

$$\chi=H_0^{-1}\int_{\ln a_i}^{\ln a}a^{\frac{1}{2}(1+3w)}=\frac{2H_0^{-1}}{(1+3w)}\left[a^{\frac{1}{2}(1+3w)}-a_i^{\frac{1}{2}(1+3w)}\right] \tag{23}$$

To properly analyze Eq.23, it is useful to consider its limits as time approaches zero:

$$\mathrm{w}>-(1/3): \qquad \lim_{a_i\to 0}\tau_i=0 \qquad \Longrightarrow \qquad \chi\to\tau\sim R_H \tag{24}$$

$$\mathrm{w}<-(1/3): \qquad \lim_{a_i\to 0}\tau_i=-\infty \qquad \Longrightarrow \qquad \chi\to\infty \tag{25}$$

In addition, if $w<-1/3$ in Eq.7, the following features can be derived [25]:

$$\frac{d}{dt}(aH)^{-1}=-\frac{a''}{(a')^2}<0 \qquad\qquad a''>0 \tag{26}$$

These limits apply to different phases of the evolution of the universe. Throughout matter and radiation-dominated eras ($w>-1/3$), the particle horizon is dominated by late times and, while increasing, the horizon distance is finite. The same cannot be said for eras dominated by fluids with $w<-1/3$. In these particular phases, χ is dominated by early times. As a result, the particle horizon is unbounded at the beginning of the universe. It naturally follows that, if the universe began with a phase dominated by a fluid with $w<-1/3$, it would have been completely causally connected at one point in time (Fig.4b). This would allow disconnected patches of the sky to be in thermal equilibrium at later times. In addition, the cosmological expansion would have been accelerating while the Hubble radius would have been decreasing. Indeed, these are well-established features of inflation.

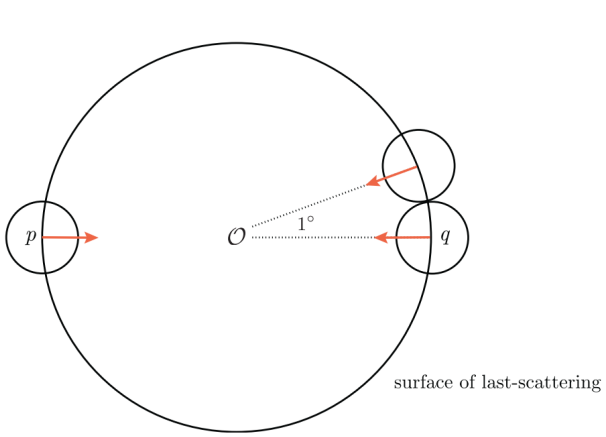

(a) *Photons streaming from the surface of last-scattering, a spherical shell with a radius equal to the distance traveled by photons since the time of decoupling. Smaller circles have a radius corresponding to the particle horizon at the time of decoupling. p and q correspond to photons in thermal equilibrium originating at two diametrically opposite points in the sky. The observer is at position O. Figure from [25].*

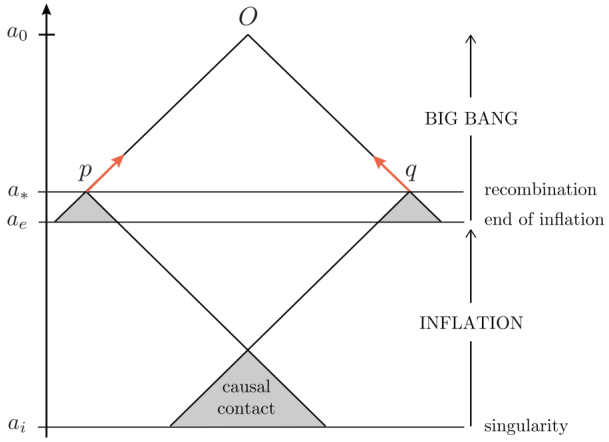

(b) *Light-cone diagram of two patches of the sky. The Hot Big Bang evolution considers the evolution of two causally disconnected patches. The addition of inflation ensures that the two patches were in causal contact before recombination. The start of the standard evolution corresponds with the end of inflation while the beginning of the universe/time singularity is before inflation. Figure from [11].*

Figure 4: *Diagrammatic representation of the horizon problem and its solution.*

2.4.2 Main Features of Slow-Roll Inflation

Inflation is an early period of accelerating growth, characterized by a decreasing Hubble radius and $w < -1/3$. These attributes can be produced by a wide range of models. One of the most common is the single-field slow-roll inflation model. This model is extensively treated in [6, 25] and here only the relevant details are reported.

For slow-roll inflation to be effective, the inflaton must satisfy a set of conditions. In particular, the slow-roll parameters ε and η, must be much smaller than one (i.e. $\varepsilon, \eta \ll 1$). Similarly, one can define potential slow-roll parameters ε_V, η_V. These parameters are defined as follows:

$$\varepsilon = -\frac{H'}{H^2} = \frac{\phi'^2}{2M_p^2 H^2} \qquad \eta = \frac{\varepsilon'}{H\varepsilon} \tag{27}$$

$$\varepsilon_V = \frac{M_p^2}{2}\left(\frac{\partial_\phi V}{V}\right)^2 \qquad |\eta_V| = M_p^2 \frac{\partial_\phi^2 V}{V} \tag{28}$$

Using Eq.28, one can deduce whether the inflaton's potential can be associated with inflationary expansion. Therefore, in this mode, only particularly flat regions of the potential meet these requirements. As inflation progresses, the inflaton slowly moves away from these regions, as if it were slowly rolling over the potential. Eventually, the potential becomes steeper and results in the end of inflation.

3 Quantum Fluctuations and Their Statistics

This section briefly outlines the concepts of power spectra, bispectra, and their connection to random fields. It discusses Gaussianity and elements of cosmological perturbation theory. With this knowledge as a basis, the reader should be adequately equipped for the calculations and analyses of Sec.4.6.

3.1 Quantum Fluctuations

In the previous section, the universe and its energy content have been treated as homogeneous and isotropic. Even though this approximation is valid on cosmological scales, fields are often characterized by local quantum fluctuations. These are (mostly) small variations of the field value at specific points in spacetime. Therefore, quantum fluctuations evolve into small inhomogeneities and anisotropies. In the following sections, the origin and inflationary evolution of quantum fluctuations in single-field inflation are discussed.

3.1.1 Vacuum Fluctuations and Sourced Fluctuations

Quantum fluctuations can be of two main types depending on their origin: i) *vacuum fluctuations* or ii) *"sourced" fluctuations*. Vacuum fluctuations are virtual particles that arise as a temporary violation of energy conservation as allowed by the *Energy-Time uncertainty principle*. The latter states that the energy can vary by an amount ΔE for a time period Δt as long as $\Delta E \Delta t > (1/2)$ [26]. One can consider this energy as being "borrowed" from the vacuum and used to excite the field temporarily, resulting in virtual particles. On the other hand, sourced fluctuations are quantum fluctuations arising from the self-interactions or interactions with other fields. While these concepts will be expanded upon in Sec.4, Fig.5 provides a visualization of the origin of sourced quantum fluctuations in the case of self and external interactions.

(a) *Tree-level Feynman diagram of a self-interaction involving three inflaton fluctuations. No external fields are involved. This interaction leads to the production of two quantum fluctuations.*

(b) *Tree-level Feynman diagram of an external interaction involving two external fields* φ *and one inflaton fluctuation. This interaction leads to the production of one quantum fluctuation.*

Figure 5: *Examples of interactions leading to sourced quantum fluctuations.*

3.1.2 Evolution of Scalar Fluctuations: The Mukhanov-Sasaki Equation

During Inflation, the universe's evolution is governed by the scalar field ϕ, which has so far been treated as maximally symmetric due to the negligible contribution of quantum fluctuations. Nonetheless, the fluctuations can affect late-time observables such as the CMB and LSS distribution (Sec. 1).

Therefore, their evolution is highly relevant to current cosmological research.

The appropriate framework to determine the fluctuation's evolution is cosmological perturbation theory [9]. In this approach, the focus is put on inflaton fluctuations. Nonetheless, this method is viable for fluctuations of additional scalar fields which might be responsible for the generation of anisotropies. In perturbation theory, the inflaton's fluctuations $\delta\phi^{(n)}$ are treated as n^{th}-order corrections to the background (homogeneous) field $\phi^{(0)}$. Similarly, the metric is expanded around the background FLRW metric $g^{(0)}_{\alpha\beta}$ to treat small deviations arising from inhomogeneities in the energy content as perturbations. The expansions are evaluated as follows [9]:

$$\phi = \phi^{(0)} + \delta\phi^{(1)} + \frac{1}{2}\delta\phi^{(2)} + \cdots \simeq \phi^{(0)} + \delta\phi^{(1)} \tag{29}$$

$$g_{\alpha\beta} = g^{(0)}_{\alpha\beta} + \delta g^{(1)}_{\alpha\beta} + \frac{1}{2}\delta g^{(2)}_{\alpha\beta} + \cdots \simeq g^{(0)}_{\alpha\beta} \tag{30}$$

In principle, perturbative expansions can be carried out to infinite order. However, higher-order corrections are often negligible and expansions can be stopped at first order. In addition, metric perturbations generally introduce sub-leading corrections, especially when acting on energy contents weakly coupled to gravity. Therefore, it is useful to fix the gauge such that metric perturbations are zero.

Within this framework, it is thus possible to derive the evolution equations for the perturbations. Considering the previously discussed assumption, the equation of motion for $\delta\phi^{(1)}$ can be obtained by direct substitution of Eq.29 into Eq.11. The resulting equation can then be further simplified by expressing it in terms of the $\tilde{\phi} = a\phi$ field and later substituting its Fourier transform. The final equation is known as the *Mukhanov-Sasaki* (MS) equation for the Fourier modes $u_k(\tau)$ (Eq.31). Note that for light slow-roll fields $\varepsilon \ll 1$ and $\eta_\phi = (m_\phi^2/3H^2) \ll 1$.

$$\ddot{u}_k(\tau) + \left(k^2 - \frac{1}{\tau^2}\left(\nu_\phi^2 - \frac{1}{4}\right)\right) u_k(\tau) = 0 \qquad \nu_\phi^2 = \left(\frac{9}{4} - \frac{m_\phi^2}{H^2}\right) \simeq \frac{3}{2} - \varepsilon + \eta_\phi \tag{31}$$

The general solution to the MS equation is given, in terms of the n$^{\text{th}}$-order Hankel functions $H^{(n)}_{(3/2)}(-k\tau)$, by Eq.32 [9]. The behavior of the Hankel functions is shown in Fig.6.

$$u_k(\tau) = \sqrt{-\tau}\left[c_1(k)H^{(1)}_{\nu_\phi}(-k\tau) + c_2(k)H^{(2)}_{\nu_\phi}(-k\tau)\right] \tag{32}$$

It is interesting to analyze Eq.32 in the subhorizon and superhorizon limits. The former is characterised by a fluctuations's wavelength λ that is much smaller than Hubble Radius $R_H = (aH)^{-1}$ ($-k\tau \gg 1$). On the other hand, in the superhorizon limit, the fluctuation's wavelength is greater than the Hubble radius ($-k\tau \ll 1$). The approximations in these limits are the following:

$$\textit{Subhorizon limit:} \qquad H^{(1)}_{\nu_\chi}(x \gg 1) \sim \sqrt{\frac{2}{\pi x}} e^{i\left(x - \frac{\pi}{2}\nu_\phi - \frac{\pi}{4}\right)} \qquad H^{(2)}_{\nu_\phi}(x \gg 1) \sim \sqrt{\frac{2}{\pi x}} e^{-i\left(x - \frac{\pi}{2}\nu_\phi - \frac{\pi}{4}\right)} \tag{33}$$

$$\textit{Superhorizon limit:} \qquad H^{(1)}_{\nu_\chi}(x \ll 1) \sim \sqrt{2/\pi} e^{-i\frac{\pi}{2}} 2^{(\nu_\phi - \frac{3}{2})} \left(\Gamma\left(\nu_\phi\right)/\Gamma(3/2)\right) x^{-\nu_\phi} \tag{34}$$

To recover the plane-wave solution of the flat, non-expanding vacuum in the subhorizon limit, it is possible to discard the Hankel function of the second kind ($c_2 = 0$) and choose an appropriate constant c_1 [6, 9]. The result and its superhorizon limit for light fields are presented in Eq.35.

$$u_k(\tau) = \frac{\sqrt{\pi}}{2} e^{i\left(\nu_\phi + \frac{1}{2}\right)\frac{\pi}{2}} \sqrt{-\tau} H^{(1)}_{\nu_\phi}(-k\tau) \qquad |u_k(\tau)| \simeq \frac{aH}{\sqrt{2k^3}} \left(\frac{k}{aH}\right)^{\frac{3}{2} - \nu_\phi} \tag{35}$$

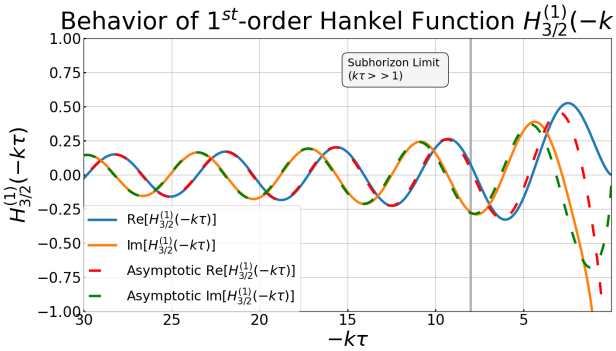

(a) *Behavior of Hankel function $H^{(1)}_{(3/2)}(-k\tau)$ as a function of $-k\tau$. The behavior is reported for both the real and imaginary parts, together with their asymptotic approximation for the sub-horizon limit ($-k\tau \gg 1$). The grey line indicates the start of the region in which the asymptotic approximation is valid.*

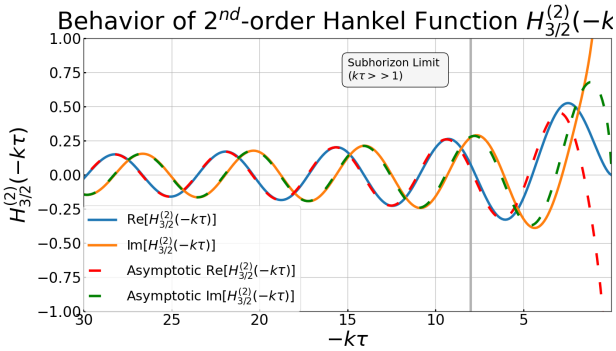

(b) *Behavior of Hankel function $H^{(2)}_{(3/2)}(-k\tau)$ as a function of $-k\tau$. The behavior is reported for both the real and imaginary parts, together with their asymptotic approximation for the sub-horizon limit ($-k\tau \gg 1$). The grey line indicates the start of the region in which the asymptotic approximation is valid.*

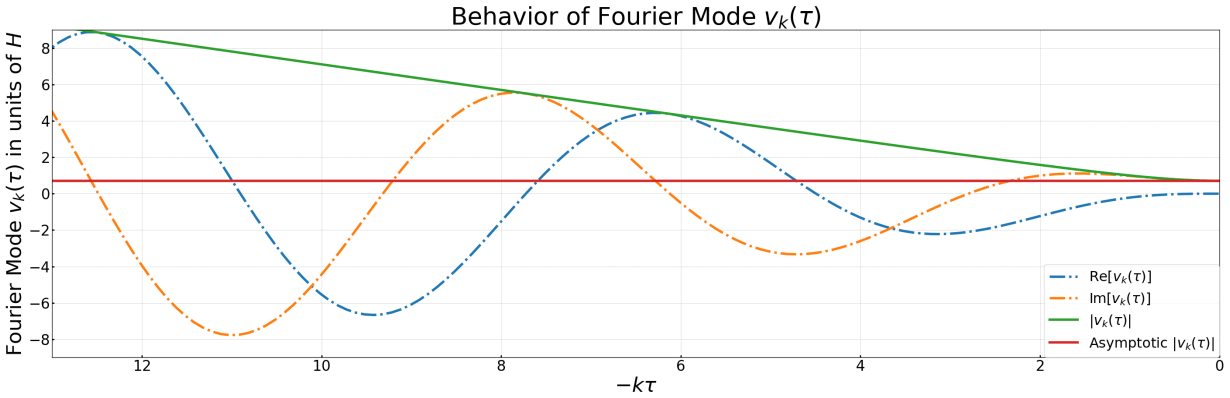

(c) *Evolution of the Fourier modes $v_k(\tau) = a^{-1}u_k(\tau)$ and their asymptotic behavior in the superhorizon limit ($-k\tau \ll 1$) given in Eq.35. The graphs are produced for $\nu = (3/2)$. The real (blue, dashed) and imaginary (orange, dashed) parts are plotted separately. The absolute value is represented as the continuous green line. The asymptotic absolute value is shown as a continuous red line.*

Figure 6: *Behavior of first and second order Hankel functions, together with the evolution of Fourier modes, as a function of $-k\tau$ for $\nu = 3/2$.*

3.1.3 The Importance of Quantum Fluctuations

As discussed in Sec.2.4, during Inflation the Hubble Radius $R = (aH)^{-1} = -\tau$ decreases and so does the size of local sky patches. If the decrease is large enough, the wavelength of quantum fluctuations can quickly enter superhorizon scales.

The growth of quantum fluctuations, as predicted by the Mukhanov-Sasaki equation, can be seen in Fig.6c. In this visualization, Field perturbations are produced at early times ($\tau \to -\infty$) with a comoving wavenumber k. During inflation ($\tau \to 0$), the amplitude of such fluctuations steadily decreases until it is frozen to a constant value in the superhorizon limit [6, 9]. Alternatively, in expanding coordinates, the wavelength rapidly grows to superhorizon scales while the amplitude decreases until it reaches a constant value at late times. The superhorizon freezing of the fluctuation amplitude can be physically interpreted by looking at the equation of motion of scalar fields. The second term of

the equation is the "Hubble Drag", which acts as a friction term and counteracts the gravitational growth of the amplitude presented in the fourth term. The Hubble drag dominates on subhorizon scales, resulting in a gradual decrease of the amplitude. However, gravitational amplification becomes increasingly relevant at larger scales. Eventually, the two effects counteract each other and, on superhorizon scales, the amplitude is frozen [9]. If the Hubble drag extended its dominance to the superhorizon limit, the large-scale fluctuation's amplitude would eventually vanish.

After inflation, the Hubble Radius starts increasing. In addition, the inflaton and its fluctuations decay into matter and radiation through a process known as *reheating*[2] [25]. As a result, quantum fluctuations that previously grew to superhorizon scales slowly re-enter the horizon as density perturbations (Fig.7) [9]. The perturbations locally alter the geometry of spacetime and gravitational potential, which ultimately affect the CMB and LSS distribution.

Finally a last remark on subhorizon and superhorizon fluctuations. So far, the discussion has been limited to the latter. Ignoring subhorizon fluctuations is a valid approximation as long as their effects on late-time observables are negligible. Thankfully, to significantly affect the gravitational evolution of the CMB and LSS distribution, perturbations must be characterized by wavelengths comparable to cosmological scales [9]. Therefore, in this treatment, only superhorizon fluctuations have been considered.

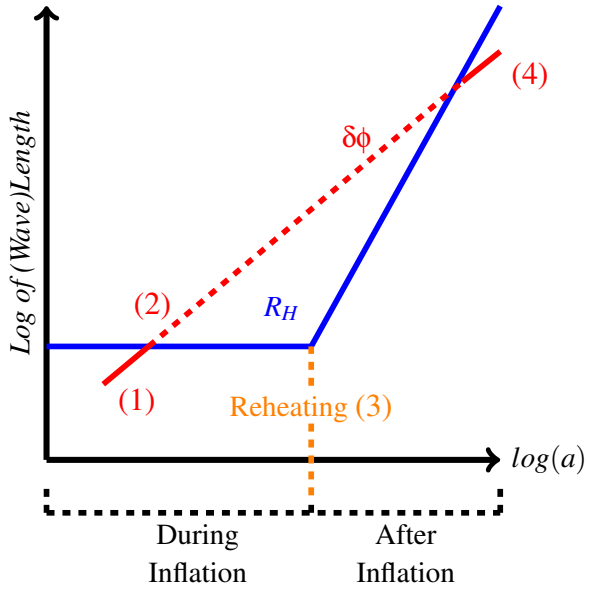

Figure 7: *Diagrammatic representation of the evolution, as a function of scale factor $a(t)$, of superhorizon quantum fluctuations (red) during and after inflation. This is compared to the physical Hubble radius $R_H = H^{-1}$ (blue). Diagram inspired by [9]. Quantum fluctuations are created as subhorizon perturbations during inflation (1). They then grow to superhorizon scales (2). During reheating, they decay into matter/radiation perturbations (3). They then rejoin the horizon after inflation (4).*

[2]While reheating is an important aspect of inflation, its discussion goes beyond the scope of this research. However, a brief discussion of the physics of reheating can be found in [25].

3.1.4 Sourced Quantum Fluctuations and The Mukhanov-Sasaki Equation

The Mukhanov-Sasaki equation is derived by excluding the effects of interactions. However, most fields interact with themselves and other fields. As explained in Sec.3.1.1, these interactions can result in additional (sourced) quantum fluctuations which manifest in the equations of motion as additional "source" terms. while this idea is explored in more detail in Sec.4, in this section a treatment of sourced quantum fluctuations is presented. To maintain this treatment as general as possible, an unspecified source term $J(\tau,\vec{x})$ is considered. It follows that the equations of motion in momentum space can be written as follows:

$$\ddot{u}_k(\tau) + \left(k^2 - \frac{1}{\tau^2}\left(\nu_\phi^2 - \frac{1}{4}\right)\right) u_k(\tau) = J_{\vec{k}}(\tau) \tag{36}$$

The solution to the above equation contains the "homogeneous" solution, which satisfies the equation when the source term vanishes (Sec.3.1.2), and a "particular" solution. In this case, the two solutions correspond to vacuum and sourced quantum fluctuations. To find the particular solution, it is useful to analyze the impulsive response of the system. Analogously to classical electrodynamics, one can model the source term as a collection of various instantaneous sources, which are mathematically described as Dirac Delta functions. The response of the system to such sources is described by Green's function $G(\tau,\tau')$, which satisfies the following equation:

$$\ddot{G}_k(\tau,\tau') + \left(k^2 - \frac{1}{\tau^2}\left(\nu_\phi^2 - \frac{1}{4}\right)\right) G_k(\tau,\tau') = \delta(\tau-\tau') \tag{37}$$

Physically, one can use the superposition principle to relate Green's function to the particular solution. This process is treated in detail in [27]. Here, a simplified version is reported. In particular, as the partial derivatives in Eq.37 depend on τ only, it is possible to multiply by $J_{\vec{k}}(\tau')$ both sides of the equation. This results in the following expression:

$$\left[\partial_\tau^2 + \left(k^2 - \frac{1}{\tau^2}\left(\nu_\phi^2 - \frac{1}{4}\right)\right)\right] G_k(\tau,\tau') J_{\vec{k}}(\tau') = \delta(\tau-\tau') J_{\vec{k}}(\tau') \tag{38}$$

Therefore, by integrating with respect to τ', the following integral solution satisfies Eq.36:

$$u_{\mathrm{k}}^{part}(\tau) = \int d\tau' G_{\mathrm{k}}(\tau,\tau') J_k(\tau') \tag{39}$$

The precise expression of the particular solution $u_k^{part}(\tau)$ depends on the form of the source term $J_k(\tau)$ and of Green's function $G_k(\tau,\tau')$. The latter can be derived using the following time-ordered expectation value [22]:

$$G(\tau,\tau') = \langle 0|T\left(\delta\tilde{\phi}(\tau,\vec{x})\delta\tilde{\phi}(\tau',\vec{x})\right)|0\rangle \tag{40}$$

The computation of the above expression is given in Sec.A.1.4. Discarding the advanced solution and maintaining only the physically relevant retarded expression, the final expression for Green's function in momentum space reads:

$$G_{\mathrm{k}}(\tau,\tau') = -i\Theta(\tau-\tau')\left[u_{\mathrm{k}}(\tau)u_{\mathrm{k}}^*(\tau') - u_{\mathrm{k}}^*(\tau)u_{\mathrm{k}}(\tau')\right] \tag{41}$$

3.2 Field Statistics

The measured statistics of late-time observables are compared to predicted values to distinguish between various inflationary scenarios. Out of the many valuable quantities, the most important statistical measures are the 2-point and 3-point correlation functions. These observables quantify the average relationship between the various fields evaluated at different points in spacetime [25, 28]. For example, a zero correlation function means that the quantities are completely independent.

The *n-point correlation* function is defined mathematically as the *ensemble average* of the product of one (or multiple) fields evaluated at n different points [9, 25, 28]. Classically, the term ensemble average refers to the average, over multiple (fictitious) universes, of all possible realizations of the aforementioned product (Fig.8) [28]. This interpretation can be expanded to quantum mechanics. Cosmological observations cause the collapse of the universe's wavefunction into one of its specific realizations. Quantum averages of these observations are thus averages over all possible realizations of the universe and are thus equivalent to ensemble averages [28]. This allows the following definition of the n-point correlation function:

$$\langle \delta\phi(\tau_1,\vec{x}_1)\delta\phi(\tau_2,\vec{x}_2)\dots\delta\phi(\tau_n,\vec{x}_n)\rangle = \langle 0|\delta\phi(\tau_1,\vec{x}_1)\delta\phi(\tau_2,\vec{x}_2)\dots\delta\phi(\tau_n,\vec{x}_n)|0\rangle \tag{42}$$

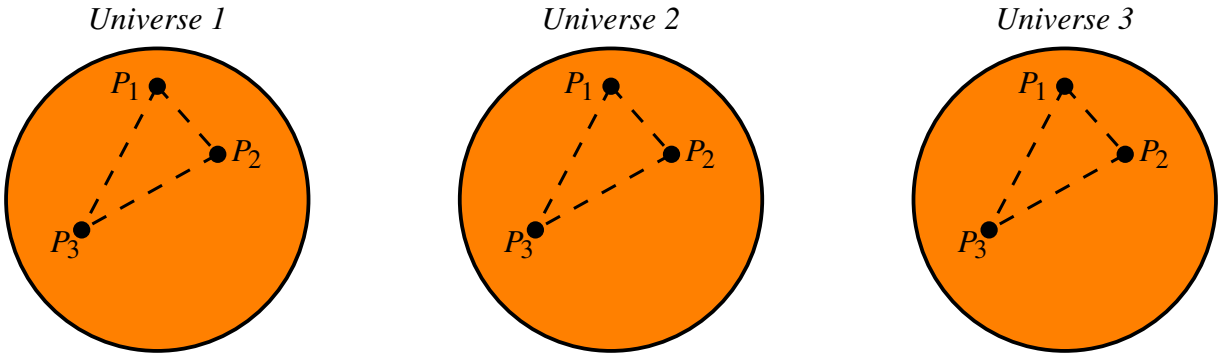

Figure 8: *Diagrammatic representation of the ensemble average. In this example, the 3-point correlation function is evaluated in three separate universes and the ensemble average is the average between the three realizations.*

3.2.1 (Non-)Gaussian Random Fields

Random fields are fields whose realizations are drawn from a probability distribution function. If the probability distribution is Gaussian the field is known as a *Gaussian random field* [28]. Gaussian random fields are entirely described by 2-point correlators [9, 28]. In fact, due to the nature of the distribution, higher-order statistics either vanish (odd n) or can be written in terms of multiple 2-point correlators (even n) [28]. This concept can be generalized to any random field $f(\tau,\vec{x})$ by expressing the n-point correlation functions as follows [23]:

$$\begin{aligned}\langle f(\tau_1,\vec{x}_1)\dots f(\tau_n,\vec{x}_n)\rangle =& \lambda\big(\langle f(\tau_1,\vec{x}_1)f(\tau_2,\vec{x}_2)\rangle\langle f(\tau_3,\vec{x}_3)f(\tau_4,\vec{x}_4)\rangle\dots + \text{combinations}\big) + \\ &+ \langle f(\tau_1,\vec{x}_1)\dots f(\tau_n,\vec{x}_n)\rangle_c\end{aligned} \tag{43}$$

In the above equation, λ vanishes for odd values of n while it is unitary for even values. The product $\langle f(\tau_1,\vec{x}_1)\dots f(\tau_n,\vec{x}_n)\rangle_c$ is the *connected* part of the correlation function which contains terms that cannot be expressed as products of 2-point correlators. If this last term is non-vanishing, the field is non-Gaussian. It is thus clear that the 3-point correlation function is the lowest-order statistical measure able to find deviations from Gaussian distributions.

3.2.2 Power Spectrum and Bispectrum

Correlation functions are often computed in momentum space. Therefore, it is common to look at the Fourier transform of the 2-point and 3-point correlators of the random field f: the power spectrum $P_f(\vec{\mathrm{k}},\vec{\mathrm{k}}')$ and bispectrum $B_f(\vec{\mathrm{k}}_1,\vec{\mathrm{k}}_2,\vec{\mathrm{k}}_3)$. From this definition it is possible to derive the more useful results of Eq.44-45 [17, 25].

$$\langle f_{\vec{\mathrm{k}}}(\tau)f_{\vec{\mathrm{k}}'}(\tau)\rangle = (2\pi)^{(3/2)}\delta(\vec{\mathrm{k}}+\vec{\mathrm{k}}')P(\mathrm{k}) = \frac{2\pi^2}{k^3}\delta(\vec{\mathrm{k}}+\vec{\mathrm{k}}')P_f(\mathrm{k}) \tag{44}$$

$$\langle f_{\vec{\mathrm{k}}_1}(\tau)f_{\vec{\mathrm{k}}_2}(\tau)f_{\vec{\mathrm{k}}_3}(\tau)\rangle = (2\pi)^3\delta(\vec{\mathrm{k}}_1+\vec{\mathrm{k}}_2+\vec{\mathrm{k}}_3)B_f(\mathrm{k}_1,\mathrm{k}_2,\mathrm{k}_3) \tag{45}$$

In the context of this research, the random fields taken into consideration are the quantum fluctuations $\delta\phi$ and the related density perturbation[3] $\zeta = -(H/\bar{\phi}')\delta\phi$, where $\bar{\phi}$ is the background value of the field. In the absence of interactions, one can use the solutions to the Mukhanov-Sasaski equation (Sec.3.1.2) to evaluate the power spectrum and bispectrum (Sec.A.2). This results in the following expressions:

$$P_\zeta(\mathrm{k}) = \Delta_P(-\mathrm{k}\tau)^{(n_s-1)} \qquad B_\zeta(\mathrm{k}_1,\mathrm{k}_2,\mathrm{k}_3) = 0 \tag{46}$$

where the spectral index is defined as $n_s = 1+3-2\nu \sim 1$ and the primordial amplitude is given by $\Delta_P^{1/2} = H^2/(2\pi|\bar{\phi}'|)$. The vanishing bispectrum, like any other odd n-point correlator, vanishes as a result of its dependency on the expectation value of an odd number of creation/annihilation operators. On the other hand, the bilinearity of even n-point correlators allows for vanishing connected parts. Therefore, vacuum fluctuations are Gaussian random fields. However, it is highly unlikely that the inflaton was in a true vacuum. As such, self-interactions or interactions with auxiliary fields might introduce additional terms that are relevant to the calculation of correlation functions. If these terms are bilinear, the associated bispectrum might not vanish and the associated field is not Gaussian. The extent of this non-Gaussianity is analyzed in Sec.4.

3.2.3 Characteristics of The Bispectrum

As three-point correlation functions are evaluated at three different points in spacetime, the momenta associated with said points must form a triangle in the sky. This *triangle condition* is enforced by the delta-function of Eq.45.

Even though bispectra have common domains, they vary in magnitude and differ based on their dependency on the shape and size of the momentum triangle. These three characteristics are known as the *size*, *shape*, and *running* of the bispectrum [24]. To analyze these three characteristics, it is useful to reparametrize the momenta as in Eq.47. After setting $x_1 = 1$, it is possible to define the *shape function* $S(\mathrm{k},x_2,x_3)$ which is shown below in Eq.48:

[3] The definition of the density perturbation ζ requires challenging expansions of the action and the metric. These computations go beyond the scope of this research but are treated in the following papers [24, 29, 30]

$$\mathrm{k}_1 = x_1\mathrm{k} \qquad \mathrm{k}_2 = x_2\mathrm{k} \qquad \mathrm{k}_3 = x_3\mathrm{k} \tag{47}$$

$$S(\mathrm{k}, x_2, x_3) = \frac{1}{N}\mathrm{k}^6 (x_2 x_3)^2 B(\mathrm{k}, x_2, x_3) \tag{48}$$

In Eq.48 The factor N is an arbitrary normalization constant. Some examples of the possible bispectrum shape functions are presented in the next sections.

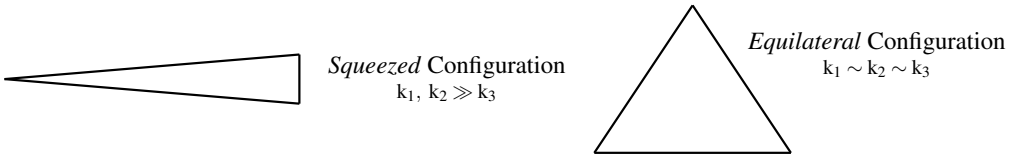

Figure 9: *Two examples of possible configurations of the momentum triangle. The equilateral configuration is characterised by momenta of similar lengths* ($\mathrm{k}_1 \sim \mathrm{k}_2 \sim \mathrm{k}_3$)*. On the other hand, the squeezed configuration arises when two sides are much larger than the third* ($\mathrm{k}_1,\ \mathrm{k}_2 \gg \mathrm{k}_3$)*. For further examples see [17, 18].*

3.2.4 The Local and Equilateral Bispectrum

Depending on the physical nature of the model and the origin of the non-Gaussianity, the bispectra can be broadly classified into two main categories: *local*, which peaks for the squeezed configuration, and *equilateral*, which peaks for the equilateral configuration.

The local bispectrum is typical of models in which the non-Gaussianity arises on superhorizon scales [31, 32]. This relates to the discussion presented in Sec.3.1.3. Superhorizon fluctuations are generally the most relevant for late-time observables' anisotropies and inhomogeneities and are thus expected to greatly contribute to their non-Gaussianity. However, because of the triangle condition, not all wavelengths can grow deep into the superhorizon regime. Therefore, the local bispectrum peaks for configurations in which one wavelength is much larger than the other two. As such, wavevectors are expected to produce the most non-Guassianity in the "squeezed triangle" configuration (Fig.9) [31]. In this case, the superhorizon fluctuation acts as a background for the subhorizon fluctuations, which are much smaller in size. Therefore, the non-Gaussianity is generated by the two smaller perturbations over the superhorizon background. As such, the bispectrum can be decomposed into products of the subhorizon power spectra.

Indeed, this is a feature of the most common model for the production of local bispectra. In this model, the density perturbation $\zeta(\tau,\vec{x})$ is divided into two terms: a dominating Gaussian term $\zeta_L(\tau,\vec{x})$ and a sub-leading non-Gaussian term $\zeta_{NL}(\tau,\vec{x})$, which can be expanded in terms of the first term. This expansion, together with its equivalent in momentum space, is as follows [17, 28]:

$$\zeta(\tau,\vec{x}) = \zeta_L(\tau,\vec{x}) + \zeta_{NL}(\tau,\vec{x}) = \zeta_L(\tau,\vec{x}) + \frac{3}{5} f_{NL}^{loc} \left(\zeta_L^2(\tau,\vec{x}) - \langle \zeta_L^2(\tau,\vec{x})\rangle\right) \tag{49}$$

$$\zeta(\tau,\vec{\mathrm{k}}) = \zeta_L(\tau,\vec{\mathrm{k}}) + \frac{3}{5} f_{NL}^{loc} \left(\int \frac{d^3p}{(2\pi)^{3/2}} \zeta_L(\tau,\vec{\mathrm{k}})\zeta_L(\tau,\vec{\mathrm{k}} - \vec{\Delta_P}) - (2\pi)^{3/2}\delta(\vec{\mathrm{k}})\langle \zeta_L^2(\tau,\vec{x})\rangle \right) \tag{50}$$

where $f_{\rm NL}^{loc}$ is the *non-linearity parameter* which quantifies the amount of non-Gaussianity. Substitution of the above equation in Eq.45 gives the bispectrum and normalized shape function of Eq.52 [17, 28]. The shape is plotted in Fig.10a and in Fig.10d.

$$B_\zeta^{loc} = 2 f_{\rm NL}^{loc} \left[P_\zeta(\mathrm{k}_1) P_\zeta(\mathrm{k}_2) + \text{ cycl. perms.} \right] = \frac{3}{10} (2\pi)^{(5/2)} P_\zeta(k) \frac{\sum_i k_i}{\prod_i k_i} f_{\rm NL}^{loc} \tag{51}$$

$$S^{loc} = \frac{1}{3} \frac{\sum_i \mathrm{k}_i^3}{\prod_i \mathrm{k}_i} = \frac{1}{3} \frac{1 + x_2^3 + x_3^3}{x_2 x_3} \tag{52}$$

The equilateral bispectrum and its shape (Eq.53-54 [17, 33]) are typical of models in which the non-Gaussianity is produced at times of horizon crossing [17, 31, 32]. This is a result of inflationary models in which spatial derivatives of quantum fluctuations have a relevant role. As these terms become increasingly smaller as wavelengths grow, they quickly vanish outside the horizon. Therefore, the maximum non-Gaussianity is expected for configurations with similar wavelengths, such that their contributions vanish together. Because of this, the bispectrum and its shape peak for the "Equilateral Configuration" (Fig.9) as it can be seen in Fig.10b and Fig.10d. Similarly to its local counterpart, the equilateral non-linearity parameter $f_{\rm NL}^{\rm equil}$ arises by dividing the bispectrum in its equilateral configuration by the power spectrum squared [30]. This is made clearer in Sec.4.5.

$$B^{equil} \propto f_{\rm NL}^{\rm equil} \left[\left(-\frac{1}{k_1^3 k_2^3} + \text{cyc. perms.} \right) - \frac{2}{(k_1 k_2 k_3)^2} + \left(\frac{1}{k_1 k_2^2 k_3^3} + 5 \text{ perms .} \right) \right] \tag{53}$$

$$S^{equil} = \frac{(\mathrm{k}_1 + \mathrm{k}_2 - \mathrm{k}_3)(\mathrm{k}_2 + \mathrm{k}_3 - \mathrm{k}_1)(\mathrm{k}_3 + \mathrm{k}_1 - \mathrm{k}_2)}{\mathrm{k}_1 \mathrm{k}_2 \mathrm{k}_3} = \frac{(1 + x_2 - x_3)(x_2 + x_3 - 1)(x_3 + 1 - x_2)}{x_2 x_3} \tag{54}$$

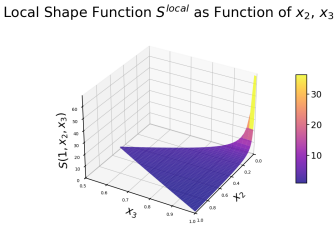

(a) *3D view of local shape function S^{loc}.*

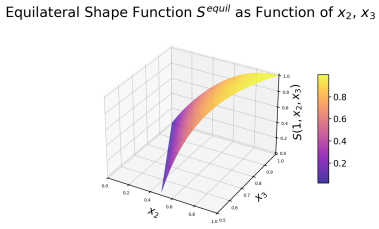

(b) *3D view of equilateral shape function S^{equil}.*

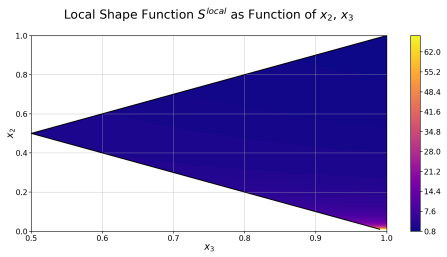

(c) *Top-down view of local shape function S^{loc}.*

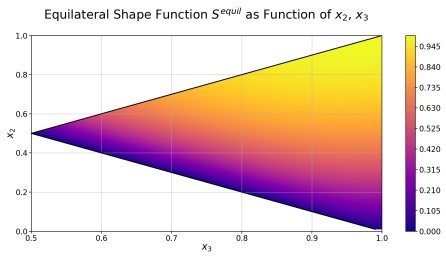

(d) *Top-down view of equilateral shape function S^{equil}.*

Figure 10: *Three-dimensional and top-down view of two shape functions S as a function of x_2, x_3 ($x_1 = 1$). The independent variables range from 0 to 1 but the shape function is plotted only for combinations that satisfy the triangle condition. To avoid comparing the same configuration twice, configurations with $x_3 \geq x_2$ are considered.*

3.2.5 Self-Interaction Bispectrum

As discussed in earlier sections, the local and equilateral shapes are a common result for the computation of many bispectra. However, many inflationary models predict deviations from these two shapes. One such case is *Maldacena's bispectrum* [29], which is computed by introducing self-interactions in single-field inflationary models.

To analyze the effects of self-interactions on the bispectrum, one has to Taylor-expand the scalar-field action up to third-order while applying the expansions in Eq.29-30. This introduces interactions between three quantum fluctuations (Fig.5a), which allow for a non-zero bispectrum. The full expansion can be found in [29] and parts of the third-order correction can be found in the following equation:

$$S_3 = \int d^4x a^3(t) \left[-\frac{\partial_t \phi^{(0)}}{4H} \delta\phi^{(1)} \left(\left(\partial_t \delta\phi^{(1)} \right)^2 - a^{-2}(t) \left(\partial_\mu \delta\phi^{(1)} \right)^2 \right) + \dots \right] \tag{55}$$

The calculation of the self-interaction bispectrum requires finding the complete equation of motion using the expansion in Eq.55. The subsequent determination of the source terms associated with the quantum fluctuations allows the use of the particular solution (Eq.39) to compute the three-point function. Even though the process appears to be simple, the computations are involved and the reader is referred to [23, 29] for the full treatment. Nonetheless, the structure of the expansion (Eq.55) provides valuable information about the bispectrum shape and size. In fact, as the third-order action contains spatial-derivative interactions and other types of interactions, the final bispectrum shape is expected to contain both local and equilateral features. Furthermore, the equilateral and local contributions are expected to decrease by a factor proportional to the slow-roll parameters. These predictions are confirmed by the complete shape function S^{Mald} [17]:

$$S^{Mald}(k_1,k_2,k_3) \simeq 2(3\varepsilon - \eta) S^{loc}(k_1,k_2,k_3) + \frac{5}{3}\varepsilon S^{equil}(k_1,k_2,k_3) \tag{56}$$

Maldacena's shape function (Eq.56) depends on the slow-roll parameters. These quantities determine the shape of the bispectrum. For instance, as $\eta \to 3\varepsilon$, Maldacena's shape becomes increasingly similar to the equilateral case. This is visualized in Fig.11 for various combinations of slow-roll parameters inconsistent with PLANCK constraints on n_s [34] but chosen for the sake of simplicity. In addition, the presence of slow-roll parameters leads to a considerable reduction of the size of the bispectrum, resulting in an effective non-linearity parameter $f_{NL} \ll 1$ [17], for all possible configurations of Eq.56. This conclusion arises directly from Maldacena's calculation [29], which can be summarised by the following formula:

$$f_{\rm NL}^{Mald} = \frac{5}{12}\left(n_{\rm s} + f(\vec{\rm k}_1, \vec{\rm k}_2, \vec{\rm k}_3) n_{\rm T} \right) \tag{57}$$

where $n_{\rm s} \sim 1$, $n_{\rm T} \simeq -2\varepsilon \ll 1$ and the function $f(\vec{\rm k}_1, \vec{\rm k}_2, \vec{\rm k}_3)$ ranges between 0 (squeezed configuration) and $5/6$ (equilateral configuration).

3.2.6 The PLANCK Constraints On $f_{\rm NL}$

As discussed in previous sections, the size of the non-Gaussianity is often analyzed through measurements of the non-linearity parameter f_{NL}. The PLANCK collaboration [33] has compared various shapes to the CMB spectrum to impose limits on the parameter. These constraints are: $f_{\rm NL}^{loc} = -0.9 \pm 5.1$, $f_{\rm NL}^{equil} = -26 \pm 47$

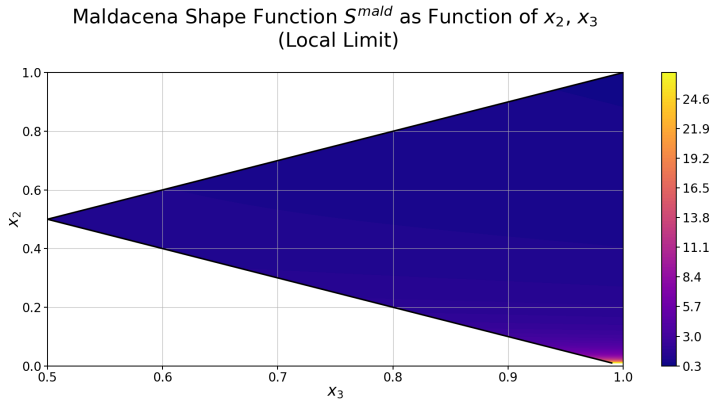

(a) *Contour plot of the Maldacena Shape function in the limit it approaches the local shape of Fig.10. In this example* $\epsilon = \eta = 0.1$. *The shape peaks at* $(x_2, x_3) = (0, 1)$.

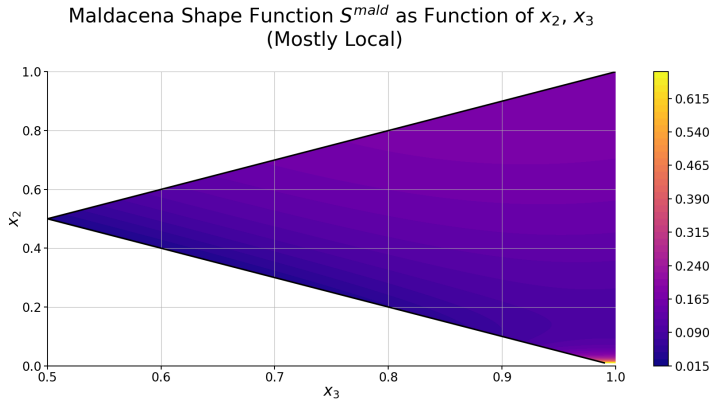

(b) *Contour plot of the Maldacena Shape for* $\epsilon = 0.1$ *and* $\eta = 0.295$. *The shape function is mostly local with a peak at* $(x_2, x_3) = (0, 1)$. *However, minor deviations typical of the equilateral shape are present. These manifest themselves as a gradual increase in value as* $(x_2, x_3) \to (1, 1)$.

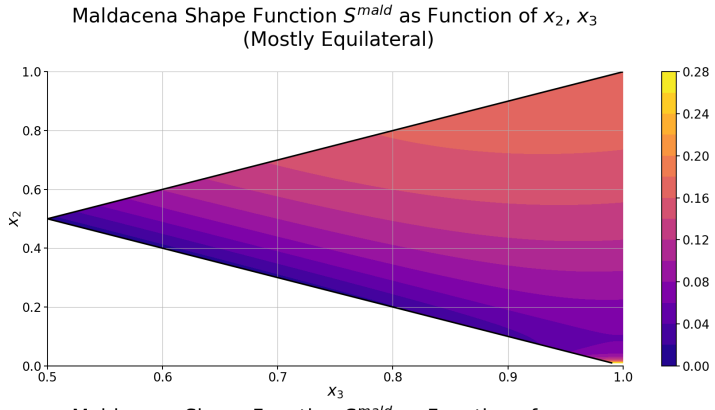

(c) *Contour plot of the Maldacena Shape for* $\epsilon = 0.1$ *and* $\eta = 0.298$. *The shape function is mostly equilateral as can be seen from the steady increase in value as* $(x_2, x_3) \to (1, 1)$. *However, similarly to the local case, the shape presents a (larger) peak at* $(x_2, x_3) = (0, 1)$.

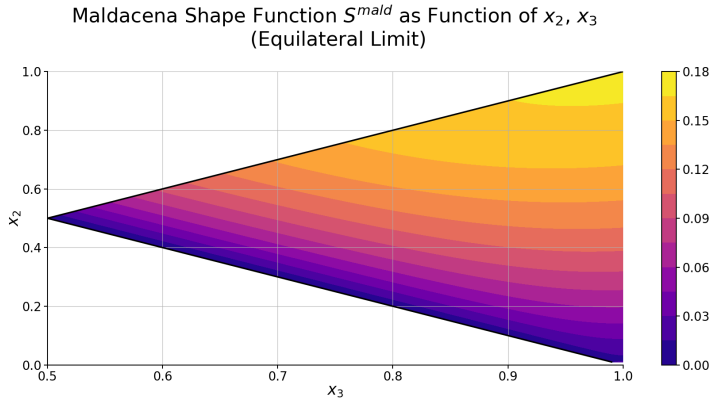

(d) *Contour plot of the Maldacena Shape function in the limit it approaches the equilateral shape of Fig.10. In this example* $\epsilon = 0.1$ $\eta = 0.2999$. *The shape peaks at* $(x_2, x_3) = (1, 1)$.

Figure 11: *Various contour plots of the Maldacena Shape as a function* x_2 *and* x_3, *for varying values of the slow-roll parameters* ϵ *and* η. *The independent variables range from* 0 *to* 1 *but the shape function is plotted only for combinations that satisfy the triangle condition. To avoid comparing the same configuration twice, configurations with* $x_3 \geq x_2$ *are considered. Note that the values of* ϵ *and* η *chosen are not consistent with the PLANCK constraints imposed on the spectral index* n_s.

4 Gauge-Interactions

Many inflationary models revolve around a single inflaton that governs the inflationary evolution of the universe. Nonetheless, there might be auxiliary fields with negligible energy contributions. Even when these fields do not affect the inflationary expansion, through interactions with the inflaton they might contribute to its quantum fluctuations.

In the following sections, the particular case of Gauge fields as auxiliary fields is considered. In particular, the model Action of Eq.58 [10] is used. This model combines the standard Lagrangians analyzed in Sec.2 to the interaction Lagrangian density $\mathcal{L}_{int}$ between the two fields. The interaction Lagrangian is given below:

$$S = \int dx^4 \left(\frac{M_p^2 R}{2} + \mathcal{L}_\phi + \mathcal{L}_{\vec{A}} + \mathcal{L}_{int} \right) \qquad \mathcal{L}_{int} = -\frac{\alpha}{4f} \frac{\eta^{\mu\nu\alpha\beta}}{\sqrt{-g}} \phi F_{\alpha\beta} F_{\mu\nu} \tag{58}$$

where $\mathcal{L}_\phi$ and $\mathcal{L}_{\vec{A}}$ correspond to the Lagrangian densities given in Eq.9 and Eq.12 respectively. In addition, $\eta^{\mu\nu\alpha\beta}$ is the Levi-Civita tensor in Minkowski space, α is the coupling constant, and f is the axion constant. The term proportional to the Ricci Scalar R quantifies the minimal coupling of the fields to gravity.

4.1 Mediator Effect of Gauge Fields

It is useful to expand $\mathcal{L}_{int}$ to first-order to analyze the interactions involving the quantum fluctuations and the gauge fields. Such an expansion can be achieved by substituting the expanded metric and scalar field (See Eq.29). This results in the following interaction Lagrangian:

$$\mathcal{L}_{int} = \ldots - \frac{\alpha}{4f} \frac{\eta^{\mu\nu\alpha\beta}}{\sqrt{-g}} \delta\phi^{(1)} F_{\alpha\beta} F_{\mu\nu} + \ldots \tag{59}$$

Eq.59 describes the cubic interaction of the gauge field with the inflaton's fluctuations (Fig.12a). For instance, the gauge particles can interact to form a "sourced" quantum fluctuation (Sec.3.1.1). Vice versa, a quantum fluctuation can decay into two gauge fields. For these reasons, this interaction is known as *inverse decay*.

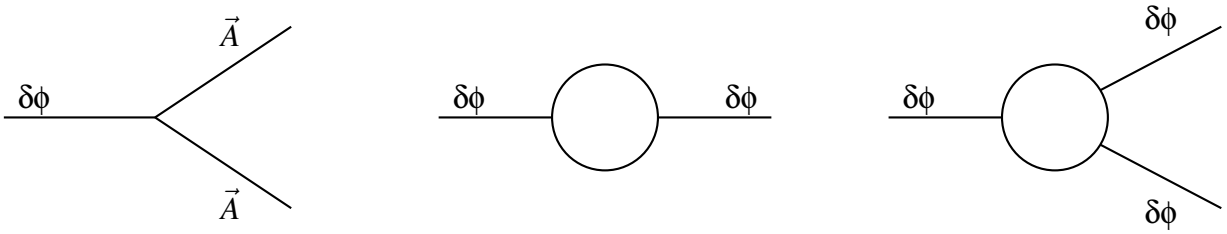

(a) *Feynman diagram of the inverse decay interaction. By inverting the diagram, the opposite interaction is possible, resulting in sourced quantum fluctuations.*

(b) *Feynman diagram of an interaction between two inflaton's fluctuations. The interaction is mediated by the gauge field $\vec{A}$ through virtual particles (loop).*

(c) *Feynman diagram of a triple interaction between inflaton's fluctuations. The interaction is mediated by the gauge field $\vec{A}$ through virtual particles (loop).*

Figure 12: *Feynman diagrams of the interactions in Eq.59.*

Due to its ability to source quantum fluctuations, the inverse decay interaction is highly relevant to the analysis of the inhomogeneities and anisotropies of late-time observables. However, on its own, it has no immediate relevance to the power spectrum or the bispectrum. As discussed in Sec. 3.2.2, these quantities are computed from the 2-point and 3-point correlation functions which require interactions between two and three quantum fluctuations respectively. These can be achieved by combining several inverse decay interactions. Examples include the interaction depicted in Fig.12b where a fluctuation decays into two gauge fields, producing a second quantum fluctuation. This concept can be extended to Fig.12c in which the interaction is between three quantum fluctuations.

It is important to note that gauge fields appear as virtual particles in Fig.12b-12c. Therefore, they mediate the interaction and provide a "one-loop" correction to the tree-level diagrams. While these corrections are negligible in the case of self-interactions between inflaton fluctuations [35], by appropriate tuning of the interaction parameters in Eq.59 it is possible to achieve large contributions by one-loop corrections arising from gauge-interactions. This idea is explored in the following sections.

4.2 The Modified Equations of Motion

The additional interaction term (Eq.59) modifies the equations of motion with respect to the case where the gauge field Lagrangian is only made up of a kinetic term. By appropriately minimizing the action, the modified equations of motion can be derived in terms of ϕ, $\vec{A}$, $\vec{E} = -a^{-2}\dot{\vec{A}}$, and $\vec{B} = a^{-2}\vec{\nabla}\times\vec{A}$. the result is [10, 24]:

$$\ddot{\vec{A}} - \nabla^2\vec{A} - \frac{\alpha}{f}\dot{\phi}\vec{\nabla}\times\vec{A} = 0 \tag{60}$$

$$\ddot{\phi} + 2\mathcal{H}\dot{\phi} - \nabla^2\phi + a^2\partial_\phi V = a^2\frac{\alpha}{f}\vec{E}\cdot\vec{B} \tag{61}$$

Eq.61 can be expanded by direct substitution of Eq.29 (See Sec.A.1.3). To complete the task, the source term's background value is separated from its local deviations. The resulting equations are:

$$\ddot{\phi}^{(0)} + 2\mathcal{H}\dot{\phi}^{(0)} + a^2\partial_\phi V(\phi) = a^2\frac{\alpha}{f}\langle\vec{E}\cdot\vec{B}\rangle \tag{62}$$

$$\left[\partial_\tau^2 + 2\mathcal{H}\partial_\tau - \nabla^2 + a^2 m_\phi^2\right]\delta\phi^{(1)} = a^2\frac{\alpha}{f}\left(\vec{E}\cdot\vec{B} - \langle\vec{E}\cdot\vec{B}\rangle\right) \tag{63}$$

Eq.62 describes how the inflaton background is affected by the presence of Gauge fields and their *backreaction* on the background inflaton field. On the other hand, Eq.63 describes how the evolution of inflaton fluctuations is affected by the inverse decay interaction involving the Gauge field's fluctuations. To properly analyze these effects, it is useful to consider the evolution of scalar and gauge field modes, which are governed by the following equations:

$$\left[\partial_\tau^2 + k^2 - \frac{1}{\tau^2}\left(\nu_\phi^2 - \frac{1}{4}\right)\right]u_k(\tau) = a(\tau)J_{\vec{k}}(\tau) \qquad J_{\vec{k}}(\tau) = a^2\frac{\alpha}{f}\int\frac{d^3x}{(2\pi)^{(3/2)}}\left(\vec{E}\cdot\vec{B} - \langle\vec{E}\cdot\vec{B}\rangle\right)e^{-i\vec{q}\cdot\vec{x}} \tag{64}$$

$$\left[\partial_\tau^2 + k^2\left(1 - \lambda\frac{2\xi}{(-k\tau)}\right)\right]A_\lambda(\tau,k) = 0 \qquad \xi = \frac{\alpha}{2fH}\phi^{\prime(0)} \simeq O(\varepsilon) \sim const \tag{65}$$

4.3 Gauge Field Modes

The inflationary evolution of Gauge field modes can be partially understood by direct inspection of Eq.65. For instance, it is possible to note that when $2|\xi| \gg -k\tau$ the modes can be described by the (limiting) equation:

$$\ddot{A}_\lambda(\tau,k) \simeq \mp\lambda(2|\xi|k/\tau)A_\lambda(\tau,k) \gg \mp\lambda A_\lambda(\tau,k) \tag{66}$$

where $\mp$ depends on the sign of ξ. Therefore, in this particular limit, the $\lambda = \pm$ mode undergoes a period of large growth while the remaining mode decays rapidly. If $\xi > 0$, this result can be achieved for $\xi \geq 2$ in the superhorizon limit ($-k\tau \ll 1$). On the other hand, in the subhorizon limit ($-k\tau \gg 1$), Eq.65 reduces to its unmodified version (Eq.16) and thus initially reproduces its vacuum behavior.

The solutions to Eq.65 are examined in detail in [10, 24] for the case $\xi > 0$. Ignoring the decaying mode A_-, the general solution for the A_+ includes irregular Coulomb functions. As expected from the inspection of Eq.65, the solution has the largest magnitude for values of $-k\tau \ll 2\xi$ (Fig.13). More specifically, the solution rapidly decays outside of the interval $(8\xi)^{-1} < -k\tau < 2\xi$. Within this range, the growing mode $A_+(\tau,k)$ and its conformal time derivative can be approximated by the following expressions:

$$A_+(\tau,k) \simeq \frac{1}{\sqrt{2k}}\left(\frac{-k\tau}{2\xi}\right)^{1/4} e^{\pi\xi-2\sqrt{-k\tau(2\xi)}} \tag{67}$$

$$\dot{A}_+(\tau,k) \simeq \sqrt{-\frac{2k\xi}{\tau}}A_+(\tau,k) \tag{68}$$

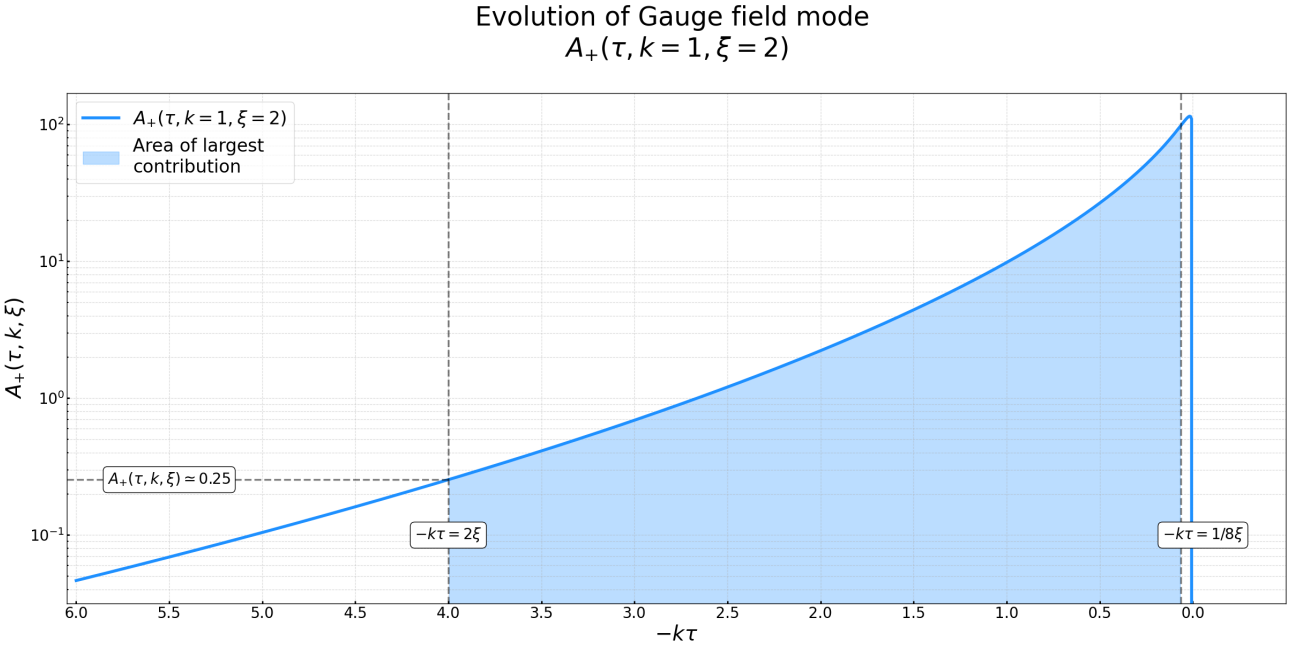

Figure 13: *Graph of the Gauge field mode A_+ (Eq.67) for $k = 1$ and $\xi = 2$, against $-k\tau$. The largest values of $-k\tau$ correspond to the earliest times during inflation. The mode is plotted in blue and the region of largest contribution to observables is shaded. The mode rapidly decays outside the interval $(8\xi)^{-1} < -k\tau < 2\xi$.*

4.4 The Power Spectrum

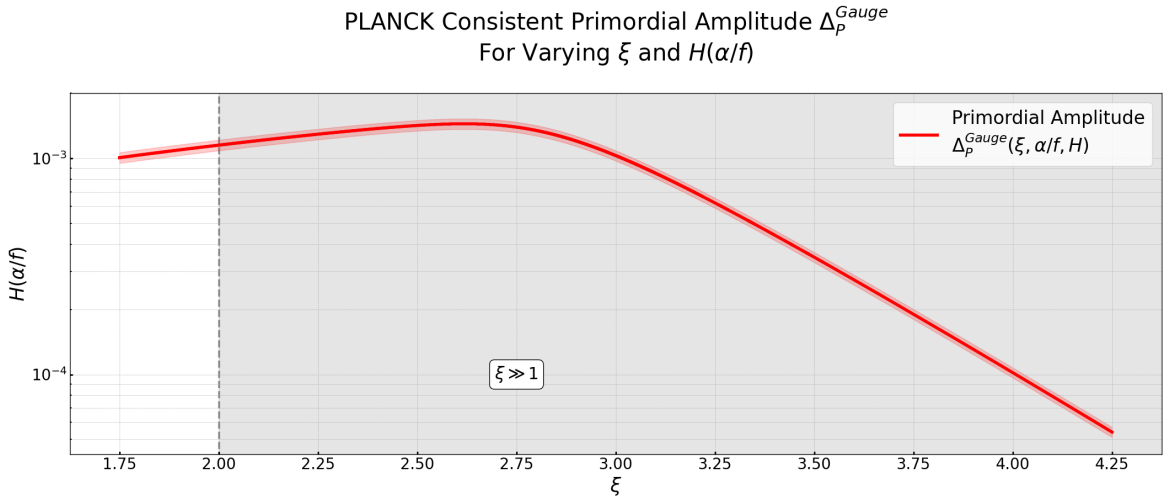

Figure 14: *Plots of the primordial amplitude Δ_P^{Gauge} (Eq.69) for various configurations of the parameters ξ and (α/f). The plot is restricted to regions of parameter space that produce values consistent with PLANCK measurements [36]. Solid lines correspond to configurations that approximately match $\Delta_P^{Gauge} \sim 2.101 \cdot 10^{-9}$ while shaded regions correspond to amplitude values within the measured interval. The width of these regions is increased by 10% for better readability. The gray-shaded area corresponds to values satisfying $\xi >> 1$.*

After finding the particular solution to the modified equations of motion one can derive the two and three-point correlators. In this section, only the results of these calculations are reported and analyzed while the computations are reported in detail in Sec.A.3. In the presence of Gauge interactions, the power spectrum is modified according to the following equation:

$$P_\zeta(k) = \Delta_P \left[1 + \Delta_P e^{4\pi\xi} f_2(\xi)\right] (-k\tau)^{n_s - 1} = \Delta_P^{Gauge} (-k\tau)^{n_s - 1} \tag{69}$$

$$\Delta_P = \frac{H^2}{2\pi|\phi'^{(0)}|} = \frac{H}{4\pi\xi}\frac{\alpha}{f} \tag{70}$$

where the functions $f_2(\xi)$ is a convoluted combination of integrals that need to be numerically integrated. Fits for this function have been performed by [24] and are reported in Tab.2. In addition, it can be noted that Eq.69 can be written in power-law form (Eq.44) after the redefinition of the primordial amplitude $\Delta_P \to \Delta_P^{Gauge}$. The value of Δ_P^{Gauge} depends on combinations of the ξ and $H(\alpha/f)$[4] parameters. However, not all combinations are allowed. The PLANCK constraint $\Delta_P^{Gauge} = 2.101^{+0.031}_{-0.034} \cdot 10^{-9}$ [36] ($0.005\text{Mpc}^{-1} \leq k \leq 0.2\text{Mpc}^{-1}$, $-1/\tau = 0.05\text{Mpc}^{-1}$) reduces the allowed configurations to a thin region of parameter space (Fig.14). Therefore, only this region is taken into consideration for further discussions.

[4]The three parameters H, α and f are considered as a single parameter to allow for a simpler analysis of the parameter space. In addition, all three parameters lack distinct limits (except for the upper limit in some cases) while the ξ parameter has the important condition $\xi \gg 1$. It is thus natural to combine them and analyze ξ as a separate parameter.

Function	ξ Range	Fit ($\times 10^5$)
$f_2(\xi)$	$\xi \gg 1$	$7.5 \cdot \xi^{-6}$
	$2 \leq \xi \leq 3$	$3 \cdot \xi^{-5.4}$

Table 2: *Fits of $f_2(\xi)$ for two relevant ranges of ξ. To avoid clutter, the fit functions are multiplied by a factor of 10^5. The fits have been performed by [24].*

4.5 The Bispectrum

Similarly to the power spectrum, the bispectrum is modified by the presence of sourced quantum fluctuations. The details of how Gauge interactions affect the bispectrum can be found in Sec.A.3. The calculations lead to the following expression:

$$B_\zeta(k,x_2,x_3) = \frac{3}{10}(2\pi)^{(5/2)}\Delta_P^3 \frac{e^{6\pi\xi}}{k^6} \frac{1+x_2^3+x_3^3}{x_2^3 x_3^3} f_3(\xi,x_2,x_3) \tag{71}$$

where $f_3(\xi,1,1)$, just like $f_2(\xi)$, is a convoluted ensemble of integrals that need to be numerically evaluated for appropriate results. The complexity of these integrals is further increased by the dependence of f_3 on the triangle configuration through the parameters x_2 and x_3.

Function	ξ Range	Fit ($\times 10^7$)
$f_3(\xi,1,1)$	$\xi \gg 1$	$2.8 \cdot \xi^{-9}$
	$2 \leq \xi \leq 3$	$7.4 \cdot \xi^{-8.1}$

Table 3: *Fits of $f_3(\xi,1,1)$ for two relevant ranges of ξ. To avoid clutter, the fit functions are multiplied by a factor of 10^7. The fits have been performed by [24].*

Because of the above-mentioned reasons, performing a numerical analysis of the shape and size of the bispectrum (Eq.71) is difficult. Nonetheless, the task is greatly simplified by an analysis of the mechanism at play. As discussed in Sec.4.3, Gauge field modes quickly decay outside the interval $(8\xi)^{-1} < -k\tau < 2\xi$. On the other hand, within this range, they can be approximated by Eq.67, and thus contribute non-trivially to interactions. Therefore, modes appearing in the calculation for the power spectrum and bispectrum must all satisfy the constraint $-k\tau \in ((8\xi)^{-1}, 2\xi)$ at the same time. Physically, this means that Gauge modes are produced with similar wavelengths and thus leave the horizon at similar times. However, as the modes exit the allowed interval, they rapidly decay. As this behavior is typical of equilateral bispectra, the bispectrum of Eq.71 is expected to be (mostly) of such a type. Indeed, this hypothesis was confirmed by [24], as the overlap between the two bispectrum shapes was determined to be 0.94 (low ξ) and 0.93 (high ξ).

Having established the shape of the bispectrum as equilateral, the size of the non-Gaussianity can be determined through $f_{\rm NL}^{\rm equil}$. This parameter can be defined by dividing the equilateral bispectrum ($x_2 = x_3 = 1$) by the square of the power spectrum [30]. Therefore, the parameter can be defined as in Eq.72. Its behavior in the relevant regions of parameter space is shown in Fig.15.

$$f_{\rm NL}^{\rm equil} = \frac{f_3(\xi,1,1)\Delta_P^3 e^{6\pi\xi}}{P_\zeta^2(k)} \tag{72}$$

4.6 The Value Of $f_{\rm NL}^{\rm equil}$ and A Comparison With Maldacena's Bispectrum

As discussed in Sec.4.4, applying the power spectrum PLANCK constraint [36] to the Gauge interaction correlators results in a shrinking of the allowed region of parameter space. This region shrinks further once the PLANCK $f_{\rm NL}^{\rm equil}$ constraints [33] are imposed. This is shown, for two different values of $-k\tau$, in Fig.15. From this figure, one can infer that, for most parameter configurations, the non-Gaussianity is many times higher than the maximum allowed value of 21. This results from the exponential factor in Eq.72.

It is useful to compare the behavior of $f_{\rm NL}^{\rm equil}$ for various values of $-k\tau$ to understand the impact of the non-unitary spectral index $n_{\rm s} = 0.9649 \pm 0.0042$ measured by the PLANCK Collaboration[36]. To emphasize these effects, Eq.72 has been plotted in Fig.15 using the lowest allowed value of $n_{\rm s}$ and two values of $-k\tau$. These values are within the range used for the measurement of the primordial amplitude [36], and include the smallest allowed value ($-k\tau \simeq 0.1$). While Fig.15b and Fig.15c do not present visible differences compared to the scale-invariant case (Fig.15a), it is possible to notice that the change in spectral index and value of $-k\tau$ affect the maximum allowed parameters ξ and $H(\alpha/f)$. More precisely, the lower spectral index increases both parameters, which increase further as $-k\tau$ decreases. Even though this is not shown in Fig.15, these effects become stronger the lower $n_{\rm s}$ gets, as the effects of $-k\tau \ll 1$ become more important.

Considering the least restrictive option given by the combination proposed in Fig.15c, one can impose upper limits on parameter values. In this particular case, both Planck constraints are met for $\xi \leq 2.5$ and $H(\alpha/f) \leq 1.44 \cdot 10^{-3}$. In this allowed section of parameter space, the residual between the two primordial amplitudes Δ_P^{Gauge} and Δ_P is always less than 1.98%. This value suggests a sub-leading effect of Gauge interactions and sourced quantum fluctuations on correlators and inflationary dynamics. This is consistent with the inflationary assumption of a dominating inflaton energy density and smaller, negligible contribution from other sources.

The previously treated results do not include additional sources of non-Gaussianity. For instance, the non-Gaussianity arising from the non-linear gravitational evolution of density perturbations or the one arising from reheating are ignored. These are often part of more advanced treatments. These contributions are generally highly relevant and often increase the $f_{\rm NL}$ parameter significantly. Therefore, their contribution would make it possible to restrict the allowed parameters further. Their inclusion would thus help validate or exclude the presence of Gauge interactions but, without a proper determination of the ξ and $H(\alpha/f)$ parameters, this cannot be done. For instance, a measured value $\xi = 2.6$ would allow for the exclusion of Gauge field effects while $\xi = 2.4$ would require the determination of $H(\alpha/f)$. While these parameters can in principle be measured by matching the power spectrum formula to PLANCK data, there currently are no precise limits on these two parameters. This, combined with the narrow allowed region of parameter space, suggests that Gauge interactions were probably irrelevant at the time of inflation.

It is interesting to compare the magnitude of the Gauge interaction non-Gaussianity with its self-interaction counterpart. As previously discussed, Maldacena's bispectrum predicts $f_{\rm NL} \ll 1$ for both local, equilateral, and mixed shapes. As this value is within the PLANCK constraints (Sec.3.2.6), there is no additional information that can be extracted. In addition, current limits on slow roll parameters ($\epsilon < 0.0097$, $\eta = 0.032^{+0.009}_{-0.007}$ [34]) are not precise enough to accurately determine its shape. However, the upper limit $f_{\rm NL} \ll 1$ suggests that the effects of self-interactions on the bispectrum are

many times smaller than the effects of Gauge interactions. Therefore, Maldacena's bispectrum acts as a minor correction to the Gauge interaction three-point correlator. While the shape of this correction is highly sensitive to slow-roll parameters, the total bispectrum is expected to be equilateral because of the dominance of the inverse-decay bispectrum. However, these conclusions can likely be extended to comparisons between self-interaction and any other type of external interaction. As a result, it is highly unlikely that Maldacena's bispectrum will ever be measured. For these reasons, the presence of self-interaction cannot be excluded from measurements with $f_{\mathrm{NL}} > 1$.

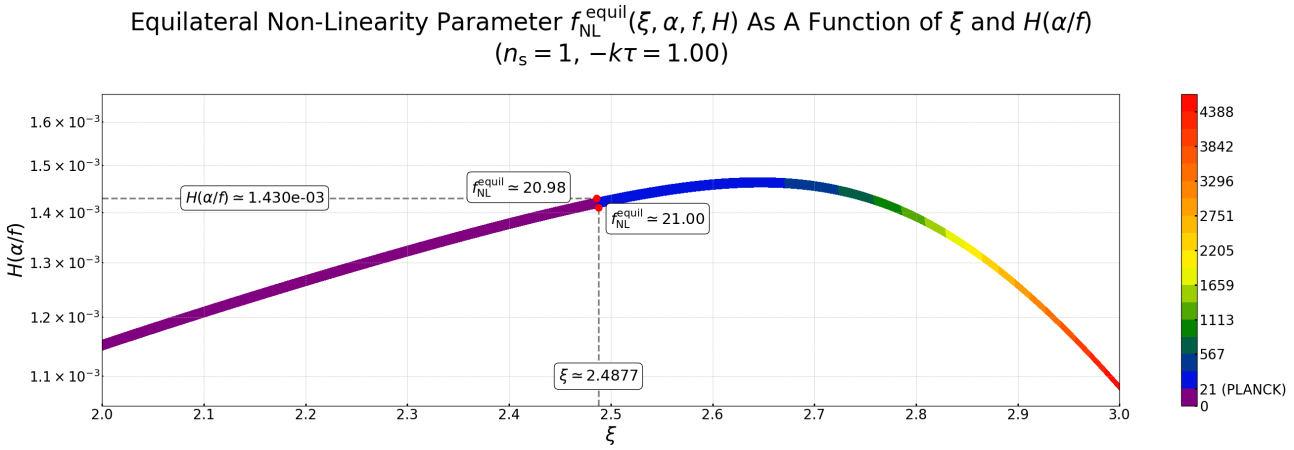

(a) *Contour plot of the scale-invariant* f_{NL}^{equil}.

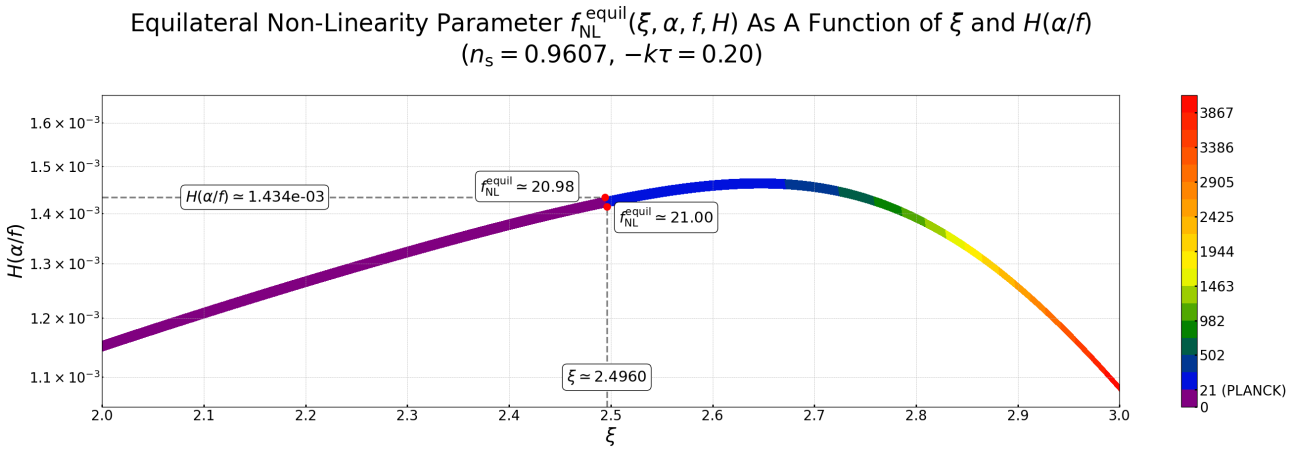

(b) *Contour plot of* f_{NL}^{equil} *for* $-k\tau = 0.2$.

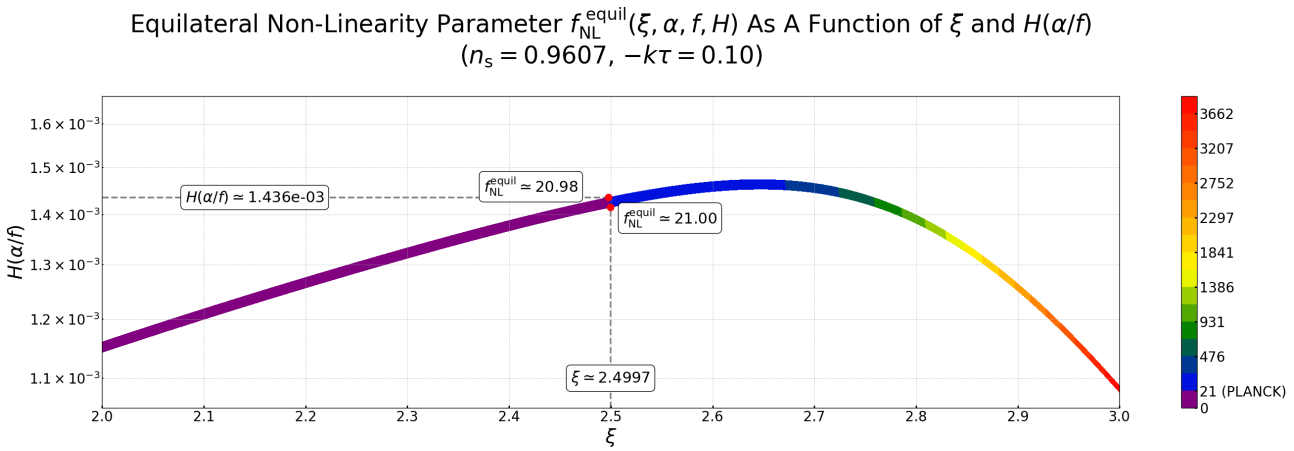

(c) *Contour plot of* f_{NL}^{equil} *for* $-k\tau = 0.1$.

Figure 15: *Contour plot of* f_{NL}^{equil} *in its parameter space for the scale invariant case (a) and for the PLANCK measured non-unitary spectral index (b, c). The contour plot is restricted to configurations for which the primordial amplitude agrees with PLANCK measurements (Fig.14). The purple region of the contour plot agrees with PLANCK* ($-73 \leq f_{NL}^{equil} \leq 21$). *The maximum allowed values of* ξ *and* $H(\alpha/f)$ *are reported. For the plots (b) and (c), the pivot scale is chosen as* $k_0 = (-1/\tau)^{-1} = 0.05\text{Mpc}^{-1}$ *and* k *is chosen to vary between* $0.005\text{Mpc}^{-1} \leq k \leq 0.01\text{Mpc}^{-1}$ *[36]. The lowest allowed value of the spectral index* $n_s = 0.9607$ *[36] has been chosen to emphasize scale effects.*

5 Conclusion

FLRW Cosmology is based on the assumption that the universe is homogeneous and isotropic. However, accurate measurements of late-time observables show various inhomogeneities and anisotropies. The statistics of these deviations, often determined through two- and three-point correlation functions, tend to be of a Gaussian nature (Sec.3.2.2). This results in (almost) vanishing bispectra.

The origin of inhomogeneities and anisotropies can be traced back to the presence of quantum fluctuations during inflation. As inflation progresses, these fluctuations evolve and ultimately affect later stages of the cosmological evolution. In the case of vacuum scalar fluctuations, the evolution is governed by the Mukhanov-Sasaki equation (Sec.3.1.2). It predicts that the wavelength of the quantum fluctuations produced during inflation suffers rapid growth. If inflation lasts for a long enough time, fluctuations can grow to superhorizon scales, where their amplitude remains constant. Eventually, at the end of inflation, they decay into matter and radiation perturbations. As the horizon grows, the perturbations re-enter the horizon and affect late-time observables. Fluctuations of this type are nearly Gaussian and have small, slow-roll suppressed three-point correlators which are non-vanishing due to the always-present self-interactions.

Self and external interactions may lead to the production of additional ("sourced") quantum fluctuations. The additional term in the Lagrangian modifies the Mukhanov-Sasaki equation, altering the evolution of scalar fluctuations (Sec.3.1.4). In addition, sourced fluctuations might allow for non-vanishing three-point correlators and thus introduce non-Gaussian features (Sec.4.1). This concept has been analyzed for the case of Gauge interactions, which have been partially compared to self-interactions. The resulting bispectrum, computed using Green's functions, peaks for the equilateral configuration. For this particular triangle, most parameter combinations predict a non-Gaussianity many times larger than the values measured by the PLANCK collaboration. Nonetheless, PLANCK constraints are met for a narrow region of parameter space in which $\xi \leq 2.50$ and $H(\alpha/f) \leq 1.44 \cdot 10^{-3}$. In this region, the primordial amplitude Δ_P^{Gauge} deviates from the Gaussian Δ_P (Eq.44) by a maximum of 1.98%, suggesting a small contribution of sourced quantum fluctuations to the inhomogeneities and anisotropies. In addition, comparisons with the self-interaction bispectrum ($f_{\mathrm{NL}} \ll 1$) suggest that this type of interaction is sub-dominant compared to the external Gauge interactions.

In conclusion, these results do not entirely exclude the presence of inflaton-gauge field interactions during inflation, as the exact values of the relevant parameters are unknown. However, the generally large non-Gaussianity, combined with the narrow region of allowed parameters and the imprecise limits on ξ and $H(\alpha/f)$, disfavor the model and majorly rule it out. Furthermore, these calculations do not include additional sources of non-Gaussianity (e.g. Gravitational evolution of density perturbations and reheating) which are included in more complex treatments. These more accurate calculations reduce the range of allowed parameters even further and, if performed, would help falsify the model. Nonetheless, the exclusion of Gauge interactions does not necessarily exclude other models that might produce non-Gaussianities within the measured constraints.

Bibliography

[1] A. H. Guth, "Inflationary universe: A possible solution to the horizon and flatness problems," *Physical Review D*, vol. 23, no. 2, pp. 347–356, Jan. 1981, ISSN: 05562821. DOI: 10.1103/PHYSREVD.23.347.

[2] A. A. Starobinsky, "Spectrum of relict gravitational radiation and the early state of the universe," *Soviet Journal of Experimental and Theoretical Physics Letters*, vol. 30, p. 682, Dec. 1979. [Online]. Available: https://ui.adsabs.harvard.edu/abs/1979JETPL..30..682S.

[3] *ESA - The history of the Universe*. [Online]. Available: https://www.esa.int/ESA_Multimedia/Images/2015/02/The_history_of_the_Universe.

[4] *What happened in the early universe? — Center for Astrophysics — Harvard & Smithsonian*. [Online]. Available: https://www.cfa.harvard.edu/big-questions/what-happened-early-universe.

[5] B. Ryden, *Introduction to cosmology*. Cambridge University Press, 2017, ISBN: 9781107154834.

[6] P. Peter and J.-P. Uzan, *Primordial cosmology*. Oxford University Press, 2009, ISBN: 9780199209910.

[7] D. Baumann, "TASI Lectures on Inflation," 2012. [Online]. Available: https://doi.org/10.48550/arXiv.0907.5424.

[8] D. Lyth, *Cosmology for Physicists*. Boca Raton, UNITED KINGDOM: Taylor & Francis Group, 2016, ISBN: 9781498755337. DOI: 10.1201/9781315368016. [Online]. Available: https://doi.org/10.1201/9781315368016.

[9] N. Bartolo, E. Komatsu, S. Matarrese, and A. Riotto, "Non-Gaussianity from Inflation: Theory and Observations," *Physics Reports*, vol. 402, no. 3-4, pp. 103–266, Jun. 2004. DOI: 10.1016/j.physrep.2004.08.022. [Online]. Available: https://www.sciencedirect.com/science/article/abs/pii/S0370157304003151.

[10] M. M. Anber and L. Sorbo, "Naturally inflating on steep potentials through electromagnetic dissipation," *Physical Review D - Particles, Fields, Gravitation and Cosmology*, vol. 81, no. 4, Aug. 2009. DOI: 10.1103/PhysRevD.81.043534. [Online]. Available: https://journals.aps.org/prd/abstract/10.1103/PhysRevD.81.043534.

[11] D. Baumann, "TASI Lectures on Primordial Cosmology," Jul. 2018. [Online]. Available: https://doi.org/10.48550/arXiv.1807.03098.

[12] *ESA - Planck CMB*. [Online]. Available: https://www.esa.int/ESA_Multimedia/Images/2013/03/Planck_CMB.

[13] Springel et Al., *Millennium Simulation Project*. [Online]. Available: https://wwwmpa.mpa-garching.mpg.de/galform/virgo/millennium/index.shtml.

[14] *COBE - Cosmic Background Explorer*. [Online]. Available: https://lambda.gsfc.nasa.gov/product/cobe/.

[15] *Wilkinson Microwave Anisotropy Probe (WMAP)*. [Online]. Available: https://map.gsfc.nasa.gov/.

[16] *ESA - Planck*. [Online]. Available: https://www.esa.int/Science_Exploration/Space_Science/Planck.

[17] M. Liguori, E. Sefusatti, J. R. Fergusson, and E. P. S. Shellard, "Primordial non-Gaussianity and Bispectrum Measurements in the Cosmic Microwave Background and Large-Scale Structure," *Advances in Astronomy*, vol. 2010, Jan. 2010. DOI: 10.1155/2010/980523. [Online]. Available: https://onlinelibrary.wiley.com/doi/10.1155/2010/980523.

[18] E. Komatsu, "Hunting for Primordial Non-Gaussianity in the Cosmic Microwave Background," *Classical and Quantum Gravity*, vol. 27, no. 12, p. 124 010, May 2010. DOI: 10.1088/0264-9381/27/12/124010. [Online]. Available: https://iopscience.iop.org/article/10.1088/0264-9381/27/12/124010.

[19] A. Salam, "Fundamental interaction," *AccessScience*, Jun. 2020. DOI: 10.1036/1097-8542.275600. [Online]. Available: https://www.accessscience.com/content/article/a275600.

[20] E. Hubble, "A RELATION BETWEEN DISTANCE AND RADIAL VELOCITY AMONG EXTRA-GALACTIC NEBULAE," *Proceedings of the National Academy of Sciences of the United States of America*, vol. 15, no. 3, p. 168, Mar. 1929, ISSN: 0027-8424. DOI: 10.1073/PNAS.15.3.168. [Online]. Available: https://www.ncbi.nlm.nih.gov/pmc/articles/PMC522427/.

[21] D. Tong, *Quantum Field Theory*. Cambridge: University of Cambridge, 2006. [Online]. Available: http://www.damtp.cam.ac.uk/user/tong/qft.html.

[22] L. H. Ryder, *Quantum field theory*. Cambridge university press, 1996, ISBN: 0521478146.

[23] N. Bartolo, S. Matarrese, and A. Riotto, "Evolution of second-order cosmological perturbations and non-Gaussianity," *Journal of Cosmology and Astroparticle Physics*, no. 1, pp. 47–70, Jan. 2004, ISSN: 14757516. DOI: 10.1088/1475-7516/2004/01/003. [Online]. Available: https://iopscience.iop.org/article/10.1088/1475-7516/2004/01/003.

[24] N. Barnaby, R. Namba, and M. Peloso, "Phenomenology of a pseudo-scalar inflaton: naturally large nongaussianity," *Journal of Cosmology and Astroparticle Physics*, vol. 2011, no. 04, p. 009, Apr. 2011, ISSN: 1475-7516. DOI: 10.1088/1475-7516/2011/04/009. [Online]. Available: https://iopscience.iop.org/article/10.1088/1475-7516/2011/04/009.

[25] D. Baumann, *Cosmology*. University of Amsterdam. [Online]. Available: http://cosmology.amsterdam/education/cosmology/.

[26] J. J. Sakurai and J. Napolitano, *Modern Quantum Mechanics*, 3rd ed. Cambridge University Press, Sep. 2020, ISBN: 9781108629447.

[27] S. Bayin, *Mathematical methods in science and engineering*, English, Second edition. Hoboken, NJ: John Wiley & Sons, 2018, ISBN: 9781119425458.

[28] E. A. Lim, *Advanced Cosmology : Primordial non-Gaussianities*. Cambridge, 2012. [Online]. Available: https://nms.kcl.ac.uk/eugene.lim/AdvCos/lecture2.pdf.

[29] J. Maldacena, "Non-gaussian features of primordial fluctuations in single field inflationary models," *Journal of High Energy Physics*, vol. 2003, no. 05, p. 013, May 2003, ISSN: 1126-6708. DOI: 10.1088/1126-6708/2003/05/013. [Online]. Available: https://iopscience.iop.org/article/10.1088/1126-6708/2003/05/013.

[30] X. Chen, M.-X. Huang, S. Kachru, and G. Shiu, "Observational signatures and non-Gaussianities of general single-field inflation," *Journal of Cosmology and Astroparticle Physics*, no. 01, Jan. 2007, ISSN: 1475-7516. DOI: 10.1088/1475-7516/2007/01/002. [Online]. Available: https://iopscience.iop.org/article/10.1088/1475-7516/2007/01/002.

[31] J. R. Fergusson and E. P. S. Shellard, "Primordial non-Gaussianity and the CMB bispectrum," *Physical Review D*, vol. 76, no. 8, Oct. 2007. DOI: 10.1103/PhysRevD.76.083523. [Online]. Available: https://journals.aps.org/prd/abstract/10.1103/PhysRevD.76.083523.

[32] D. Babich, P. Creminelli, and M. Zaldarriaga, "The shape of non-Gaussianities," *Journal of Cosmology and Astroparticle Physics*, no. 08, p. 09, 2004. DOI: 10.1088/1475-7516/2004/08/009. [Online]. Available: https://iopscience.iop.org/article/10.1088/1475-7516/2004/08/009.

[33] R. C. Butler *et al.*, "Planck 2018 results. IX. Constraints on Primordial non-Gaussianity," *A&A*, vol. 641, A9, 2020. DOI: https://doi.org/10.1051/0004-6361/201935891. [Online]. Available: https://www.aanda.org/articles/aa/full_html/2020/09/aa35891-19/aa35891-19.html.

[34] F. K. Hansen *et al.*, "Planck 2018 Results X. Constraints on Inflation," *A&A*, vol. 641, A10, 2020. DOI: 10.1051/0004-6361/201833887. [Online]. Available: https://www.aanda.org/articles/aa/full_html/2020/09/aa33887-18/aa33887-18.html.

[35] S. Weinberg, "Quantum contributions to cosmological correlations," *Physical Review D*, vol. 72, no. 4, p. 043 514, Aug. 2005, ISSN: 15507998. DOI: 10.1103/PhysRevD.72.043514. [Online]. Available: https://journals.aps.org/prd/abstract/10.1103/PhysRevD.72.043514.

[36] S. D. M. White, A. Zacchei, and A. Zonca, "Planck2018 Results. VI. Cosmological parameters," *A&A*, vol. 641, A6, 2020. DOI: https://doi.org/10.1051/0004-6361/201833910. [Online]. Available: https://www.aanda.org/articles/aa/full_html/2020/09/aa33910-18/aa33910-18.html.

Appendix

To improve clarity, many calculations and results have previously been reported without step-by-step explanations. In this section, a detailed description of such calculations is provided. In particular, Sec.A.2 discusses the power spectrum and bispectrum of vacuum fluctuations while Sec.A.3 concerns the power spectrum and bispectrum arising from sourced quantum fluctuations. In addition, one can find the source code for all the graphs and plots at the following link.

A.1 Equations of Motions

A.1.1 Scalar Field Dynamics

Eq.10 can be derived by minimizing the Lagrangian density $\mathcal{L} = \sqrt{-g}\mathcal{L}_\phi$ with respect to the variations in the scalar field $\phi(t,\vec{x})$. This can be done by explicitly evaluating the Lagrange equations (Eq. 8). The terms are computed as follows:

$$\frac{\partial \mathcal{L}}{\partial \phi} = \sqrt{-g}\frac{\partial \mathcal{L}_\phi}{\partial \phi} = -\sqrt{-g}\partial_\phi V(\phi) \tag{A.1}$$

$$\frac{\partial \mathcal{L}}{\partial\left(\partial_\mu \phi\right)} = \sqrt{-g}\frac{\partial \mathcal{L}_\phi}{\partial\left(\partial_\mu \phi\right)} = -\frac{1}{2}\sqrt{-g}g^{\alpha\beta}\left[\delta^\mu{}_\alpha \partial_\beta\phi + \partial_\alpha\phi\delta^\mu{}_\beta\right] = -\sqrt{-g}g^{\mu\alpha}\partial_\alpha\phi \tag{A.2}$$

Combining the terms according to Eq.8 and diving by $-\sqrt{-g}$ leads to the following equations of motion:

$$\frac{1}{\sqrt{-g}}\partial_\alpha\left(\sqrt{-g}g^{\alpha\beta}\partial_\beta\phi\right) - \partial_\phi V(\phi) = 0 \tag{A.3}$$

Using the FRLW metric in its conformal time definition, the first term can be expanded into:

$$\begin{aligned}
\frac{1}{\sqrt{-g}}\partial_\alpha\left(\sqrt{-g}g^{\alpha\beta}\partial_\beta\phi\right) &= (-g)^{-1/2}\partial_\mu\left[(-g)^{1/2}\left(g^{\mu 0}\left(\partial_0\phi\right)\right) + (-g)^{1/2}\left(g^{\mu j}\left(\partial_j\phi\right)\right)\right] = \\
&= (-g)^{-1/2}\Big\{\partial_0\left[(-g)^{1/2}\left(g^{00}\left(\partial_0\phi\right) + g^{0j}\left(\partial_j\phi\right)\right)\right] + \\
&\quad + \partial_i\left[(-g)^{1/2}\left(g^{i0}\left(\partial_0\phi\right) + g^{ij}\left(\partial_j\phi\right)\right]\right\} = \\
&= (-g)^{-1/2}\left\{\partial_0\left[(-g)^{1/2}g^{00}\partial_0\phi\right] + (-g)^{1/2}a^2\gamma^{ij}\partial_i\partial_j\phi\right\}
\end{aligned} \tag{A.4}$$

In flat space ($K = 0$), this reduces to:

$$\begin{aligned}
-\frac{1}{\sqrt{-g}}\partial_\alpha\left(\sqrt{-g}g^{\alpha\beta}\partial_\beta\phi\right) &= a^{-4}\left[-\partial_0\left(a^2\dot{\phi}\right) + a^2\delta^{ij}\partial_i\partial_j\phi\right] = \\
&= a^{-4}\left[-\partial_0\left(2a\dot{a}\dot{\phi} + a^2\ddot{\phi}\right) + a^2\nabla^2\phi\right] = \\
&= -a^{-2}\left[\ddot{\phi} + 2\mathcal{H}\dot{\phi} - \nabla^2\phi\right]
\end{aligned} \tag{A.5}$$

Putting everything together leads to the following equation:

$$\ddot{\phi} + 2\mathcal{H}\dot{\phi} - \nabla^2\phi + a^2\partial_\phi V(\phi) = 0 \tag{A.6}$$

A.1.2 Gauge Field Dynamics

As in Sec.A.1.2, the equations of motion of the gauge field can be derived by appropriately minimizing the Lagrangian. As there is no explicit dependence on A^μ but only on $\partial_\mu A^\nu$, it enough to compute the $\partial\mathcal{L}/\partial(\partial_\mu A^\nu)$ term. The process is reported below:

$$\begin{aligned} F^{\alpha\beta}F_{\alpha\beta} &= g^{\alpha\rho}g^{\beta\sigma}\left(F_{\rho\sigma}F_{\alpha\beta}\right) = \\ &= g^{\alpha\rho}g^{\beta\sigma}\left(\partial_\rho A_\sigma \partial_\alpha A_\beta + \partial_\sigma A_\rho \partial_\beta A_\alpha - \partial_\rho A_\sigma \partial_\beta A_\alpha - \partial_\sigma A_\rho \partial_\alpha A_\beta\right) \end{aligned} \tag{A.7}$$

The first term can be computed in the following way:

$$\begin{aligned} g^{\alpha\rho}g^{\beta\sigma}\partial_\mu \frac{\partial}{\partial(\partial_\mu A^\nu)}\left(\partial_\rho A_\sigma \partial_\alpha A_\beta\right) &= g^{\alpha\rho}g^{\beta\sigma}g_{\sigma\lambda}g_{\beta\omega}\frac{\partial}{\partial(\partial_\mu A^\nu)}\left(\partial_\rho A^\lambda \partial_\alpha A^\omega\right) = \\ &= g^{\alpha\rho}g^{\beta\sigma}g_{\sigma\lambda}g_{\beta\omega}\left(\delta^\mu_\rho \delta^\lambda_\nu \partial_\alpha A^\omega + \delta^\mu_\alpha \delta^\omega_\nu \partial_\rho A^\lambda\right) = \\ &= g^{\alpha\rho}g^{\beta\sigma}\left(g_{\sigma\lambda}\partial_\rho \partial_\alpha A_\beta + g_{\beta\nu}\partial_\rho \partial_\alpha A_\sigma\right) = \\ &= g^{\alpha\rho}g^{\beta\sigma}\left(g^{\alpha\rho}\delta^\beta_\nu \partial_\rho \partial_\alpha A_\beta + g^{\alpha\rho}\delta^\sigma_\nu \partial_\rho \partial_\alpha A_\sigma\right) \end{aligned} \tag{A.8}$$

By permutation of the indices, one can use the result of Eq.A.8 to compute the fully minimized Lagrangian density. The result is as follows:

$$\partial_\mu \frac{\partial\mathcal{L}}{\partial(\partial_\mu A^\nu)} = -g^{\alpha\beta}\partial_\alpha F_{\beta\nu} = 0 \tag{A.9}$$

The equations of motion can be simplified by choice of the FLRW metric (Eq.2) and of the Coulomb Gauge which sets $A^0 = 0$ and $\vec{\nabla}\cdot\vec{A} = \partial_i A^i = 0$. The simplifications are detailed below:

$$\begin{aligned} -\sqrt{-g}g^{\alpha\beta}\partial_\alpha F_{\beta\nu} &= -a^4\left(g^{\beta 0}\partial_0 F_{\beta\nu} + g^{\beta i}\partial_i F_{\beta\nu}\right) = \\ &= -a^4\left(g^{00}\partial_0 F_{0\nu} + g^{ji}\partial_i F_{j\nu}\right) = \\ &= -a^4\left[g^{00}\partial_0\partial_0 A_\nu + g^{ji}\left(\partial_i\partial_j A_\nu - \partial_\nu \partial_i A_j\right)\right] = \\ &= -a^2\left(-\partial_0\partial_0 A_\nu + \partial_0\partial_\nu A_0 + \partial^i\partial_i A_\nu - \partial_\nu \partial_i A^i\right) = \\ &= a^2\left(\partial^2_\tau \vec{A} - \nabla^2\vec{A}\right) = 0 \end{aligned} \tag{A.10}$$

The equations of motion can thus be expressed as:

$$\partial^2_\tau \vec{A} - \nabla^2\vec{A} = 0 \tag{A.11}$$

A.1.3 The Mukhanov-Sasaki Equation

One can solve Eq.A.5 for the field $\tilde{\phi} = a\phi$. Direct substitution leads to the following final expression (Eq.A.12):

$$\frac{1}{\sqrt{-g}}\partial_\alpha\left(\sqrt{-g}g^{\alpha\beta}\partial_\beta\phi\right) + \partial_\phi V = a^{-3}\left(\ddot{\tilde{\phi}} - \frac{\ddot{a}}{a}\tilde{\phi} - \nabla^2\tilde{\phi}\right) + \partial_\phi V \tag{A.12}$$

The Mukhanov-Sasaki equation can be derived by Taylor expanding $\tilde{\phi}(\tau,\vec{x})$ around the background value $\tilde{\phi}^{(0)}(\tau)$. The first order corrections are the quantum fluctuations $\delta\tilde{\phi}(\tau,\vec{x})$. The Taylor expansion up to first order is the following:

$$\tilde{\phi}(\tau,\vec{x}) = \tilde{\phi}^{(0)}(\tau) + \delta\tilde{\phi}(\tau,\vec{x}) \qquad \partial_\phi V = a\partial_{\tilde{\phi}}V = a\left(\partial_{\tilde{\phi}}V|_0 + \partial^2_{\tilde{\phi}}V|_0\delta\tilde{\phi}\right) \tag{A.13}$$

Substituting the Taylor expanded values in Eq.A.12 produces the Mukhanov-Sassaki equation in position space. Defining $m_\phi = \partial^2_{\tilde{\phi}}V|_0$, the equation reads:

$$\textit{Background Equation:} \qquad \ddot{\tilde{\phi}}^0 - \frac{\ddot{a}}{a}\tilde{\phi}^{(0)} + a^4\left(\partial_{\tilde{\phi}}V|_0\right) = 0 \tag{A.14}$$

$$\textit{MS Equation:} \qquad \ddot{\delta\tilde{\phi}} - \frac{\ddot{a}}{a}\delta\tilde{\phi} + a^4 m_\phi\delta\tilde{\phi} = 0 \tag{A.15}$$

By substituting the Fourier transform $\delta\tilde{\phi}_{\vec{k}}(\tau)$ of $\delta\tilde{\phi}(\tau,\vec{x})$, the Mukhanov-Sasaki equation can be expressed in momentum-space. The result is the following:

$$\ddot{u}_k(\tau) + \left(k^2 + m_\phi^2 - \frac{\ddot{a}}{a}\right)u_k(\tau) = \ddot{u}_k(\tau) + \left(k^2 - \frac{1}{\tau^2}\left(\nu_\phi^2 - \frac{1}{4}\right)\right)u_k(\tau) = 0 \tag{A.16}$$

$$\nu_\phi^2 = \left(\frac{9}{4} - \frac{m_\phi^2}{H^2}\right) \tag{A.17}$$

A.1.4 Green's Function

To compute the time-order expectation value of Eq.40, it is useful to exploit Wick's theorem together with the definition of the Feynman propagator Δ_F, which are extensively discussed in [21, 22]. Wick's theorem allows for the following expansion of Eq.40:

$$\begin{aligned} G(\tau,\tau',\vec{x},\vec{x}') &= \langle 0|T\left(\delta\tilde{\phi}(\tau,\vec{x})\delta\tilde{\phi}(\tau',\vec{x}')\right)|0\rangle = \\ &= \langle 0| : \delta\tilde{\phi}(\tau,\vec{x})\delta\tilde{\phi}(\tau',\vec{x}') : |0\rangle + \Delta_F = \\ &= \langle 0| : \delta\tilde{\phi}(\tau,\vec{x})\delta\tilde{\phi}(\tau',\vec{x}') : |0\rangle - i\Theta(\tau-\tau')\langle[\delta\tilde{\phi}(\tau,\vec{x}),\delta\tilde{\phi}(\tau',\vec{x}')]\rangle + \\ &\quad + i\Theta(\tau'-\tau)\langle[\delta\tilde{\phi}(\tau',\vec{x}'),\delta\tilde{\phi}(\tau,\vec{x}')]\rangle \end{aligned} \tag{A.18}$$

The advanced solution, in which contributions from later times are considered, is not physically relevant. In addition, the normal ordered product $\langle 0| : \delta\tilde{\phi}(\tau,\vec{x})\delta\tilde{\phi}(\tau',\vec{x}') : |0\rangle$ vanishes. Therefore, in momentum space, the (retarded) Green's function is given by:

$$
\begin{aligned}
&\int \frac{d^3x d^3x'}{(2\pi)^3} G(\tau,\tau',\vec{x},\vec{x}') e^{-i(\vec{k}\cdot\vec{x}-\vec{k}'\cdot\vec{x}')} = \\
&\quad = i\Theta(\tau-\tau') \int \frac{d^3x d^3x'}{(2\pi)^3} \langle [\delta\tilde{\phi}(\tau,\vec{x}), \delta\tilde{\phi}(\tau',\vec{x}')] \rangle e^{i(\vec{k}'-\vec{k})\cdot\vec{x} - i\vec{k}'\cdot(\vec{x}-\vec{x}')} = \\
&\quad = -i\Theta(\tau-\tau') \int \frac{d^3x d^3r}{(2\pi)^3} \langle [\delta\tilde{\phi}(\tau,\vec{x}), \delta\tilde{\phi}(\tau',\vec{x}-\vec{r})] \rangle e^{i(\vec{k}'-\vec{k})\cdot\vec{x} - i\vec{k}'\cdot\vec{r}} = \\
&\quad = -i\Theta(\tau-\tau') \int \frac{d^3x d^3r d^3q}{(2\pi)^3} \left[u_q(\tau) u_q^*(\tau') - u_q^*(\tau) u_q(\tau') \right] e^{i(\vec{k}'-\vec{k})\cdot\vec{x} - i(\vec{q}-\vec{k}')\cdot\vec{r}} = \\
&\quad = -i\Theta(\tau-\tau') \left[u_k(\tau) u_k^*(\tau') - u_k^*(\tau) u_k(\tau') \right] \delta(\vec{k}-\vec{k}') = \\
&\quad = G_{\vec{k}}(\tau,\tau') \delta(\vec{k}-\vec{k}')
\end{aligned}
\tag{A.19}
$$

As discussed in Sec.3.1.3, the most physically relevant fluctuations are the ones that grow to super-horizon scales. Therefore, it is safe to assume that τ satisfies the superhorizon limit condition

A.2 Vacuum Statistics

A.2.1 The Vacuum Power Spectrum

The two-point correlation function in momentum space can be evaluated in the following manner:

$$\begin{aligned}\langle\zeta_{\vec{k}}(\tau)\zeta_{\vec{k}'}(\tau')\rangle &= \int \frac{d^3x d^3x'}{(2\pi)^3}\langle\zeta(\tau,\vec{x})\zeta(\tau',\vec{x}')\rangle \exp\left[-i\left(\vec{k}\cdot\vec{x}+\vec{k}'\cdot\vec{x}'\right)\right] = \\ &= \int \frac{d^3x' d^3r}{(2\pi)^3}\langle\zeta(\tau,\vec{x}'+\vec{r})\zeta(\tau',\vec{x}')\rangle \exp\left[-i\left(\left(\vec{k}+\vec{k}'\right)\cdot\vec{x}'+\vec{k}\cdot\vec{r}\right)\right] = \\ &= \int \frac{d^3r}{(2\pi)^{(3/2)}}\langle\zeta(\tau,\vec{r})\zeta(\tau',0)\rangle e^{-i(\vec{k}\cdot\vec{r})}\int \frac{d^3x'}{(2\pi)^{(3/2)}}e^{-i(\vec{k}+\vec{k}')\cdot\vec{x}'} = \\ &= (2\pi)^{(3/2)}\delta(\vec{k}+\vec{k}')P(\vec{k}) = \frac{2\pi^2}{k^3}\delta(\vec{k}+\vec{k}')P_\zeta(\vec{k})\end{aligned} \tag{A.20}$$

where the variable $\vec{r} = \vec{x} - \vec{x}'$ has been introduced and the integrals have been separated by exploiting statistical isotropy. Using the expression above, it is possible to find the power spectrum associated with vacuum fluctuations. To do so one has to calculate the two-point correlation function using the solutions to the Mukhanov-Sasaki equation (Eq.35). This can be done as follows:

$$\begin{aligned}\langle\zeta_{\vec{k}}(\tau)\zeta_{\vec{k}'}(\tau)\rangle &= \left(\frac{H}{\bar{\phi}'}\right)^2\langle\prod_{j=1}^{2}\left[b_{\vec{k}_j}v_{\vec{k}_j}(\tau)+b^\dagger_{-\vec{k}_j}v^*_{-\vec{k}_j}(\tau)\right]\rangle = \\ &= \left(H/\bar{\phi}'\right)^2\langle b_{\vec{k}}b^\dagger_{-\vec{k}'}\rangle v_{\vec{k}}(\tau)v^*_{-\vec{k}'}(\tau) = \\ &= \delta(\vec{k}+\vec{k}')\left(H/\bar{\phi}'\right)^2 a^{-2}(\tau)u_{\vec{k}}(\tau)u^*_{-\vec{k}'}(\tau) = \\ &= \delta(\vec{k}+\vec{k}')(4\pi^2\Delta_P)(-\tau)^2 u_{\vec{k}}(\tau)u^*_{-\vec{k}}(\tau) = \\ &= \delta(\vec{k}+\vec{k}')(4\pi^2\Delta_P)(-\tau)^2|u_{\vec{k}}(\tau)|^2\end{aligned} \tag{A.21}$$

The equation above can be further simplified by considering only the superhorizon fluctuations, which are the only ones that are relevant for late-time observables anisotropies, and inhomogeneities. If $-k\tau, -k'\tau' \ll 1$, $H^{(1)}_{\nu_\phi}(-k\tau)$ and $H^{(1)}_{\nu_\phi}(-k'\tau')$ approach similar, fully imaginary, values (See Fig.6c. This allows the use of Eq.35 to obtain the following result:

$$\begin{aligned}\langle\zeta_{\vec{k}}(\tau)\zeta_{\vec{k}'}(\tau)\rangle &= \delta(\vec{k}+\vec{k}')(4\pi^2\Delta_P)(-\tau)^2|u_{\vec{k}}(\tau)|^2 = \\ &\simeq \frac{2\pi^2}{k^3}\Delta_P(-k\tau)^{(3-2\nu_\phi)}\delta(\vec{k}+\vec{k}')\end{aligned} \tag{A.22}$$

Combining this expression with Eq.44 leads to the following final expression for the scale-invariant power spectrum $P_\zeta(k)$:

$$P_\zeta(k) = \Delta_P(-k\tau)^{(3-2\nu_\phi)} = \Delta_P(-k\tau)^{(n_s-1)} \tag{A.23}$$

A.2.2 The Vacuum Bispectrum and Higher-Order Correlators

Similarly to the power spectrum, the vacuum bispectrum is computed using the solutions to the Mukhanov-Sasaki equation (Eq.35), which are employed in the calculation of the three-point correlator in momentum space. Ignoring expectation values that vanish because of the properties of the creation/annihilation operators, the three-point correlation function is computed as follows:

$$\begin{aligned}\langle\zeta_{\vec{k}_1}(\tau_1)\zeta_{\vec{k}_2}(\tau_2)\zeta_{\vec{k}_3}(\tau_3)\rangle &= -\left(\frac{H}{\bar{\phi}'}\right)^3\langle\delta\phi(\tau_1,\vec{k}_1)\delta\phi(\tau_2,\vec{k}_2)\delta\phi(\tau_3,\vec{k}_3)\rangle = \\ &= -\left(\frac{H}{\bar{\phi}'}\right)^3\langle\prod_{j=1}^{3}\left[b_{\vec{k}_j}v_{\vec{k}_j}(\tau_j)+b^{\dagger}_{-\vec{k}_j}v^{*}_{-\vec{k}_j}(\tau_j)\right]\rangle = \\ &= -\left(\frac{H}{\bar{\phi}'}\right)^3\left[\langle b_{\vec{k}_1}b_{\vec{k}_2}b^{\dagger}_{-\vec{k}_3}\rangle v_{\vec{k}_1}v_{\vec{k}_2}v^{*}_{-\vec{k}_3}+\langle b_{\vec{k}_1}b^{\dagger}_{-\vec{k}_2}b^{\dagger}_{-\vec{k}_3}\rangle v_{\vec{k}_1}v^{*}_{-\vec{k}_2}v^{*}_{-\vec{k}_3}\right]\end{aligned}$$

To find the full expression for the three-point correlators one has to evaluate the expectation values. However, because of the action of creation and annihilation operators on vacuum states, the expectation values of strings of an odd number of operators vanish. This can be seen in the following calculation:

$$\langle b_{\vec{k}_1}b_{\vec{k}_2}b^{\dagger}_{-\vec{k}_3}\rangle = \langle b_{\vec{k}_1}b^{\dagger}_{-\vec{k}_3}b_{\vec{k}_2}\rangle + [b_{\vec{k}_2},b^{\dagger}_{-\vec{k}_3}]\langle b_{\vec{k}_1}\rangle = 0 \tag{A.24}$$

$$\langle b_{\vec{k}_1}b^{\dagger}_{-\vec{k}_2}b^{\dagger}_{-\vec{k}_3}\rangle = \langle b^{\dagger}_{-\vec{k}_2}b_{\vec{k}_1}b^{\dagger}_{-\vec{k}_3}\rangle + [b_{\vec{k}_1},b^{\dagger}_{-\vec{k}_2}]\langle b^{\dagger}_{-\vec{k}_3}\rangle = 0 \tag{A.25}$$

Using the above results, it becomes clear that the three-point correlator is zero and that the vacuum bispectrum vanishes. However, this does not entirely exclude traces of non-Gaussianity. Higher-order statistics may be characterized by a non-vanishing connected component. To check the presence of such a term, it is useful to consider the four-point correlation function. By following a similar procedure to the one employed to compute the three-point correlation function, it is clear that the four-point correlator will depend on the following expectation values:

$$\langle b_{\vec{k}_1}b_{\vec{k}_2}b_{\vec{k}_3}b^{\dagger}_{-\vec{k}_4}\rangle = [b_{\vec{k}_3},b^{\dagger}_{-\vec{k}_4}]\langle b_{\vec{k}_1}b_{\vec{k}_2}\rangle + \langle b_{\vec{k}_1}b_{\vec{k}_2}b^{\dagger}_{-\vec{k}_4}b_{\vec{k}_3}\rangle = 0 \tag{A.26}$$

$$\begin{aligned}\langle b_{\vec{k}_1}b_{\vec{k}_2}b^{\dagger}_{-\vec{k}_3}b^{\dagger}_{-\vec{k}_4}\rangle &= [b_{\vec{k}_2}b^{\dagger}_{-\vec{k}_3}]\langle b_{\vec{k}_1}b^{\dagger}_{-\vec{k}_4}\rangle + \langle b_{\vec{k}_1}b^{\dagger}_{-\vec{k}_3}b_{\vec{k}_2}b^{\dagger}_{-\vec{k}_4}\rangle = \\ &= [b_{\vec{k}_2}b^{\dagger}_{-\vec{k}_3}]\langle b_{\vec{k}_1}b^{\dagger}_{-\vec{k}_4}\rangle + [b_{\vec{k}_1}b^{\dagger}_{-\vec{k}_3}]\langle b_{\vec{k}_2}b^{\dagger}_{-\vec{k}_4}\rangle = \\ &= \langle b_{\vec{k}_2}b^{\dagger}_{-\vec{k}_3}\rangle\langle b_{\vec{k}_1}b^{\dagger}_{-\vec{k}_4}\rangle + \langle b_{\vec{k}_1}b^{\dagger}_{-\vec{k}_3}\rangle\langle b_{\vec{k}_2}b^{\dagger}_{-\vec{k}_4}\rangle\end{aligned} \tag{A.27}$$

$$\begin{aligned}\langle b_{\vec{k}_1}b^{\dagger}_{-\vec{k}_2}b_{\vec{k}_3}b^{\dagger}_{-\vec{k}_4}\rangle &= \langle b_{\vec{k}_1}b^{\dagger}_{-\vec{k}_2}\rangle[b_{\vec{k}_3},b^{\dagger}_{-\vec{k}_4}] + \langle b_{\vec{k}_1}b^{\dagger}_{-\vec{k}_2}b^{\dagger}_{-\vec{k}_4}b_{\vec{k}_3}\rangle \\ &= \langle b_{\vec{k}_1}b^{\dagger}_{-\vec{k}_2}\rangle\langle b_{\vec{k}_3},b^{\dagger}_{-\vec{k}_4}\rangle\end{aligned} \tag{A.28}$$

$$\langle b_{\vec{k}_1}b^{\dagger}_{-\vec{k}_2}b^{\dagger}_{-\vec{k}_3}b^{\dagger}_{-\vec{k}_4}\rangle = [b_{\vec{k}_1},b^{\dagger}_{-\vec{k}_2}]\langle b^{\dagger}_{-\vec{k}_3}b^{\dagger}_{-\vec{k}_4}\rangle + \langle b^{\dagger}_{-\vec{k}_2}b_{\vec{k}_1}b^{\dagger}_{-\vec{k}_3}b^{\dagger}_{-\vec{k}_4}\rangle = 0 \tag{A.29}$$

These expressions show that the four-point correlation function can be entirely written using two-point correlators. This procedure yields similar results for all even n-point correlation functions. These results, combined with the previous discussion on odd n correlators, demonstrate that vacuum quantum fluctuations are a Gaussian random field.

A.3 Gauge Interaction Statistics

A.3.1 "Electric" And "Magnetic" Fields

In Sec.4.2, the "electric" ($\vec{E} = -a^{-2}\dot{\vec{A}}$) and "magnetic" ($\vec{B} = a^{-2}\vec{\nabla}\times\vec{A}$) fields have been introduced to simplify the notation in various equations of motion. The general formula for these fields can be derived as follows:

$$\begin{aligned}
\vec{\nabla}\times\vec{A} &= \sum_{\lambda}\int \frac{d^3k}{(2\pi)^{3/2}}\left[a_\lambda(\vec{k})A_\lambda(\tau,\vec{k})\left(\vec{\nabla}\times e^{i\vec{k}\cdot\vec{x}}\hat{\varepsilon}_\lambda(\vec{k})\right) + a^\dagger_\lambda(-\vec{k})A^*_\lambda(\tau,-\vec{k})\left(\vec{\nabla}\times e^{i\vec{k}\cdot\vec{x}}\hat{\varepsilon}^*_\lambda(-\vec{k})\right)\right] \\
&= \sum_{\lambda}\int \frac{d^3k}{(2\pi)^{3/2}}\left[a_\lambda(\vec{k})A_\lambda(\tau,\vec{k}) + a^\dagger_\lambda(-\vec{k})A^*_\lambda(\tau,-\vec{k})\right]\left(\vec{\nabla}\times e^{i\vec{k}\cdot\vec{x}}\hat{\varepsilon}_\lambda(\vec{k})\right) \\
&= \sum_{\lambda}\int \frac{\int^3 k}{(2\pi)^{3/2}}\left[a_\lambda(\vec{k})A_\lambda(\tau,\vec{k}) + a^\dagger_\lambda(-\vec{k})A^*_\lambda(\tau,-\vec{k})\right]\left[e^{i\vec{k}\cdot\vec{x}}\left(\vec{\nabla}\times\hat{\varepsilon}_\lambda(\vec{k})\right) + \left(\vec{\nabla}e^{i\vec{k}\cdot\vec{x}}\right)\hat{\varepsilon}_\lambda(\vec{k})\right] = \\
&= \sum_{\lambda}\int \frac{d^3k}{(2\pi)^{3/2}}\left[a_\lambda(\vec{k})A_\lambda(\tau,\vec{k}) + a^\dagger_\lambda(-\vec{k})A^*_\lambda(\tau,-\vec{k})\right]\left[\left(\vec{\nabla}\times\hat{\varepsilon}_\lambda(\vec{k})\right) + \left(i\vec{k}\times\hat{\varepsilon}_\lambda(\vec{k})\right)\right]e^{i\vec{k}\cdot\vec{x}} = \\
&= \sum_{\lambda}\int \frac{d^3k}{(2\pi)^{3/2}}\lambda k\left[a_\lambda(\vec{k})A_\lambda(\tau,\vec{k}) + a^\dagger_\lambda(-\vec{k})A^*_\lambda(\tau,\vec{k})\right]\hat{\varepsilon}_\lambda(\vec{k})e^{i\vec{k}\cdot\vec{x}} \\
\partial_\tau\vec{A} &= \sum_{\lambda}\frac{d^3k}{(2n)^{3/2}}\left[a_\lambda(\vec{k})\dot{A}_\lambda(\tau,\vec{k}) + a^\dagger_\lambda(-\vec{k})\dot{A}_\lambda(\tau,-\vec{k})\right]\hat{\varepsilon}_\lambda(\vec{k})e^{i\vec{k}\cdot\vec{x}}
\end{aligned}$$

The above expressions lead to the following final formulas:

$$\vec{E} = -\frac{1}{a^2}\partial_\tau\vec{A} = -\frac{1}{a^2}\sum_{\lambda}\int \frac{d^3k}{(2\pi)^{3/2}}\left[a_\lambda(\vec{k})\dot{A}_\lambda(\tau,\vec{k}) + a^\dagger_\lambda(-\vec{k})\dot{A}_\lambda(\tau,-\vec{k})\right]\hat{\varepsilon}_\lambda(\vec{k})e^{i\vec{k}\cdot\vec{x}} \tag{A.30}$$

$$\vec{B} = \frac{1}{a^2}\vec{\nabla}\times\vec{A} = \frac{1}{a^2}\sum_{\lambda}\int \frac{d^3k}{(2\pi)^{3/2}}\lambda k\left[a_\lambda(\vec{k})A_\lambda(\tau,\vec{k}) + a^\dagger_\lambda(-\vec{k})A^*_\lambda(\tau,\vec{k})\right]\hat{\varepsilon}_\lambda(\vec{k})e^{i\vec{k}\cdot\vec{x}} \tag{A.31}$$

Eq.A.30-A.31 can be used to compute the inner product between the electric and magnetic field which is a relevant quantity for the source term associated with gauge interactions (Eq.65). Its Fourier transform can be computed in the following manner:

$$\begin{aligned}
\int \frac{d^3x}{(2\pi)^{(3/2)}}\left(\vec{E}\cdot\vec{B}\right)e^{-i\vec{q}\cdot\vec{x}} &= -\frac{1}{a^4}\sum_{\lambda,\lambda'}\int \frac{d^3x d^3k d^3k'}{(2\pi)^{(9/2)}}\left(\lambda'\mathrm{k}'\right)\left[a_\lambda(\vec{k})\dot{A}_\lambda(\tau,\vec{k}) + a^\dagger_\lambda(-\vec{k})\dot{A}_\lambda(\tau,-\vec{k})\right] \\
&\quad \left[a_{\lambda'}(\vec{k}')A_{\lambda'}(\tau,\vec{k}') + a^\dagger_{\lambda'}(-\vec{k}')A^*_{\lambda'}(\tau,\vec{k}')\right]\left(\hat{\varepsilon}_\lambda(\vec{k})\cdot\hat{\varepsilon}_{\lambda'}(\vec{k}')\right)e^{i(\vec{k}+\vec{k}'-\vec{q})\cdot\vec{x}} = \\
&= -\frac{1}{a^4}\sum_{\lambda,\lambda'}\int \frac{d^3k}{(2\pi)^{(3/2)}}\left(\lambda'|\vec{q}-\vec{k}|\right)\left[a_\lambda(\vec{k})\dot{A}_\lambda(\tau,\vec{k}) + a^\dagger_\lambda(-\vec{k})\dot{A}_\lambda(\tau,-\vec{k})\right] \\
&\quad \left[a_{\lambda'}(\vec{q}-\vec{k})A_{\lambda'}(\tau,\vec{q}-\vec{k}) + a^\dagger_{\lambda'}(\vec{k}-\vec{q})A^*_{\lambda'}(\tau,\vec{k}-\vec{q})\right]\left(\hat{\varepsilon}_\lambda(\vec{k})\cdot\hat{\varepsilon}_{\lambda'}(\vec{q}-\vec{k})\right)
\end{aligned}$$

A.3.2 Gauge Modes And Their Derivative

To derive Eq.65 one has to substitute the Gauge field's Fourier transform (Eq.20) in Eq.60. Using the calculations of Sec.A.3.1 for the conformal time derivative and the curl of $\vec{A}$, the substitution yields the following result:

$$\left[\partial_\tau^2 + k^2\left(1 - \lambda k\frac{\alpha}{f}\dot{\phi}^{(0)}\right)\right] A_\lambda(\tau, \mathrm{k}) = 0 \tag{A.32}$$

As $\phi'^{(0)} = a^{-1}\dot{\phi}^{(0)}$, it is useful to define the parameter $\xi = 2(\alpha/f)H\phi'^{(0)}$ such that $\dot{\phi}^{(0)} = -2(\xi/\tau)$. Therefore, by the substitution of the parameter ξ, Eq.65 is recovered. As discussed in [10, 24], the solutions to this equation can be approximated by Eq.67-68 within the range $(8\xi)^{-1} < -\mathrm{k}\tau < 2\xi$. The use of this result allows us to discard the A_- modes, leading to the following simplifications of the Fourier transform of the dot product between the electric and magnetic fields:

$$\begin{aligned}\int \frac{d^3x}{(2\pi)^{(3/2)}}\left(\vec{E}\cdot\vec{B}\right)e^{-i\vec{q}\cdot\vec{x}} = -\frac{1}{a^4}\int \frac{d^3k}{(2\pi)^{(3/2)}}|\vec{q}-\vec{k}|\left[a_+(\vec{k})\dot{A}^*_+(\tau,\vec{k}) + a^\dagger_+(-\vec{k})\dot{A}_+(\tau,-\vec{k})\right] \\ \left[a_+(\vec{q}-\vec{k})A_+(\tau,\vec{q}-\vec{k}) + a^\dagger_+(\vec{k}-\vec{q})A^*_+(\tau,\vec{k}-\vec{q})\right](\hat{\varepsilon}_+(\vec{k})\cdot\hat{\varepsilon}_+(\vec{q}-\vec{k})) \quad = \\ = -\frac{1}{a^4}\int \frac{d^3k}{(2\pi)^{(3/2)}}k|\vec{q}-\vec{k}|\sqrt{\frac{2\xi}{(-k\tau)}}\left[a_+(\vec{k})A_+(\tau,\vec{k}) + a^\dagger_+(-\vec{k})A^*_+(\tau,-\vec{k})\right] \\ \left[a_+(\vec{q}-\vec{k})A_+(\tau,\vec{q}-\vec{k}) + a^\dagger_+(\vec{k}-\vec{q})A^*_+(\tau,\vec{k}-\vec{q})\right](\hat{\varepsilon}_+(\vec{k})\cdot\hat{\varepsilon}_+(\vec{q}-\vec{k}))\end{aligned}$$

Similarly, the Fourier transform of the average of the dot product can be computed as follows:

$$\begin{aligned}\int \frac{d^3x}{(2\pi)^{(3/2)}}\langle\vec{E}\cdot\vec{B}\rangle e^{-i\vec{q}\cdot\vec{x}} = \langle\int \frac{d^3x}{(2\pi)^{(3/2)}}\left(\vec{E}\cdot\vec{B}\right)e^{-i\vec{q}\cdot\vec{x}}\rangle = \\ = -\frac{1}{a^4}\int \frac{d^3k}{(2\pi)^{(3/2)}}|\vec{q}-\vec{k}|\langle a_+(\vec{k})a^\dagger_+(\vec{k}-\vec{q})\rangle\dot{A}_+(\tau,\vec{k})A^*_+(\tau,\vec{k}-\vec{q})(\hat{\varepsilon}_+(\vec{k})\cdot\hat{\varepsilon}_+(\vec{q}-\vec{k})) = \\ = -\delta(\vec{q})\frac{1}{a^4}\int \frac{d^3k}{(2\pi)^{(3/2)}}k\dot{A}_+(\tau,\vec{k})A^*_+(\tau,\vec{k})\end{aligned}$$

A.3.3 Gauge-Interaction Power Spectrum

The two-point correlation function in momentum space is defined as the expectation value of the product between two density perturbations ($\zeta_{\vec{k}}(\tau)$ and $\zeta_{\vec{k}'}(\tau)$) evaluated at two different points. As $\delta\phi_{\vec{k}}(\tau)$ can be separated into a homogeneous and a particular solution, the two-point correlator depends on four separate terms. However, as evidenced by Eq.63 and Eq.41, the particular solution depends on pairs of gauge field modes and their operators. On the other hand, the homogeneous solution depends on single scalar modes and operators. As a result, expectation values containing an odd number of homogeneous solutions will disappear. Therefore, the correlator simplifies to:

$$\langle\zeta_{\vec{k}}(\tau)\zeta_{\vec{k}'}(\tau)\rangle = \left(\frac{H}{\phi'(0)}\right)^2\left[\langle\delta\phi^{homo}_{\vec{k}}\delta\phi^{homo}_{\vec{k}'}\rangle + \langle\delta\phi^{part}_{\vec{k}}\delta\phi^{part}_{\vec{k}'}\rangle\right] \tag{A.33}$$

$$\langle\delta\phi^{part}_{\vec{k}}\delta\phi^{part}_{\vec{k}'}\rangle = \int d\tau' d\tau'' \frac{a(\tau')a(\tau'')}{a^2(\tau)} G_{\vec{k}}(\tau,\tau')G_{\vec{k}'}(\tau,\tau'')\langle J_{\vec{k}}(\tau')J_{\vec{k}'}(\tau'')\rangle \tag{A.34}$$

The first term of Eq.A.33 is computed in Sec.A.2.1. Therefore, the evaluation of the power spectrum is reduced to the computation of $\langle\delta\phi^{part}_{\vec{k}}\delta\phi^{part}_{\vec{k}'}\rangle$ (Eq.A.34). The latter can be separated into two separate calculations: the computation of the expectation values and the computation of the product of Green's functions. The latter is shown below:

$$\begin{aligned}
G_{\vec{k}}(\tau,\tau')G_{\vec{k}'}(\tau,\tau'') &= -\Theta(\tau-\tau')\Theta(\tau-\tau'')\left[u_k(\tau)u_k^*(\tau') - u_k^*(\tau)u_k(\tau')\right]\left[u_{k'}(\tau)u_{k'}^*(\tau'') - u_{k'}^*(\tau)u_{k'}(\tau'')\right] = \\
&= 4\Theta(\tau-\tau')\Theta(\tau-\tau'')\Big[\mathrm{Im}\left[u_k(\tau)\right]\mathrm{Im}\left[u_{k'}(\tau)\right]\mathrm{Re}\left[u_k(\tau')\right]\mathrm{Re}\left[u_{k'}(\tau'')\right] \quad + \\
&\quad - \mathrm{Re}\left[u_k(\tau)\right]\mathrm{Re}\left[u_{k'}(\tau)\right]\mathrm{Im}\left[u_k(\tau')\right]\mathrm{Im}\left[u_{k'}(\tau'')\right] + \\
&\quad - \mathrm{Im}\left[u_k(\tau)\right]\mathrm{Re}\left[u_{k'}(\tau)\right]\mathrm{Re}\left[u_k(\tau')\right]\mathrm{Im}\left[u_{k'}(\tau'')\right] + \\
&\quad - \mathrm{Re}\left[u_k(\tau)\right]\mathrm{Im}\left[u_{k'}(\tau)\right]\mathrm{Im}\left[u_k(\tau')\right]\mathrm{Re}\left[u_{k'}(\tau'')\right]\Big]
\end{aligned}$$

The expression above can be simplified by considering the behavior of the real and imaginary parts of $u_k(\tau)$ separately. For instance, in the case $\nu = (3/2)$, the two parts can be expressed as follows:

$$\begin{aligned}
\mathrm{Re}\left[u_k(\tau)\right] &= \frac{\sqrt{\pi}}{2}\sqrt{-\tau}\left[\mathrm{Re}\left[e^{i\left(\nu+\frac{1}{2}\right)\frac{\pi}{2}}\right]\mathrm{Re}\left[H_\nu^{(1)}(-k\tau)\right] - \mathrm{Im}\left[e^{i\left(\nu+\frac{1}{2}\right)\frac{\pi}{2}}\right]\mathrm{Im}\left[H_\nu^{(1)}(-k\tau)\right]\right] = \\
&= \frac{\sqrt{\pi}}{2}\sqrt{-\tau}\mathrm{Re}\left[H_\nu^{(1)}(-k\tau)\right]
\end{aligned} \tag{A.35}$$

$$\begin{aligned}
\mathrm{Im}\left[u_k(\tau)\right] &= \frac{\sqrt{\pi}}{2}\sqrt{-\tau}\left[\mathrm{Re}\left[e^{i\left(\nu+\frac{1}{2}\right)\frac{\pi}{2}}\right]\mathrm{Im}\left[H_\nu^{(1)}(-k\tau)\right] + \mathrm{Im}\left[e^{i\left(\nu+\frac{1}{2}\right)\frac{\pi}{2}}\right]\mathrm{Re}\left[H_\nu^{(1)}(-k\tau)\right]\right] = \\
&= \frac{\sqrt{\pi}}{2}\sqrt{-\tau}\mathrm{Im}\left[H_\nu^{(1)}(-k\tau)\right]
\end{aligned} \tag{A.36}$$

In addition, only fluctuations that grow to superhorizon scales are physically relevant. As a result, it is possible to substitute the superhorizon limit of $u_k(\tau)$ (Eq.35) in the expression for the product of Green's functions. In this situation, $u_k(\tau)$ is purely imaginary (See Fig.6c). Therefore, the product of Green's functions simplifies to:

$$\begin{aligned}
G_{\vec{k}}(\tau,\tau')G_{\vec{k}'}(\tau,\tau'') &= 4\Theta(\tau-\tau')\Theta(\tau-\tau'')u_k(\tau)u_{k'}(\tau)\mathrm{Re}\left[u_k(\tau')\right]\mathrm{Re}\left[u_{k'}(\tau'')\right] = \\
&= \frac{\pi}{2}a^2(\tau)H^2\frac{\left[(-k\tau)(-k'\tau)\right]^{\frac{1}{2}(n_s-1)}}{(kk')^{(3/2)}}\Theta(\tau-\tau')\Theta(\tau-\tau'')\sqrt{(-\tau')(-\tau'')}\mathrm{Re}\left[H_\nu^{(1)}(-k\tau')\right]\mathrm{Re}\left[H_\nu^{(1)}(-k'\tau'')\right]
\end{aligned} \tag{A.37}$$

To complete the calculation, the expectation value $\langle J_{\vec{k}}(\tau')J_{\vec{k}'}(\tau'')\rangle$ must be computed. As can be seen from Eq.63, this product can be divided into four smaller terms. However, three out of four will depend on the Fourier transform of $\langle \vec{E}\cdot\vec{B}\rangle$. According to the results of Sec.A.3.2, these terms are only relevant when momenta are zero and thus they provide small contributions to the final results. Therefore, they can safely be discarded. The resulting formula for the expectation value is the following:

$$\begin{aligned}\langle J_{\vec{k}}(\tau')J_{\vec{k}'}(\tau'')\rangle \simeq a^2(\tau')a^2(\tau'')\left(\frac{\alpha}{f}\right)^2\Bigg\langle\Bigg[\int\frac{d^3x}{(2\pi)^{(3/2)}}\left(\vec{E}(\tau',\vec{x})\cdot\vec{B}(\tau',\vec{x})\right)e^{-i\vec{k}\cdot\vec{x}}\Bigg]\\ \times\Bigg[\int\frac{d^3x'}{(2\pi)^{(3/2)}}\left(\vec{E}(\tau'',\vec{x}')\cdot\vec{B}(\tau'',\vec{x}')\right)e^{-i\vec{k}'\cdot\vec{x}'}\Bigg]\Bigg\rangle\end{aligned} \tag{A.38}$$

Substitution of the results of Sec.A.3.2 separates the expression into 16 different terms. However, the expectation value of a string of operators that start with a creation operator always vanishes. The same applies to strings of operators that end with an annihilation operator. Therefore, only four expectation values are not necessarily zero. These are the following:

$$\begin{aligned}\langle a_+(\vec{q})a_+(\vec{k}-\vec{q})a_+(\vec{q}')a_+^\dagger(\vec{q}'-\vec{k}')\rangle &= \langle a_+(\vec{q})a_+(\vec{k}-\vec{q})a_+^\dagger(\vec{q}'-\vec{k}')a_+(\vec{q}')\rangle+\\ &+[a_+(\vec{q}'),\,a_+^\dagger(\vec{q}'-\vec{k}')]\langle a_+(\vec{q})a_+(\vec{k}-\vec{q})\rangle=\\ &=0\end{aligned} \tag{A.39}$$

$$\begin{aligned}\langle a_+(\vec{q})a_+(\vec{k}-\vec{q})a_+^\dagger(-\vec{q}')a_+^\dagger(\vec{q}'-\vec{k}')\rangle &= \langle a_+(\vec{q})a_+^\dagger(-\vec{q}')a_+(\vec{k}-\vec{q})a_+^\dagger(\vec{q}'-\vec{k}')\rangle+\\ &+[a_+(\vec{k}-\vec{q}),\,a_+^\dagger(-\vec{q}')]\langle a_+(\vec{q})a_+^\dagger(\vec{q}'-\vec{k}')\rangle=\\ &=[a_+(\vec{q}),\,a_+^\dagger(-\vec{q}')][a_+(\vec{k}-\vec{q}),\,a_+^\dagger(\vec{q}'-\vec{k}')]+\\ &+[a_+(\vec{k}-\vec{q}),\,a_+^\dagger(-\vec{q}')][a_+(\vec{q}),\,a_+^\dagger(\vec{q}'-\vec{k}')]=\\ &=\delta(\vec{q}+\vec{q}')\delta(\vec{k}+\vec{k}'-\vec{q}-\vec{q}')+\delta(\vec{k}'+\vec{q}-\vec{q}')\delta(\vec{k}-\vec{q}+\vec{q}')\end{aligned} \tag{A.40}$$

$$\begin{aligned}\langle a_+(\vec{q})a_+^\dagger(\vec{q}-\vec{k})a_+(\vec{q}')a_+^\dagger(\vec{q}'-\vec{k}')\rangle &= +\langle a_+(\vec{q})a_+^\dagger(\vec{q}-\vec{k})a_+^\dagger(\vec{q}'-\vec{k}')a_+(\vec{q}')\rangle\\ &+[a_+(\vec{k}-\vec{q}),\,a_+^\dagger(-\vec{q}')]\langle a_+(\vec{q})a_+^\dagger(\vec{q}'-\vec{k}')\rangle=\\ &=\delta(\vec{k})\delta(\vec{k}')\end{aligned} \tag{A.41}$$

$$\begin{aligned}\langle a_+(\vec{q})a_+^\dagger(\vec{q}-\vec{k})a_+^\dagger(-\vec{q}')a_+^\dagger(\vec{q}'-\vec{k}')\rangle &= \langle a_+^\dagger(\vec{q}-\vec{k})a_+(\vec{q})a_+^\dagger(-\vec{q}')a_+^\dagger(\vec{q}'-\vec{k}')\rangle\\ &+[a_+(\vec{q}),\,a_+^\dagger(\vec{q}-\vec{k})]\langle a_+^\dagger(-\vec{q}')a_+^\dagger(\vec{q}'-\vec{k}')\rangle=\\ &=0\end{aligned} \tag{A.42}$$

Eq.A.40 is the only term that is non-vanishing and that does not require momenta to be zero. It is associated with the following product of Gauge modes:

$$\begin{aligned}
&\dot{A}_+(\tau',\vec{q})A_+(\tau',\vec{\mathrm{k}}-\vec{q})\dot{A}^*_+(\tau'',-\vec{q}')A^*_+(\tau'',\vec{q}'-\vec{\mathrm{k}}') = \\
&\quad = 2\xi\sqrt{\frac{|\vec{q}||\vec{q}'|}{(-\tau')(-\tau'')}}A_+(\tau',\vec{q})A_+(\tau',\vec{\mathrm{k}}-\vec{q})A^*_+(\tau'',-\vec{q}')A^*_+(\tau'',\vec{q}'-\vec{\mathrm{k}}') \qquad \text{(A.43)} \\
&\quad = \frac{1}{4}\left(\frac{|\vec{q}||\vec{q}'|}{|\vec{\mathrm{k}}-\vec{q}||\vec{q}'-\vec{\mathrm{k}}'|}\right)^{(1/4)} e^{\left[4\pi\xi-2\sqrt{2\xi}\left[(-|\vec{q}|\tau')^{(1/2)}+(-|\vec{\mathrm{k}}-\vec{q}|\tau')^{(1/2)}+(-|\vec{q}'|\tau'')^{(1/2)}+(-|\vec{q}'-\vec{\mathrm{k}}'|\tau'')^{(1/2)}\right]\right]}
\end{aligned}$$

Using Eq.A.40 and Eq.A.43, one can compute the expectation value of the product of the source terms (Eq.A.38). The calculation is shown below:

$$\begin{aligned}
\langle J_{\vec{\mathrm{k}}}(\tau')J_{\vec{\mathrm{k}}'}(\tau'')\rangle &= \frac{1}{a^2(\tau')a^2(\tau'')}\left(\frac{\alpha}{f}\right)^2\int\frac{d^3qd^3q'}{(2\pi)^3}\Big[|\vec{\mathrm{k}}-\vec{q}||\vec{q}'-\vec{\mathrm{k}}'|\langle a_+(\vec{q})a_+(\vec{\mathrm{k}}-\vec{q})a^\dagger_+(-\vec{q}')a^\dagger_+(\vec{q}'-\vec{\mathrm{k}}')\rangle \\
&\qquad \times\dot{A}_+(\tau',\vec{q})A_+(\tau',\vec{\mathrm{k}}-\vec{q})\dot{A}^*_+(\tau'',-\vec{q}')A^*_+(\tau'',\vec{q}'-\vec{\mathrm{k}}') \\
&\qquad \times(\hat{\varepsilon}_+(\vec{q})\cdot\hat{\varepsilon}_+(\vec{\mathrm{k}}-\vec{q}))(\hat{\varepsilon}_+(\vec{q}')\cdot\hat{\varepsilon}_+(\vec{\mathrm{k}}'-\vec{q}'))\Big] = \\
&= \frac{1}{4a^2(\tau')a^2(\tau'')}\left(\frac{\alpha}{f}\right)^2\int\frac{d^3qd^3q'}{(2\pi)^3}\Big[\delta(\vec{q}+\vec{q}')\delta(\vec{\mathrm{k}}+\vec{\mathrm{k}}'-\vec{q}-\vec{q}')+\delta(\vec{\mathrm{k}}'+\vec{q}-\vec{q}')\delta(\vec{\mathrm{k}}-\vec{q}+\vec{q}') \\
&\qquad \times\left(|\vec{q}||\vec{q}'||\vec{\mathrm{k}}-\vec{q}|^3|\vec{q}'-\vec{\mathrm{k}}'|^3\right)^{(1/4)} \\
&\qquad \times e^{\left[4\pi\xi-2\sqrt{2\xi}\left[(-|\vec{q}|\tau')^{(1/2)}+(-|\vec{\mathrm{k}}-\vec{q}|\tau')^{(1/2)}+(-|\vec{q}'|\tau'')^{(1/2)}+(-|\vec{q}'-\vec{\mathrm{k}}'|\tau'')^{(1/2)}\right]\right]} \\
&\qquad \times(\hat{\varepsilon}_+(\vec{q})\cdot\hat{\varepsilon}_+(\vec{\mathrm{k}}-\vec{q}))(\hat{\varepsilon}_+(\vec{q}')\cdot\hat{\varepsilon}_+(\vec{\mathrm{k}}'-\vec{q}'))\Big] = \\
&= \frac{1}{4a^2(\tau')a^2(\tau'')}\left(\frac{\alpha}{f}\right)^2\delta(\vec{\mathrm{k}}+\vec{\mathrm{k}}')\int\frac{d^3q}{(2\pi)^3}\Big[\left(|\vec{q}|^{(1/2)}|\vec{\mathrm{k}}-\vec{q}|^{(3/2)}+|\vec{q}||\vec{\mathrm{k}}-\vec{q}|\right) \\
&\qquad \times e^{\left[4\pi\xi-2\sqrt{2\xi}\left(|\vec{q}|^{(1/2)}+|\vec{\mathrm{k}}-\vec{q}|^{(1/2)}\right)\left((-\tau')^{(1/2)}+(-\tau'')^{(1/2)}\right)\right]} \\
&\qquad \times(\hat{\varepsilon}_+(\vec{q})\cdot\hat{\varepsilon}_+(\vec{\mathrm{k}}-\vec{q}))(\hat{\varepsilon}_+(-\vec{q})\cdot\hat{\varepsilon}_+(\vec{q}-\vec{\mathrm{k}}))\Big] = \\
&= \frac{1}{4a^2(\tau')a^2(\tau'')}\left(\frac{\alpha}{f}\right)^2\delta(\vec{\mathrm{k}}+\vec{\mathrm{k}}')\int\frac{d^3q}{(2\pi)^3}\Big[|\hat{\varepsilon}_+(\vec{q})\cdot\hat{\varepsilon}_+(\vec{\mathrm{k}}-\vec{q})|^2\left(|\vec{q}|^{(1/2)}|\vec{\mathrm{k}}-\vec{q}|^{(3/2)}+|\vec{q}||\vec{\mathrm{k}}-\vec{q}|\right) \\
&\qquad \times e^{\left[4\pi\xi-2\sqrt{2\xi}\left(|\vec{q}|^{(1/2)}+|\vec{\mathrm{k}}-\vec{q}|^{(1/2)}\right)\left((-\tau')^{(1/2)}+(-\tau'')^{(1/2)}\right)\right]}\Big]
\end{aligned}$$

By direct substitution in Eq.A.34 of the above expression, the two-point correlator can be computed in the manner shown below:

$$
\begin{aligned}
\langle \delta\phi^{part}_{\vec{\mathrm{k}}} \delta\phi^{part}_{\vec{\mathrm{k}}'} \rangle &= \int d\tau' d\tau'' \frac{a(\tau')a(\tau'')}{a^2(\tau)} G_{\vec{\mathrm{k}}}(\tau,\tau') G_{\vec{\mathrm{k}}'}(\tau,\tau'') \langle J_{\vec{\mathrm{k}}}(\tau') J_{\vec{\mathrm{k}}'}(\tau'') \rangle = \\
&= \delta(\vec{\mathrm{k}}+\vec{\mathrm{k}}') \frac{\alpha^2 H^2 \pi}{8 f^2 k^3 (2\pi)^3} (-k\tau)^{n_s-1} e^{4\pi\xi} \times \\
&\quad \times \int_{-\infty}^{\tau} d\tau' d\tau'' d^3q \Bigg\{ \frac{\sqrt{(-\tau')(-\tau'')}}{a(\tau')a(\tau'')} \mathrm{Re}\left[H_\nu^{(1)}(-k\tau')\right] \mathrm{Re}\left[H_\nu^{(1)}(-k\tau'')\right] \\
&\qquad \times \Big[|\hat{\varepsilon}_+(\vec{q}) \cdot \hat{\varepsilon}_+(\vec{\mathrm{k}}-\vec{q})|^2 \left(|\vec{q}|^{(1/2)} |\vec{\mathrm{k}}-\vec{q}|^{(3/2)} + |\vec{q}||\vec{\mathrm{k}}-\vec{q}| \right) \\
&\qquad \times e^{-2\sqrt{2\xi}\left(|\vec{q}|^{(1/2)} + |\vec{\mathrm{k}}-\vec{q}|^{(1/2)}\right)\left((-\tau')^{(1/2)} + (-\tau'')^{(1/2)}\right)} \Big] \Bigg\} = \\
&= \delta(\vec{\mathrm{k}}+\vec{\mathrm{k}}') \frac{H^4 \pi}{8k^3(2\pi)^3} \left(\frac{\alpha}{f}\right)^2 (-k\tau)^{n_s-1} e^{4\pi\xi} \times \\
&\quad \times \int_{-\infty}^{\tau} d\tau' d\tau'' d^3q \Bigg\{ \left((-\tau')(-\tau'')\right)^{(3/2)} \mathrm{Re}\left[H_\nu^{(1)}(-k\tau')\right] \mathrm{Re}\left[H_\nu^{(1)}(-k\tau'')\right] \\
&\qquad \times \Big[|\hat{\varepsilon}_+(\vec{q}) \cdot \hat{\varepsilon}_+(\vec{\mathrm{k}}-\vec{q})|^2 \left(|\vec{q}|^{(1/2)} |\vec{\mathrm{k}}-\vec{q}|^{(3/2)} + |\vec{q}||\vec{\mathrm{k}}-\vec{q}| \right) \\
&\qquad \times e^{-2\sqrt{2\xi}\left(|\vec{q}|^{(1/2)} + |\vec{\mathrm{k}}-\vec{q}|^{(1/2)}\right)\left((-\tau')^{(1/2)} + (-\tau'')^{(1/2)}\right)} \Big] \Bigg\} = \\
&= \delta(\vec{\mathrm{k}}+\vec{\mathrm{k}}') \frac{H^2 \pi}{8k^3(2\pi)^3} \Delta_P (4\pi\xi)^2 (-k\tau)^{n_s-1} e^{4\pi\xi} \times \\
&\quad \times \int_{-\infty}^{\tau} d\tau' d\tau'' d^3q \Bigg\{ \left((-\tau')(-\tau'')\right)^{(3/2)} \mathrm{Re}\left[H_\nu^{(1)}(-k\tau')\right] \mathrm{Re}\left[H_\nu^{(1)}(-k\tau'')\right] \\
&\qquad \times \Big[|\hat{\varepsilon}_+(\vec{q}) \cdot \hat{\varepsilon}_+(\vec{\mathrm{k}}-\vec{q})|^2 \left(|\vec{q}|^{(1/2)} |\vec{\mathrm{k}}-\vec{q}|^{(3/2)} + |\vec{q}||\vec{\mathrm{k}}-\vec{q}| \right) \\
&\qquad \times e^{-2\sqrt{2\xi}\left(|\vec{q}|^{(1/2)} + |\vec{\mathrm{k}}-\vec{q}|^{(1/2)}\right)\left((-\tau')^{(1/2)} + (-\tau'')^{(1/2)}\right)} \Big] \Bigg\} = \\
&= \frac{2\pi^2}{k^3} \delta(\vec{\mathrm{k}}+\vec{\mathrm{k}}') \frac{H^2}{4\pi^2} \frac{\xi^2}{8\pi} \Delta_P (-k\tau)^{n_s-1} e^{4\pi\xi} \frac{\pi}{2} \times \\
&\quad \times \int_{-k\tau}^{0} dx' dx'' d^3p \Bigg\{ \left((x')(x'')\right)^{(3/2)} \mathrm{Re}\left[H_\nu^{(1)}(x')\right] \mathrm{Re}\left[H_\nu^{(1)}(x'')\right] \\
&\qquad \times \Big[|\hat{\varepsilon}_+(\vec{p}) \cdot \hat{\varepsilon}_+(\hat{k}-\vec{p})|^2 \left(4|\vec{p}|^{(1/2)} |\hat{k}-\vec{p}|^{(3/2)} + |\vec{p}||\vec{\mathrm{k}}-\vec{p}| \right) \\
&\qquad \times e^{-2\sqrt{2\xi}\left(|\vec{p}|^{(1/2)} + |\hat{k}-\vec{p}|^{(1/2)}\right)\left((x')^{(1/2)} + (x'')^{(1/2)}\right)} \Big] \Bigg\}
\end{aligned}
$$

In the last line of the expression above the substitution $\vec{p} = \vec{q}/k$, $x' = -k\tau'$ and $x'' = -k\tau''$ have been made. The power spectrum can thus be expressed as follows:

$$P_\zeta(k) = \Delta_P(-k\tau)^{n_s-1}\left[1 + \Delta_P e^{4\pi\xi} f_2(\xi, \vec{\mathrm{k}})\right] \tag{A.44}$$

$$f_2(\xi, \vec{\mathrm{k}}) = \frac{\xi^2}{8\pi}\int d^3p \left(4|\vec{p}|^{(1/2)}|\hat{k} - \vec{p}|^{(3/2)} + |\vec{p}||\hat{k} - \vec{p}|\right) \times \tag{A.45}$$
$$\times \mathrm{I}^2\left(-2\sqrt{2\xi}\left[|\vec{p}|^{(1/2)} + |\hat{k} - \vec{p}|^{(1/2)}\right]\right)$$

$$\mathrm{I}(z) = \sqrt{\frac{\pi}{2}}\int_{-k\tau}^{\infty} dx (x)^{3/2} \mathrm{Re}\left[H_\nu^{(1)}(x)\right] e^{zx^{(1/2)}} \tag{A.46}$$

A.3.4 Gauge-Interaction Bispectra

The three-point correlation function in momentum space is defined as the expectation value of the product between three density perturbations ($\zeta_{\vec{k}_1}(\tau)$, $\zeta_{\vec{k}_3}(\tau)$, and $\zeta_{\vec{k}_3}(\tau)$) evaluated at three different points. As $\delta\phi_{\vec{k}}(\tau)$ can be separated into a homogeneous and a particular solution, the two-point correlator depends on eight separate terms. Similarly to the power spectrum (Sec.A.3.3), the terms involving odd numbers of homogenous solutions vanish. In addition, the terms containing a single particular solution vanish. For example, consider the case of $\langle\delta\phi^{homo}_{\vec{k}_1}\delta\phi^{homo}_{\vec{k}_2}\delta\phi^{part}_{\vec{k}_3}\rangle$. The expectation value is evaluated as follows:

$$\begin{aligned}\langle\delta\phi^{homo}_{\vec{k}_1}\delta\phi^{homo}_{\vec{k}_2}\delta\phi^{part}_{\vec{k}_3}\rangle &= \langle\delta\phi^{homo}_{\vec{k}_1}\delta\phi^{homo}_{\vec{k}_2}\rangle\langle\delta\phi^{part}_{\vec{k}_3}\rangle = \\ &= \langle\delta\phi^{homo}_{\vec{k}_1}\delta\phi^{homo}_{\vec{k}_2}\rangle\int d\tau' a^{-1}(\tau)G_{\vec{k}_3}(\tau,\tau')\langle J_{\vec{k}_3}(\tau')\rangle \\ &= a(\tau)\frac{\alpha}{f}\langle\delta\phi^{homo}_{\vec{k}_1}\delta\phi^{homo}_{\vec{k}_2}\rangle\int\frac{d\tau' d^3x}{(2\pi)^{(3/2)}}G_{\vec{k}_3}(\tau,\tau')\left[\langle\vec{E}\cdot\vec{B}\rangle-\langle\vec{E}\cdot\vec{B}\rangle\right]e^{-i\vec{q}\cdot\vec{x}} = \\ &= 0\end{aligned}$$

Therefore, the three-point correlator is entirely described by a single term:

$$\begin{aligned}\langle\zeta_{\vec{q}_1}(\tau)\zeta_{\vec{q}_2}(\tau)\zeta_{\vec{q}_3}(\tau)\rangle &= -\left(\frac{H}{\phi'(0)}\right)^3\langle\delta\phi^{part}_{\vec{q}_1}\delta\phi^{part}_{\vec{q}_2}\delta\phi^{part}_{\vec{q}_3}\rangle = \\ &= -\left(\frac{H}{\phi'(0)}\right)^3\int d\tau_1 d\tau_2 d\tau_3\frac{a(\tau_1)a(\tau_2)a(\tau_3)}{a^3(\tau)}\big[G_{\vec{q}_1}(\tau,\tau_1)G_{\vec{q}_2}(\tau,\tau_2)G_{\vec{q}_3}(\tau,\tau_3)\times \\ &\qquad\times\langle J_{\vec{q}_1}(\tau_1)J_{\vec{q}_2}(\tau_2)J_{\vec{q}_3}(\tau_3)\rangle\big]\end{aligned} \tag{A.47}$$

To simplify expressions, these substitutions are often made in the next calculations:

$$\nu=\frac{3}{2}\qquad z_n=-|\vec{q}_n|\tau_n\qquad \vec{p}=\vec{k}/|\vec{q}_1|\qquad x_n=|\vec{q}_n|/|\vec{q}_1| \tag{A.48}$$

Similarly to the calculation of the power spectrum, one has to compute the product of Green functions. This results in the following expression:

$$\begin{aligned}G_{\vec{q}_1}(\tau,\tau_1)G_{\vec{q}_2}(\tau,\tau_2)G_{\vec{q}_2}(\tau,\tau_3) &= 8\Theta(\tau-\tau_1)\Theta(\tau-\tau_2)\Theta(\tau-\tau_3)\left(a(\tau)H\frac{\sqrt{\pi}}{2}\right)^3\times \\ &\quad\times\frac{1}{\sqrt{8|\vec{q}_1|^3|\vec{q}_2|^3|\vec{q}_3|^3}}\left[(-\tau_1)(-\tau_2)(-\tau_3)\right]^{(1/2)}\times \\ &\quad\times\left[(-|\vec{q}_1|\tau_1)(-|\vec{q}_2|\tau_2)(-|\vec{q}_3|\tau_3)\right]^{\frac{1}{2}(n_s-1)}\times \\ &\quad\times\mathrm{Re}\left[H^{(1)}_\nu(-|\vec{q}_1|\tau_1)\right]\mathrm{Re}\left[H^{(1)}_\nu(-|\vec{q}_2|\tau_2)\right]\mathrm{Re}\left[H^{(1)}_\nu(-|\vec{q}_3|\tau_3)\right] \\ &= \Theta(\tau-\tau_1)\Theta(\tau-\tau_2)\Theta(\tau-\tau_3)a^3(\tau)H^3\left(\frac{\pi}{2}\right)^{(3/2)}\times \\ &\quad\times\frac{1}{|\vec{q}_1|^6x_2^2x_3^2}\left(z_1z_2z_3\right)^{\frac{1}{2}}\times \\ &\quad\times\mathrm{Re}\left[H^{(1)}_\nu(z_1)\right]\mathrm{Re}\left[H^{(1)}_\nu(z_2)\right]\mathrm{Re}\left[H^{(1)}_\nu(z_3)\right]\end{aligned} \tag{A.49}$$

The second step of the calculation involves the computation of the product of source terms and its expectation value. While the procedure is similar to the one used for the power spectrum, the number of terms is four times larger. Thankfully, out of the 64 terms, 60 can be ignored as they are vanishing due to the properties of creation/annihilation operators or are irrelevant at non-zero momenta. Out of the four remaining terms, two evaluate to zero. Therefore, only the following two expectation values survive:

$$\begin{aligned}\langle a_+\left(\vec{k}_1\right)a_+\left(\vec{q}_1-\vec{k}_1\right)a_+\left(\vec{k}_2\right)a_+^\dagger\left(\vec{k}_2-\vec{q}_2\right)a_+^\dagger\left(-\vec{k}_3\right)a_+^\dagger\left(\vec{k}_3-\vec{q}_3\right)\rangle = \\ = \delta(\vec{q}_1-\vec{\mathrm{k}}_1+\vec{\mathrm{k}}_3)\delta(\vec{q}_2-\vec{\mathrm{k}}_2+\vec{\mathrm{k}}_1)\delta(\vec{q}_3-\vec{\mathrm{k}}_3+\vec{\mathrm{k}}_2)+ \\ +\delta(\vec{q}_1+\vec{q}_2-\vec{\mathrm{k}}_1-\vec{\mathrm{k}}_2)\delta(\vec{q}_3-\vec{\mathrm{k}}_3+\vec{\mathrm{k}}_2)\delta(\vec{\mathrm{k}}_1+\vec{\mathrm{k}}_3)+ \\ +\delta(\vec{q}_1+\vec{q}_3-\vec{\mathrm{k}}_1-\vec{\mathrm{k}}_3)\delta(\vec{q}_3-\vec{\mathrm{k}}_3+\vec{\mathrm{k}}_2)\delta(\vec{\mathrm{k}}_2+\vec{\mathrm{k}}_3)+ \\ +\delta(\vec{q}_1+\vec{q}_2-\vec{\mathrm{k}}_1-\vec{\mathrm{k}}_2)\delta(\vec{q}_3-\vec{\mathrm{k}}_3+\vec{\mathrm{k}}_1)\delta(\vec{\mathrm{k}}_2+\vec{\mathrm{k}}_3)\end{aligned} \tag{A.50}$$

$$\begin{aligned}\langle a_+\left(\vec{k}_1\right)a_+\left(\vec{q}_1-\vec{k}_1\right)a_+^\dagger\left(-\vec{k}_2\right)a_+\left(\vec{q}_2-\vec{k}_2\right)a_+^\dagger\left(-\vec{k}_3\right)a_+^\dagger\left(\vec{k}_3-\vec{q}_3\right)\rangle = \\ = \delta(\vec{q}_1-\vec{\mathrm{k}}_1+\vec{\mathrm{k}}_2)\delta(\vec{q}_2-\vec{\mathrm{k}}_2+\vec{\mathrm{k}}_3)\delta(\vec{q}_3-\vec{\mathrm{k}}_3+\vec{\mathrm{k}}_1)+ \\ +\delta(\vec{q}_1+\vec{q}_3-\vec{\mathrm{k}}_1-\vec{\mathrm{k}}_3)\delta(\vec{q}_2-\vec{\mathrm{k}}_2+\vec{\mathrm{k}}_3)\delta(\vec{\mathrm{k}}_1+\vec{\mathrm{k}}_2)+ \\ +\delta(\vec{q}_2+\vec{q}_3-\vec{\mathrm{k}}_2-\vec{\mathrm{k}}_3)\delta(\vec{q}_1-\vec{\mathrm{k}}_1+\vec{\mathrm{k}}_3)\delta(\vec{\mathrm{k}}_1+\vec{\mathrm{k}}_2)+ \\ +\delta(\vec{q}_2+\vec{q}_3-\vec{\mathrm{k}}_2-\vec{\mathrm{k}}_3)\delta(\vec{q}_1-\vec{\mathrm{k}}_1+\vec{\mathrm{k}}_2)\delta(\vec{\mathrm{k}}_1+\vec{\mathrm{k}}_3)\end{aligned} \tag{A.51}$$

In addition to the constraint $\vec{q}_1+\vec{q}_2+\vec{q}=0$, the δ-functions enforce the following conditions:

$$\delta(\vec{q}_1-\vec{\mathrm{k}}_1+\vec{\mathrm{k}}_3)\delta(\vec{q}_2-\vec{\mathrm{k}}_2+\vec{\mathrm{k}}_1)\delta(\vec{q}_3-\vec{\mathrm{k}}_3+\vec{\mathrm{k}}_2)\rightarrow \quad \vec{\mathrm{k}}_2=\vec{q}_2+\vec{\mathrm{k}}_1 \qquad \vec{\mathrm{k}}_3=\vec{q}_3+\vec{\mathrm{k}}_2 \tag{A.52}$$

$$\delta(\vec{q}_1+\vec{q}_2-\vec{\mathrm{k}}_1-\vec{\mathrm{k}}_2)\delta(\vec{q}_3-\vec{\mathrm{k}}_3+\vec{\mathrm{k}}_2)\delta(\vec{\mathrm{k}}_1+\vec{\mathrm{k}}_3)\rightarrow \quad \vec{\mathrm{k}}_2=-(\vec{\mathrm{k}}_1+\vec{q}_3) \qquad \vec{\mathrm{k}}_3=-\vec{\mathrm{k}}_1 \tag{A.53}$$

$$\delta(\vec{q}_1+\vec{q}_3-\vec{\mathrm{k}}_1-\vec{\mathrm{k}}_3)\delta(\vec{q}_3-\vec{\mathrm{k}}_3+\vec{\mathrm{k}}_2)\delta(\vec{\mathrm{k}}_2+\vec{\mathrm{k}}_3)\rightarrow \quad \vec{\mathrm{k}}_2=\vec{q}_2+\vec{\mathrm{k}}_1 \qquad \vec{\mathrm{k}}_3=-\vec{\mathrm{k}}_2 \tag{A.54}$$

$$\delta(\vec{q}_1+\vec{q}_2-\vec{\mathrm{k}}_1-\vec{\mathrm{k}}_2)\delta(\vec{q}_3-\vec{\mathrm{k}}_3+\vec{\mathrm{k}}_1)\delta(\vec{\mathrm{k}}_2+\vec{\mathrm{k}}_3)\rightarrow \quad \vec{\mathrm{k}}_2=\vec{q}_1+\vec{q}_2-\vec{\mathrm{k}}_1 \qquad \vec{\mathrm{k}}_3=-\vec{\mathrm{k}}_2 \tag{A.55}$$

$$\delta(\vec{q}_1-\vec{\mathrm{k}}_1+\vec{\mathrm{k}}_2)\delta(\vec{q}_2-\vec{\mathrm{k}}_2+\vec{\mathrm{k}}_3)\delta(\vec{q}_3-\vec{\mathrm{k}}_3+\vec{\mathrm{k}}_1)\rightarrow \quad \vec{\mathrm{k}}_2=\vec{\mathrm{k}}_1-\vec{q}_1 \qquad \vec{\mathrm{k}}_3=\vec{\mathrm{k}}_2-\vec{q}_2 \tag{A.56}$$

$$\delta(\vec{q}_1+\vec{q}_3-\vec{\mathrm{k}}_1-\vec{\mathrm{k}}_3)\delta(\vec{q}_2-\vec{\mathrm{k}}_2+\vec{\mathrm{k}}_3)\delta(\vec{\mathrm{k}}_1+\vec{\mathrm{k}}_2)\rightarrow \quad \vec{\mathrm{k}}_2=-\vec{\mathrm{k}}_1 \qquad \vec{\mathrm{k}}_3=-\vec{\mathrm{k}}_1-\vec{q}_2 \tag{A.57}$$

$$\delta(\vec{q}_2+\vec{q}_3-\vec{\mathrm{k}}_2-\vec{\mathrm{k}}_3)\delta(\vec{q}_1-\vec{\mathrm{k}}_1+\vec{\mathrm{k}}_3)\delta(\vec{\mathrm{k}}_1+\vec{\mathrm{k}}_2)\rightarrow \quad \vec{\mathrm{k}}_2=-\vec{\mathrm{k}}_1 \qquad \vec{\mathrm{k}}_3=\vec{\mathrm{k}}_1-\vec{q}_1 \tag{A.58}$$

$$\delta(\vec{q}_2+\vec{q}_3-\vec{\mathrm{k}}_2-\vec{\mathrm{k}}_3)\delta(\vec{q}_1-\vec{\mathrm{k}}_1+\vec{\mathrm{k}}_2)\delta(\vec{\mathrm{k}}_1+\vec{\mathrm{k}}_3)\rightarrow \quad \vec{\mathrm{k}}_2=\vec{\mathrm{k}}_1-\vec{q}_1 \qquad \vec{\mathrm{k}}_3=-\vec{\mathrm{k}}_1 \tag{A.59}$$

The terms of Eq.A.50-A.51 are associated with the products of modes shown in Eq.A.60 and Eq.A.61.

$$\begin{aligned}|\vec{q}_1-\vec{\mathrm{k}}_1||\vec{q}_2-\vec{\mathrm{k}}_2||\vec{q}_3-\vec{\mathrm{k}}_3|\big[\dot{A}_+(\tau_1,\vec{\mathrm{k}}_1)A_+(\tau_1,\vec{q}_1-\vec{\mathrm{k}}_1)\dot{A}_+(\tau_2,\vec{\mathrm{k}}_2)\times \\ \times A_+^*(\tau_2,\vec{\mathrm{k}}_2-\vec{q}_2)\dot{A}_+^*(\tau_3,-\vec{\mathrm{k}}_3)A_+^*(\tau_3,\vec{\mathrm{k}}_3-\vec{q}_3)\big]\end{aligned} \tag{A.60}$$

$$\begin{aligned}|\vec{q}_1-\vec{\mathrm{k}}_1||\vec{q}_2-\vec{\mathrm{k}}_2||\vec{q}_3-\vec{\mathrm{k}}_3|\big[\dot{A}_+(\tau_1,\vec{\mathrm{k}}_1)A_+(\tau_1,\vec{q}_1-\vec{\mathrm{k}}_1)\dot{A}_+^*(\tau_2,-\vec{\mathrm{k}}_2)\times \\ \times A_+(\tau_2,\vec{q}_2-\vec{\mathrm{k}}_2)\dot{A}_+^*(\tau_3,-\vec{\mathrm{k}}_3)A_+^*(\tau_3,\vec{\mathrm{k}}_3-\vec{q}_3)\big]\end{aligned} \tag{A.61}$$

Applying these results, one can compute $\langle J_{\vec{q}_1}(\tau_1)J_{\vec{q}_2}(\tau_2)J_{\vec{q}_3}(\tau_3)\rangle$. The expectation value can be expressed as follows:

$$\langle J_{\vec{q}_1}(\tau_1)J_{\vec{q}_2}(\tau_2)J_{\vec{q}_3}(\tau_3)\rangle = \frac{8\pi^3\xi^3 e^{6\pi\xi}}{a(\tau_1)a(\tau_2)a(\tau_3)}\frac{z_1z_2z_3}{|\vec{q}_1|^3x_2x_3}\Delta_P^{(3/2)}\delta(\vec{q}_1+\vec{q}_2+\vec{q}_2)\times \tag{A.62}$$

$$\times\int\frac{d^3p}{(2\pi)^{(9/2)}}\Bigg\{\gamma(\vec{p},\vec{q}_3)|\hat{q}_1-\vec{p}|\Big[|\vec{p}|^{(1/2)}||\hat{q}_1-\vec{p}|^{(1/2)}|x_3\hat{q}_3+\vec{p}|+|\vec{p}|^{(1/2)}||x_3\hat{q}_3+\vec{p}|^{(3/2)}+$$
$$+|\vec{p}|||\hat{q}_1-\vec{p}|^{(1/2)}|x_3\hat{q}_3+\vec{p}|^{(1/2)}+|\vec{p}|^{(3/2)}||x_3\hat{q}_3+\vec{p}|^{(1/2)}\Big]\times$$
$$\times e^{-2\sqrt{2\xi}\left[(|\vec{p}|^{(1/2)}+|\hat{q}_1-\vec{p}|^{(1/2)})(z_1)^{(1/2)}\right]}\times$$
$$\times e^{-2\sqrt{\frac{2\xi}{x_2}}\left[(|\hat{q}_1-\vec{p}|^{(1/2)}+|x_3\hat{q}_3+\vec{p}|^{(1/2)})(z_2)^{(1/2)}\right]}\times$$
$$\times e^{-2\sqrt{\frac{2\xi}{x_3}}\left[(|\vec{p}|^{(1/2)}+|x_3\hat{q}_3+\vec{p}|^{(1/2)})(z_3)^{(1/2)}\right]}+$$
$$+\gamma(\vec{p},\vec{q}_2)|\hat{q}_1-\vec{p}|\Big[|\vec{p}|^{(1/2)}||\hat{q}_1-\vec{p}|^{(1/2)}|x_2\hat{q}_2+\vec{p}|+|\vec{p}|^{(1/2)}||x_2\hat{q}_2+\vec{p}|^{(3/2)}+$$
$$+|\vec{p}|||\hat{q}_1-\vec{p}|^{(1/2)}|x_2\hat{q}_2+\vec{p}|^{(1/2)}+|\vec{p}|^{(3/2)}||x_2\hat{q}_2+\vec{p}|^{(1/2)}\Big]\times$$
$$\times e^{-2\sqrt{2\xi}\left[(|\vec{p}|^{(1/2)}+|\hat{q}_1-\vec{p}|^{(1/2)})(z_1)^{(1/2)}\right]}\times$$
$$\times e^{-2\sqrt{\frac{2\xi}{x_2}}\left[(|\vec{p}|^{(1/2)}+|x_2\hat{q}_2+\vec{p}|^{(1/2)})(z_2)^{(1/2)}\right]}\times$$
$$\times e^{-2\sqrt{\frac{2\xi}{x_3}}\left[(|\hat{q}_1-\vec{p}|^{(1/2)}+|x_2\hat{q}_2+\vec{p}|^{(1/2)})(z_3)^{(1/2)}\right]}\Bigg\}$$

where $\gamma(\vec{p},\vec{q}_n)$ is defined as:

$$\gamma=\left[\hat{\varepsilon}_+(\vec{p})\cdot\hat{\varepsilon}_+(\hat{q}_1-\vec{p})\right]\left[\hat{\varepsilon}_+^*(\vec{p})\cdot\hat{\varepsilon}_+(x_n\hat{q}_n+\vec{p})\right]\left[\hat{\varepsilon}_+^*(\hat{q}_1-\vec{p})\cdot\hat{\varepsilon}_+^*(x_n\hat{q}_n+\vec{p})\right] \tag{A.63}$$

By substitution of Eq.A.49 and Eq.A.62 in Eq.A.47 it is possible to get the following expression:

$$\langle\zeta_{\vec{q}_1}(\tau)\zeta_{\vec{q}_2}(\tau)\zeta_{\vec{q}_3}(\tau)\rangle = (2\pi)^{(3/2)}\frac{\xi^3 e^{6\pi\xi}}{|\vec{q}_1|^6 x_2^4 x_3^4}\Delta_P^3\delta(\vec{q}_1+\vec{q}_2+\vec{q}_3)\times \tag{A.64}$$

$$\times\int_{-|\vec{q}_1|\tau}^{0}\int_{-|\vec{q}_2|\tau}^{0}\int_{-|\vec{q}_3|\tau}^{0}\int dz_1dz_2dz_3d^3p\Bigg\{(z_1z_2z_3)^{(3/2)}\mathrm{Re}\left[H_\nu^{(1)}(z_1)\right]\mathrm{Re}\left[H_\nu^{(1)}(z_2)\right]\mathrm{Re}\left[H_\nu^{(1)}(z_3)\right]\times$$

$$\Big\{\gamma(\vec{p},\vec{q}_3)|\hat{q}_1-\vec{p}|\Big[|\vec{p}|^{(1/2)}||\hat{q}_1-\vec{p}|^{(1/2)}|x_3\hat{q}_3+\vec{p}|+|\vec{p}|^{(1/2)}||x_3\hat{q}_3+\vec{p}|^{(3/2)}+$$

$$+|\vec{p}|||\hat{q}_1-\vec{p}|^{(1/2)}|x_3\hat{q}_3+\vec{p}|^{(1/2)}+|\vec{p}|^{(3/2)}||x_3\hat{q}_3+\vec{p}|^{(1/2)}\Big]\times$$

$$\times e^{-2\sqrt{2\xi}\left[(|\vec{p}|^{(1/2)}+|\hat{q}_1-\vec{p}|^{(1/2)})(z_1)^{(1/2)}\right]}\times$$

$$\times e^{-2\sqrt{\frac{2\xi}{x_2}}\left[(|\hat{q}_1-\vec{p}|^{(1/2)}+|x_3\hat{q}_3+\vec{p}|^{(1/2)})(z_2)^{(1/2)}\right]}\times$$

$$\times e^{-2\sqrt{\frac{2\xi}{x_3}}\left[(|\vec{p}|^{(1/2)}+|x_3\hat{q}_3+\vec{p}|^{(1/2)})(z_3)^{(1/2)}\right]}+$$

$$+\gamma(\vec{p},\vec{q}_2)|\hat{q}_1-\vec{p}|\Big[|\vec{p}|^{(1/2)}||\hat{q}_1-\vec{p}|^{(1/2)}|x_2\hat{q}_2+\vec{p}|+|\vec{p}|^{(1/2)}||x_2\hat{q}_2+\vec{p}|^{(3/2)}+$$

$$+|\vec{p}|||\hat{q}_1-\vec{p}|^{(1/2)}|x_2\hat{q}_2+\vec{p}|^{(1/2)}+|\vec{p}|^{(3/2)}||x_2\hat{q}_2+\vec{p}|^{(1/2)}\Big]\times$$

$$\times e^{-2\sqrt{2\xi}\left[(|\vec{p}|^{(1/2)}+|\hat{q}_1-\vec{p}|^{(1/2)})(z_1)^{(1/2)}\right]}\times$$

$$\times e^{-2\sqrt{\frac{2\xi}{x_2}}\left[(|\vec{p}|^{(1/2)}+|x_2\hat{q}_2+\vec{p}|^{(1/2)})(z_2)^{(1/2)}\right]}\times$$

$$\times e^{-2\sqrt{\frac{2\xi}{x_3}}\left[(|\hat{q}_1-\vec{p}|^{(1/2)}+|x_2\hat{q}_2+\vec{p}|^{(1/2)})(z_3)^{(1/2)}\right]}\Big\}\Bigg\}$$

$$=\frac{3}{10}(2\pi)^{5/2}\Delta_P^3 e^{6\pi\xi}\frac{\delta(\vec{q}_1+\vec{q}_2+\vec{q}_3)}{|\vec{q}_1|^6}\frac{1+x_2^3+x_3^3}{x_2^3x_3^3}f_3(\xi,x_2,x_3)=\delta(\vec{q}_1+\vec{q}_2+\vec{q}_3)B_\zeta \tag{A.65}$$

where $f_3(\xi,x_2,x_3)$ is defined as in Eq.A.66:

$$
\begin{aligned}
f_3(\xi,x_2,x_3) &= \frac{5}{3\pi}\frac{\xi^3}{x_2x_3\left[1+x_2+x_3\right]} \qquad (A.66)\\
&\times\int d^3p\Bigg\{\gamma(\vec{p},\vec{q}_3)|\hat{q}_1-\vec{p}|\Big[|\vec{p}|^{(1/2)}||\hat{q}_1-\vec{p}|^{(1/2)}|x_3\hat{q}_3+\vec{p}|+|\vec{p}|^{(1/2)}||x_3\hat{q}_3+\vec{p}|^{(3/2)}+\\
&\qquad+|\vec{p}|||\hat{q}_1-\vec{p}|^{(1/2)}|x_3\hat{q}_3+\vec{p}|^{(1/2)}+|\vec{p}|^{(3/2)}||x_3\hat{q}_3+\vec{p}|^{(1/2)}\Big]\times\\
&\times\mathrm{I}\left(-2\sqrt{2\xi}\left[|\vec{p}|^{(1/2)}+|\hat{q}_1-\vec{p}|^{(1/2)}\right]\right)\mathrm{I}\left(-2\sqrt{\frac{2\xi}{x_2}}\left[|\hat{q}_1-\vec{p}|^{(1/2)}+|x_3\hat{q}_3+\vec{p}|^{(1/2)}\right]\right)\times\\
&\times\mathrm{I}\left(-2\sqrt{\frac{2\xi}{x_3}}\left[|\vec{p}|^{(1/2)}+|x_3\hat{q}_3+\vec{p}|^{(1/2)}\right]\right)+\\
&+\gamma(\vec{p},\vec{q}_2)|\hat{q}_1-\vec{p}|\Big[|\vec{p}|^{(1/2)}||\hat{q}_1-\vec{p}|^{(1/2)}|x_2\hat{q}_2+\vec{p}|+|\vec{p}|^{(1/2)}||x_2\hat{q}_2+\vec{p}|^{(3/2)}+\\
&\qquad+|\vec{p}|||\hat{q}_1-\vec{p}|^{(1/2)}|x_2\hat{q}_2+\vec{p}|^{(1/2)}+|\vec{p}|^{(3/2)}||x_2\hat{q}_2+\vec{p}|^{(1/2)}\Big]\times\\
&\times\mathrm{I}\left(-2\sqrt{2\xi}\left[|\vec{p}|^{(1/2)}+|\hat{q}_1-\vec{p}|^{(1/2)}\right]\right)\mathrm{I}\left(-2\sqrt{\frac{2\xi}{x_2}}\left[|\vec{p}|^{(1/2)}+|x_2\hat{q}_2+\vec{p}|^{(1/2)}\right]\right)\times\\
&\times\mathrm{I}\left(-2\sqrt{\frac{2\xi}{x_3}}\left[|\hat{q}_1-\vec{p}|^{(1/2)}+|x_2\hat{q}_2+\vec{p}|^{(1/2)}\right]\right)\Bigg\}
\end{aligned}
$$